

Aus der
Kinderchirurgischen Klinik und Poliklinik im Dr. von Haunerschen Kinderspital
Klinikum der Ludwig-Maximilians-Universität München



**Improving persistence of anti-CD19 CAR T cells
via overexpression of the IL-21 receptor**

Dissertation

zum Erwerb des Doktorgrades der Medizin
an der Medizinischen Fakultät der Ludwig-
Maximilians-Universität zu München

vorgelegt von

Vasil Toskov

aus

Plovdiv, Bulgarien

Jahr 2023

Mit Genehmigung der Medizinischen Fakultät
der Universität München

Erstes Gutachten: Prof. Dr. med. Tobias Feuchtinger

Zweites Gutachten: Prof. Dr. med. Marion Subklewe

Drittes Gutachten: Prof. Dr. med. Andreas Humpe

Promovierter Mitbetreuer: Dr. med. Semjon Willier

Dekan: Prof. Dr. med. Thomas Gudermann

Tag der mündlichen Prüfung: 11.10.2023

Eidesstattliche Erklärung

Ich, Vasil Toskov, geboren am 17.12.1992 in Plovdiv, Bulgarien, erkläre hiermit an Eides statt, dass ich die vorliegende Dissertation mit dem Thema **Improving persistence of anti-CD19 CAR T cells via overexpression of the IL-21 receptor** selbständig verfasst, mich außer der angegebenen keiner weiteren Hilfsmittel bedient und alle Erkenntnisse, die aus dem Schrifttum ganz oder annähernd übernommen sind, als solche kenntlich gemacht und nach ihrer Herkunft unter Bezeichnung der Fundstelle einzeln nachgewiesen habe.

Ich erkläre des Weiteren, dass die hier vorgelegte Dissertation nicht in gleicher oder in ähnlicher Form bei einer anderen Stelle zur Erlangung eines akademischen Grades eingereicht wurde.

Freiburg, 20.10.23

Ort, Datum

Vasil Toskov

Unterschrift des Autors

Danksagung

An dieser Stelle möchte ich allen beteiligten Personen meinen großen Dank aussprechen, die mich bei der Anfertigung meiner Dissertation unterstützt haben.

Besonders danken möchte ich Herrn Prof. Dr. med. Tobias Feuchtinger und Herrn Dr. med. Semjon Willier für die hervorragende Betreuung und die große Unterstützung bei der Durchführung der gesamten Arbeit.

Außerdem möchte ich mich bei allen Mitgliedern der Arbeitsgruppe Feuchtinger bedanken, die mich auf meinem Weg mit Rat und produktiven Gesprächen begleitet haben.

Des Weiteren möchte ich Frau Prof. Dr. med. Marion Subklewe und Herrn Prof. Dr. med. Sebastian Kobold meinen Dank äußern, die meine Arbeit durch Ihre konstruktiven Ratschläge positiv beeinflusst haben.

Für die ideelle und finanzielle Förderung danke ich das Mildred-Scheel-Programm der Deutschen Krebshilfe und die Studienstiftung des deutschen Volkes.

Die Arbeit an dieser Dissertation wäre ohne die grenzenlose Unterstützung meiner Eltern nicht möglich gewesen. Ihr seid meine Vorbilder und meine Inspiration. Danke!

Table of Contents

| | | |
|----------|--|-----------|
| 1 | ABBREVIATIONS | 1 |
| 2 | INTRODUCTION | 4 |
| 2.1 | ACUTE LYMPHOBLASTIC LEUKEMIA AND THERAPEUTIC CHALLENGES | 4 |
| 2.2 | TARGETED THERAPIES FOR THE TREATMENT OF B-CELL LEUKEMIA | 4 |
| 2.3 | IMPAIRED PERSISTENCE AND OTHER LIMITATIONS OF ADOPTIVE CELL THERAPY | 6 |
| 2.4 | GENOMIC ENGINEERING VIA THE CRISPR/Cas9 SYSTEM | 7 |
| 2.5 | THE ROLE OF INTERLEUKIN-21 AND ITS RECEPTOR IN IMMUNITY | 7 |
| 3 | HYPOTHESIS AND AIMS OF THE STUDY | 10 |
| 4 | MATERIALS | 11 |
| 4.1 | EQUIPMENT AND SOFTWARE | 11 |
| 4.2 | SOLUTIONS, MEDIA AND SERA FOR CELL CULTURE | 12 |
| 4.3 | CONSUMABLES | 15 |
| 4.4 | ANTIBODIES | 16 |
| 5 | METHODS | 19 |
| 5.1 | GENOMIC MODIFICATION OF PRIMARY T CELLS | 19 |
| 5.1.1 | <i>PBMCs and T cell isolation. Primary T cell activation</i> | 19 |
| 5.1.2 | <i>Generation of retroviral vector particles</i> | 19 |
| 5.1.3 | <i>Retroviral T cell transduction</i> | 19 |
| 5.1.4 | <i>IL-21 Receptor knock-out with CRISPR/Cas9</i> | 20 |
| 5.1.5 | <i>Characterization of the T cell product after genetic modification</i> | 20 |
| 5.2 | FUNCTIONALITY ASSAYS WITH GENETICALLY MODIFIED T CELLS | 20 |
| 5.2.1 | <i>IL-21R surface expression induction</i> | 21 |
| 5.2.2 | <i>Co-culture with blinatumomab</i> | 21 |
| 5.2.3 | <i>Co-culture with interleukin-21</i> | 21 |
| 5.2.4 | <i>Cytotoxicity assay</i> | 21 |
| 5.2.5 | <i>CD107a degranulation assay</i> | 21 |
| 5.2.6 | <i>Intracellular cytokine staining (ICS)</i> | 21 |
| 5.2.7 | <i>Proliferation assay</i> | 21 |
| 5.2.8 | <i>Phenotype, activation and exhaustion markers</i> | 22 |
| 5.2.9 | <i>Measurement of STAT3 phosphorylation</i> | 22 |
| 5.2.10 | <i>Bead-based multiplex immunoassay</i> | 22 |
| 5.3 | IL-10 AND IL-21 ENZYME-LINKED IMMUNOSORBENT ASSAY (ELISA) | 22 |
| 5.4 | GENERAL CELL CULTURE | 22 |
| 5.5 | FLOW CYTOMETRY | 22 |
| 5.6 | SOFTWARE | 23 |
| 5.7 | STATISTICAL ANALYSIS | 23 |
| 6 | RESULTS | 24 |
| 6.1 | CRISPR/Cas9 GENOMIC KNOCK-OUT AND RETROVIRAL TRANSDUCTION OF IL-21R IN PRIMARY T CELLS | 24 |
| 6.1.1 | <i>Generation of IL-21R overexpressing and CRISPR/Cas9 knock-out T cells</i> | 24 |
| 6.1.2 | <i>Functionality of IL-21R overexpressing and CRISPR/Cas9 knock-out T cells</i> | 28 |
| 6.2 | RETROVIRAL TRANSDUCTION OF IL-21R AND COMMON GAMMA CHAIN IN PRIMARY T CELLS | 33 |
| 6.2.1 | <i>Generation of IL-21R and common gamma chain overexpressing T cells</i> | 33 |
| 6.2.2 | <i>Functionality of IL-21R and common gamma chain overexpressing T cells</i> | 35 |
| 6.3 | CRISPR/Cas9 KNOCK-OUT AND RETROVIRAL TRANSDUCTION OF IL-21R IN ANTI-CD19 CAR T CELLS | 39 |
| 6.3.1 | <i>Generation of first- and second-generation anti-CD19 CAR T cells overexpressing IL-21R</i> | 39 |
| 6.3.2 | <i>Functionality of first- and second-generation IL-21R overexpressing anti-CD19 CAR T cells</i> | 43 |
| 6.3.3 | <i>Generation of IL-21R CRISPR/Cas9 knock-out in second-generation anti-CD19 CAR T cells</i> | 46 |
| 6.3.4 | <i>Functionality of IL-21R overexpressing and knock-out anti-CD19 CAR T cells</i> | 49 |

| | | |
|-----------|--|-----------|
| 6.3.5 | <i>Cytokine secretion and T helper phenotype of IL-21R overexpressing and knock-out anti-CD19 CAR T cells</i> | 53 |
| 6.4 | RETROVIRAL TRANSDUCTION OF IL-21R AND IL-21 IN PURIFIED CD4 ⁺ AND CD8 ⁺ ANTI-CD19 CAR T CELLS | 57 |
| 6.4.1 | <i>Generation of CD4⁺ and CD8⁺ anti-CD19 CAR T cells</i> | 57 |
| 6.4.2 | <i>Functionality of IL-21R and IL-21 overexpressing CD4⁺ and CD8⁺ anti-CD19 CAR T cells</i> | 58 |
| 7 | DISCUSSION | 60 |
| 7.1 | ALTERED IL-21R EXPRESSION AND ITS EFFECT ON PRIMARY T CELLS | 60 |
| 7.2 | OVEREXPRESSION OF THE COMMON GAMMA CHAIN DOES NOT IMPROVE IL-21/IL-21R SIGNALING | 61 |
| 7.3 | SUCCESSFUL GENERATION OF FUNCTIONAL ANTI-CD19 CAR T CELLS OVEREXPRESSIONG IL-21R | 63 |
| 7.4 | ALTERED IL-21R EXPRESSION AND ITS EFFECT ON SECOND-GENERATION CAR T CELLS WITH 4-1BB CO-STIMULATION | 63 |
| 7.5 | SUPERIOR FUNCTIONALITY AFTER COMBINATION OF IL-21 PRODUCING CD4 ⁺ AND IL-21R OVEREXPRESSIONG CD8 ⁺ CAR T CELLS | 65 |
| 7.6 | OUTLOOK | 66 |
| 8 | SUMMARY/ABSTRACT | 67 |
| 9 | ZUSAMMENFASSUNG | 68 |
| 10 | REFERENCES | 69 |
| 11 | SUPPLEMENTS | 79 |
| 11.1 | SUPPLEMENTARY FIGURES | 79 |
| 11.2 | PRIMER SEQUENCES | 79 |
| 11.3 | T CELL SEQUENCES | 80 |
| 11.3.1 | <i>Sequence of _{RV19z} CAR</i> | 80 |
| 11.3.2 | <i>Sequence of _{RV19z_IL-21R^{OE}} CAR</i> | 80 |
| 11.3.3 | <i>Sequence of _{RV19-28z} CAR</i> | 81 |
| 11.3.4 | <i>Sequence of _{RV19-28z_IL-21R^{OE}} CAR</i> | 81 |
| 11.3.5 | <i>Sequence of _{RV19-BBz} CAR</i> | 82 |
| 11.3.6 | <i>Sequence of _{RV19-BBz_IL-21R^{OE}} CAR</i> | 83 |
| 11.3.7 | <i>Sequence of _{RVCD132^{OE}}</i> | 84 |
| 11.3.8 | <i>Sequence of _{RVIL-21R^{OE}}</i> | 84 |
| 11.3.9 | <i>Sequence of _{RVIL-21R_CD132^{OE}}</i> | 84 |

Table of Figures

| | |
|--|----|
| Figure 6.1 Generation of IL-21R overexpressing and CRISPR/Cas9 knock-out T cells | 25 |
| Figure 6.2 Characterization of the final cell product and measurement of signal transduction via pSTAT3 in IL-21R overexpressing and CRISPR/Cas9 knock-out T cells | 27 |
| Figure 6.3 Overview of functionality assays and CD19-specific cytotoxicity of IL-21R overexpressing and CRISPR/Cas9 knock-out T cells | 29 |
| Figure 6.4 CD19-specific CD107a degranulation and phenotype of IL-21R overexpressing and CRISPR/Cas9 knock-out T cells | 31 |
| Figure 6.5 Intracellular cytokine staining of IL-21R overexpressing and CRISPR/Cas9 knock-out T cells | 32 |
| Figure 6.6 Generation of IL-21R and common gamma chain overexpressing T cells | 34 |
| Figure 6.7 Characterization of the final cell product and measurement of pSTAT3 in IL-21R and common gamma chain overexpressing T cells | 35 |
| Figure 6.8 Overview of functionality assays and CD19-specific cytotoxicity of IL-21R and common gamma chain overexpressing T cells | 36 |
| Figure 6.9 Intracellular cytokine staining and phenotype of IL-21R and common gamma chain overexpressing T cells | 38 |
| Figure 6.10 Generation of first- and second-generation anti-CD19 CAR T cells overexpressing IL-21R | 40 |
| Figure 6.11 Characterization of the final CAR T cell product | 42 |
| Figure 6.12 CD19-specific cytotoxicity and proliferation of IL-21R overexpressing CAR T cells | 44 |
| Figure 6.13 Intracellular cytokine staining of IL-21R overexpressing CAR T cells | 46 |
| Figure 6.14 Generation of IL-21R CRISPR/Cas9 knock-out and overexpressing second-generation CAR T cells and characterization of the final cell product | 48 |
| Figure 6.15 CD19-specific cytotoxicity and proliferation of IL-21R knock-out and overexpressing CAR T cells | 50 |
| Figure 6.16 Intracellular cytokine staining and expression of co-inhibitory markers in IL-21R knock-out and overexpressing CAR T cells | 52 |
| Figure 6.17 Cytokine profile of IL-21R overexpressing and knock-out anti-CD19 CAR T cells | 54 |
| Figure 6.18 T helper phenotype of CD4 ⁺ IL-21R overexpressing and knock-out anti-CD19 CAR T cells | 56 |
| Figure 6.19 Generation of purified CD4 ⁺ and CD8 ⁺ second-generation CAR T cells with IL-21R and IL-21 overexpression | 57 |
| Figure 6.20 Overview of the intracellular cytokine staining assay and IFN- γ secretion of CD8 ⁺ CAR T cells with IL-21R and IL-21 overexpression | 59 |
| Supplementary figure 11.1 Proliferation and intracellular cytokine staining of IL-21R knock-out and overexpressing CAR T cells | 79 |

1 Abbreviations

| | |
|------------------------------|---|
| γ_c | Gamma chain |
| AIEOP-BFM ALL | Associazione italiana ematologia oncologia pediatrica – Berlin-Frankfurt-Munster acute lymphoblastic leukemia study |
| ALL | Acute lymphoblastic leukemia |
| BCP | B cell precursor |
| BiTe | Bispecific T-cell engaging antibody |
| BFM-ALL | Berlin-Frankfurt-Munster acute lymphoblastic leukemia study |
| CAR | Chimeric antigen receptor |
| Cas | CRISPR-associated protein |
| CCR | C-C Motif Chemokine Receptor |
| CD | Cluster of differentiation |
| CNS | Central nervous system |
| CoALL | Cooperative acute lymphoblastic leukemia study |
| CR | Complete remission |
| crControl | Electroporated control cells |
| crIL-21R^{KO} | CRISPR/Cas9 genomic knock-out of IL-21R alpha chain in primary T cells |
| CRISPR | Clustered regularly interspersed short palindromic repeats |
| crRNA | CRISPR RNA |

| | |
|---------------|---|
| CRS | Cytokine release syndrome |
| CTLA-4 | Cytotoxic T-lymphocyte-associated protein 4 |
| CTV | CellTrace Violet |
| DMSO | Dimethyl sulfoxide |
| DSB | DNA double-stranded break |
| E:T | Effector-to-target |
| EC | Extracellular |
| ELISA | Enzyme-linked immunosorbent assay |
| EMA | European Medicine Agency |
| FACS | Fluorescence-activated cell sorting |
| FBS | Fetal bovine serum |
| FC | Fold change |
| FDA | U.S. Food and Drug Administration |
| HDR | Homology-directed repair |
| HLA | Human leukocyte antigen |
| HSCT | Hematopoietic stem cell transplantation |
| HSA | Human serum albumin |
| IC | Intracellular |
| ICS | Intracellular cytokine staining |
| Ig | Immunoglobulin |
| IL | Interleukin |

| | |
|-------------------------------------|--|
| IFN-γ | Interferon gamma |
| IntReALL | International study for treatment of childhood relapsed acute lymphoblastic leukemia |
| JAK | Janus-kinase |
| KLGR-1 | Killer cell lectin-like receptor subfamily G member 1 |
| MHC | Major histocompatibility complex |
| MRD | Minimal residual disease |
| n | Number |
| NHEJ | Nonhomologous end joining |
| NK | Natural killer cells |
| NKT | Natural killer T cells |
| ns | Not significant |
| PAM | Protospacer adjacent motif |
| PBMC | Peripheral blood mononuclear cells |
| PCR | Polymerase chain reaction |
| PD-1 | Programmed cell death 1 |
| RPMI | Roswell Park Memorial Institute medium |
| R/R | Relapsed and/or refractory |
| RV19z | 1 st generation CAR construct |
| RV19z_IL-21R^{OE} | 1 st generation CAR construct IL-21R alpha chain overexpression |
| RV19-28z | 2 nd generation CAR construct with CD28 endodomain |
| RV19-28z_IL-21R^{OE} | 2 nd generation CAR construct with CD28 |

| | |
|---|--|
| | endodomain and IL-21R alpha chain overexpression |
| RV19-BBz | 2 nd generation CAR construct with 4-1BB endodomain |
| RV19-BBz_{CR}IL-21R^{KO} | 2 nd generation CAR construct with 4-1BB endodomain and IL-21R alpha chain knock-out |
| RV19-BBz_{CR}Control | Electroporated 2 nd generation CAR construct with 4-1BB endodomain |
| RV19-BBz_IL-21R^{OE} | 2 nd generation CAR construct with 4-1BB endodomain and IL-21R alpha chain overexpression |
| RVCD132^{OE} | Retroviral overexpression of common gamma chain in primary T cells |
| RVIL-21R_CD132^{OE} | Retroviral overexpression of common gamma chain and IL-21R alpha chain in primary T cells |
| RVIL-21R^{OE} | Retroviral overexpression of IL-21R alpha chain in primary T cells |
| scFv | Single chain variable fragment |
| sFas | Soluble FAS |
| sgRNA | single guide RNA |
| STAT | Signal Transducer And Activator Of Transcription |
| T | T cells |
| T_{CM} | Central memory T cells |
| TCR | T cell receptor |
| T_{EFF} | Effector T cells |

| | |
|--------------------------------|--|
| T_{EM} | Effector memory T cells |
| T_{fh} | T follicular helper cells |
| T_h | T helper population |
| TIM-3 | T-cell immunoglobulin and mucin domain 3 |
| TM | Transmembrane |
| T_N | Naïve T cells |
| TNF-α | Tumor necrosis factor alpha |

| | |
|------------------------|---|
| tracrRNA | trans-activating crRNA |
| Treg | Regulatory T cells |
| T_{SCM} | Stem cell-like memory T cells |
| tSNE | t-distributed stochastic neighbor embedding |
| UT | Untransduced T cells |
| XSCID | X-linked severe combined immunodeficiency |

2 Introduction

2.1 Acute lymphoblastic leukemia and therapeutic challenges

Malignancy is the most common non-violent cause of death among children and adolescents in the US¹, with acute lymphoblastic leukemia (ALL) being the predominant childhood neoplasm^{2,3}. ALL has a prevalence peak within the 3 to 5 age group, derives either from the B or T cell lineage and is a leading cancer-related cause of death among the pediatric population^{4,5}. The disease is characterized by infiltration of the bone marrow and lymphoid organs by leukemic blasts, which leads to symptoms of hematopoietic exhaustion, such as easy bruising, bone pain, hepatosplenomegaly and frequent infections⁶.

Treatment protocols require risk assignment based on patient and clinical characteristics, e.g., age, sex, white blood cell count at diagnosis, central nervous system (CNS) involvement, as well as on immunophenotypic, cytogenetic and genetic characteristics⁴. This risk stratification defines treatment regimens according to known risk factors for therapy failure. Distinct genetic alterations, such as aneuploidy, deregulated oncogenes and point mutations, have been described to drive the development of the most common form of ALL, B-cell progenitor ALL (BCP-ALL)⁷. In addition to their role in risk stratification many genetic alterations are being evaluated as therapeutic targets⁷.

Ever since the first reported remission induction of leukemia via chemotherapy⁸, long-term survival from BCP-ALL has steadily improved. Current clinical trials are based on study protocols (e.g., CoALL, AIEOP-BFM ALL and ALL-BFM) that yield 5-year overall survival rates of more than 90%^{9,10}. Newly diagnosed patients often undergo three phases of chemotherapy regimens: remission induction, consolidation and maintenance therapy¹¹. A short and intensive first phase with the aim of inducing complete remission (CR), defined as less than 5% blasts seen on microscopy, is followed by consolidation therapy for 6 to 9 months, whose goal is to eradicate residual disease. The two multidrug-intensive blocks are then followed by maintenance chemotherapy for 2 to 3 years to reduce the risk of relapse. Intrathecal chemotherapy is also administered, with application frequency depending on the risk of relapse¹².

A sensitive prognostic parameter after treatment of ALL is the post-induction detection via flow cytometry or polymerase chain reaction (PCR) of minimal residual disease (MRD), defined as one leukemia cell per 10⁴ to 10⁵ normal leukocytes. MRD-positivity entails a higher risk of standard treatment failure, which is why therapy needs to be escalated in these patients¹³. Despite the remarkable survival improvement of standard-risk patients, management of relapsed and/or refractory (R/R) leukemia remains a major challenge, since intensification of conventional chemotherapy often comes at the cost of increased critical therapy toxicity. More than 2% of patients with ALL are refractory to induction therapy¹⁴, whereas the post remission relapse rate remains at 15% to 20%¹⁵. In spite of an initial high reinduction remission rate, more than half of children would relapse again¹⁶. The 2-year event-free survival rate then starkly diminishes with each subsequent relapse and even reaches the dismal rate of 13.3% ($\pm 7.0\%$) after a third salvage therapy¹⁷.

The therapeutic aim after relapse of BCP-ALL is to induce and maintain complete remission for a period of time, which allows for stem cell transplantation¹⁸. Research into novel therapeutic agents has led to the advent of targeted therapies with the aim of improving therapeutic outcome in R/R BCP-ALL. Of note in this regard are the bispecific T cell-engaging (BiTe) antibody blinatumomab and chimeric antigen receptor (CAR) T cells, which both target the CD19 antigen on the surface of B cell leukemic blasts.

2.2 Targeted therapies for the treatment of B-cell leukemia

The emergence of antibody- and T cell-based agents which can directly target leukemic blasts, has revolutionized the therapy of relapsed/refractory B-cell precursor ALL in the last decade. Blinatumomab is a recombinant bispecific antibody, which consists of two single-chain variable fragments (scFv) joined

via a glycine-serine linker¹⁹. One antigen-binding site engages the CD3 antigen on human T cells, whereas the other binds CD19, a marker expressed by B(-precursor) lymphocytes and ubiquitous in most B cell neoplasms. The antibody bispecificity enables an interaction between CD3⁺ T cells and CD19⁺ leukemic blasts and thus activates T cell cytotoxicity after TCR engagement²⁰.

In a recent study, heavily pretreated adult patients with R/R BCP-ALL who received blinatumomab achieved higher remission rates and better overall survival compared to those treated with conventional chemotherapy regimens²¹. Similar results have been described in the pediatric setting, with a multicenter randomized control trial showing improved event-free survival in first-relapse BCP-ALL patients²². Brown et al. also reported increased disease-free and overall survival rates in the blinatumomab treatment arm, with the majority of treated patients proceeding to hematopoietic stem-cell transplantation²³. These improvements in survival led to the approval of blinatumomab by the U.S. Food and Drug Administration (FDA) for the treatment of adults and children with relapsed/refractory BCP-ALL²⁰, as well as its rapid incorporation in current treatment protocols.

Another promising immunotherapeutic approach is the adoptive transfer of chimeric antigen receptor (CAR) T cells. Chimeric antigen receptors (CARs) are synthetically engineered receptors which can HLA-independently bind to specific antigens on the surface of leukemic blasts²⁴. The presence of CD19 on BCP-ALL tumor cells makes it an attractive target for CAR T cell therapy. The anti-CD19 antigen-binding domain consists of an antibody-derived scFv and is anchored to the cell membrane via a transmembrane region based on CD28 or CD8 α , which in turn is connected to the intracellular signaling domain CD3 ζ ²⁵. This delineates the basic structure of the so-called first-generation CARs. Second- and third-generation CAR constructs may furthermore incorporate one or more endodomains from co-stimulatory molecules^{26,27} such as 4-1BB, CD28 or OX40 to improve efficacy²⁸ of adoptive cell therapy.

Even though first-generation CAR T cells were proven to be successful in mounting an immune response against CD19⁺ malignancies *in vivo*²⁹, one major limitation was the low short-term persistence of the adoptively transferred T cells³⁰. In contrast, second-generation CAR constructs containing the CD28 co-stimulatory endodomain showed enhanced proliferation and persistence³¹. Most current clinical trials, however, focus on second-generation CARs with a 4-1BB endodomain, as *in vivo* persistence was shown to be superior³².

In a landmark study of two pediatric patients with relapsed/refractory BCP-ALL, complete remission was achieved after the infusion of second-generation CAR T cells with the 4-1BB intracellular domain³³. These results could be reproduced in a larger cohort of 30 children and adults with R/R BCP-ALL, as CR was reached in 90%³⁴. The multi-center follow-up study ELIANA reported overall survival of 90% and 76% at 6 and 12 months, respectively³⁵. At 3 years follow-up overall survival was still high at 63%³⁶. Patients who responded to treatment were also found to be MRD-negative. Due to its efficacy, tisagenlecleucel (Kymriah, Novartis), a second-generation CAR T cell product consisting of the FMC63 CD19-binding domain and the 4-1BB co-stimulatory endodomain was approved by FDA and the European Medicine Agency (EMA) for pediatric relapsed and/or refractory BCP-ALL³⁷.

Manufacturing of CAR T cells follows standardized protocols. T cells from the patient are collected via leukapheresis and cultured with proliferation stimulants. The activated T cell product then undergoes lenti- or retroviral transduction of the CAR construct and expansion *in vitro*, followed by reinfusion into the patient³⁸. Patients with R/R BCP-ALL often receive bridging chemotherapy prior to CAR T cell administration with the aim of reducing disease burden and eventual complications¹⁰. Lymphodepletion is also performed a few days prior to infusion as it increases *in vivo* persistence of CAR T cells³⁹. An important consideration is prior CD19-targeted therapy with blinatumomab, as it may lessen response to adoptive cell transfer⁴⁰.

2.3 Impaired persistence and other limitations of adoptive cell therapy

Several complications of CAR T cell therapy have been described, such as cytokine release syndrome (CRS), neurotoxicity and B cell aplasia⁴¹. Most complications are on-target effects due to the interaction between immune and target cells, thus clearance of the leukemic blasts lessens therapy-associated toxicities. CRS is a systemic inflammatory reaction due to monocyte- and macrophage-derived interleukin-1 (IL-1) and -6 (IL-6) and is characterized initially by fever and subsequent potential multiorgan failure with e.g., dyspnea and arterial hypotension among others⁴². Several strategies are used to abate life-threatening CRS and associated neurotoxicity, such as the IL-6 receptor antagonist tocilizumab and the IL-1 receptor antagonist anakinra^{43,44}. The ELIANA study reported CRS in 77% and neurologic complications in 40% of enrolled patients³⁵. B cell aplasia after administration of anti-CD19 CAR T cells is another common on-target, but off-tumor complication based on CD19 expression in most cells of B cell lineage³³, even though persistence of plasma cells responsible for long-lasting immunity has been described⁴⁵. Regular immunoglobulin infusions for patients with B cell aplasia are part of the follow-up routine for patients after CD19 directed CAR T cell therapy⁴⁶.

Despite high initial remission rates, about half of B-cell ALL patients treated with CAR T cells would relapse within one year of treatment³⁵ with two major mechanisms of resistance to adoptive cell therapy: either early antigen-positive or late antigen-negative/low relapse.

In the first instance, CAR T cells show a lack of in vivo persistence and expansion, both major predictors of therapeutic efficacy⁴⁷. Several factors may affect the in vivo persistence of adoptively transferred T cells, such as patient preconditioning and differentiation status of T cells. Lymphodepletion is a form of preconditioning which improves the expansion and thus the persistence of adoptively transferred cells by limiting competition for supportive cytokines such as interleukin-7 (IL-7), IL-15 and IL-21 and by decreasing the number of CD4⁺CD25⁺ regulatory T (Treg) cells^{48,49}. The level of T cell differentiation also plays an important role: for instance, enrichment of Th17 cells has been implicated in a superior anti-tumor activity⁵⁰. In contrast, terminally differentiated T cells are characterized by phenotypic changes, such as loss of CD27, CD28 and CCR7 expression, and reduced proliferative capability⁵¹. Moreover, they perform effector functions in an antigen-dependent manner and often exhibit signs of T cell dysfunction, as defined by the expression of co-inhibitory molecules, such as PD-1, TIM-3, CTLA-4 and KLGR-1⁵². To counteract exhaustion, infusion of less differentiated, stem cell-like memory (T_{SCM}) and central memory T cells (T_{CM}) can lead to sustained proliferation and persistence due to functional STAT3 signaling⁴⁷.

Persistence may also be impaired via intrinsic signaling of the co-stimulatory domain in second-generation CAR constructs. Tonic signaling of the synthetic chimeric receptor during ex vivo expansion can drive T cell differentiation and exhaustion⁵³. CD28 co-stimulation led to accelerated T cell exhaustion compared to CAR constructs with a 4-1BB endodomain³², probably due to redundant signaling of CD28 and CD3 ζ ⁵⁴. In contrast, mutating the intracellular signaling domain in a CAR construct with CD28 co-stimulation managed to calibrate activity and improve in vivo efficacy⁵⁵. Moreover, since most scFv domains are derived from murine antibodies, anti-mouse reactivity may impair CAR T cell function. By utilizing CAR T cells with humanized anti-CD19 scFv, a remarkably high relapse-free survival of 74% was achieved in patients previously treated with tisagenlecleucel¹⁰. Long-term persistence may also depend on CAR binding affinity. A clinical trial compared a lower-affinity CAR to a high-affinity FMC63 binding-domain CAR and reported increased in vitro and in vivo efficacy when affinity was reduced⁵⁶.

The second instance of relapse is due to CD19 antigen escape. Analysis of samples from relapsed patients after CAR T cell therapy showed loss-of-function mutations in exons 2–5 of the CD19 gene, leading to translation of a truncated protein, which cannot be anchored to the cell membrane⁵⁷. In another example, alternatively spliced CD19 was not recognized by the FMC63 epitope-binding domain of the clinically used CAR construct⁵⁸. Such CD19 isoforms may even be present prior to immunotherapy and become the predominant clone after CAR T cell administration⁵⁹. Moreover, immune pressure by CAR T cells drove a lineage switch of leukemic cells, which started expressing myeloid markers^{60,61}.

Furthermore, the novel mechanism of trogocytosis describes active transfer of the CD19 antigen to T cells, thus mediating not only leukemic antigen escape but also exhaustion and fratricide of CAR T cells⁶². Loss of CD19 can also be mediated by administration of blinatumomab and thus limit subsequent adoptive anti-CD19 CAR T cell therapy⁶³. A clinically effective approach to counteract CD19 antigen escape may be the simultaneous or subsequent targeting of CD22, which is also expressed on the surface of BCP-ALL blasts^{64,65}.

Over recent years, cancer immunotherapy with CAR T cells has become an essential part of therapy regimens for refractory/relapsed B-cell ALL, with remarkable clinical responses in pediatric and adult patients, combined with well-manageable therapy-related toxicities. However, further research is necessary to counteract the mechanisms of antigen escape and reduced in vivo persistence as these limit the efficacy of adoptive cell transfer and can lead to leukemia relapse.

2.4 Genomic engineering via the CRISPR/Cas9 system

Genomic engineering has emerged as an important tool to explore immune cell functionality and even redirect immune responses toward desired therapeutic outcomes. The starting point of this field was the discovery of the DNA double-stranded break (DSB) and the ability to incorporate exogenous DNA sequences at the target site⁶⁶. However, the use of targeted technologies such as zinc fingers⁶⁷ remained limited due to the arduous process of engineering custom endonucleases for the DNA sequence in question. This all changed after the introduction of the CRISPR/Cas system.

The term CRISPR, or clustered regularly interspersed short palindromic repeats, was coined in the 1980s to describe short repetitive DNA sequences^{68,69}. It took decades to finally understand the biological meaning of CRISPR in the bacterial genome. Spacers are foreign DNA sequences of phage origin between the repetitive CRISPR segments, which are incorporated into the bacterial genome after bacteriophage challenge⁶⁹. Transcription of these regions into CRISPR RNA (crRNA) and their binding to CRISPR-associated DNA nucleases (Cas) allows for cleavage of complimentary foreign DNA⁷⁰. Thus, the CRISPR/Cas system was shown to have evolved as a rudimentary immune system in bacteria aimed against bacteriophage infection⁷¹.

The most widely used DNA nuclease in CRISPR-based genomic engineering is Cas9. The CRISPR/Cas9 system targets a discrete DNA sequence via a single guide RNA (sgRNA), consisting of trans-activating crRNA (tracrRNA) and crRNA⁷². The target DNA sequence is complementary to the crRNA and must be appropriately spaced from a protospacer adjacent motif (PAM)⁷³. After the target is recognized, DNA is cleaved by Cas9 and a DSB occurs three nucleotides upstream from the PAM. The CRISPR/Cas9 system is extremely versatile, as the DNA target can be altered by engineering different crRNAs⁷⁴. Furthermore, the introduction of DSB at a specific DNA sequence allows for unparalleled precision in genomic editing, as DSBs can be repaired by nonhomologous end joining (NHEJ) and homology-directed repair (HDR), depending on the aim of the study⁷⁵. NHEJ can be utilized for knock-out studies, as it repairs the two ends of a breakage site by randomly inserting or deleting nucleotides⁷⁶. In contrast, HDR employs DNA templates to repair DSBs in-frame and can even replace specific sequences⁷⁷. Both repair mechanisms underscore the almost unlimited possibilities of the CRISPR/Cas9 system to manipulate pro- and eukaryotic genomes quickly and precisely just by choosing crRNA complementary to the DNA sequence in question.

2.5 The role of interleukin-21 and its receptor in immunity

At the crossroad between innate and adaptive immunity, cytokines have been extensively studied to shed light on the complex interactions between immune cells regarding survival, persistence and differentiation⁷⁸. They are molecules secreted by immune cells, which bind to a specific receptor on the surface of target cells and induce a response via signal transduction. Interleukin-21 (IL-21) is a part of the common cytokine receptor gamma chain family and binds to a class I cytokine family receptor, the

interleukin-21 receptor (IL-21R)⁷⁹. The cytokines in this family (IL-7, IL-15, IL-2, IL-21) bind to heterodimeric receptors which all share the common cytokine receptor gamma chain (γ_c) as a subunit⁸⁰. Thus, the IL-21 receptor complex consists of the IL-21 binding chain (IL-21R alpha chain, or IL-21R) and the common γ_c . A loss-of-function mutation in the common γ_c gene on the X chromosome leads to X-linked severe combined immunodeficiency (X-SCID) in humans, which is characterized by an absence of T and NK cells, as well as by dysfunctional B cells⁸¹.

IL-21 was the last in this group of cytokines to be discovered⁷⁹. Production of the ligand takes place mostly in natural killer T (NKT) and CD4⁺ T cell populations⁷⁹, such as Th17 and T follicular helper (Tfh) cells, and binding to its receptor facilitates pleiotropic effects on the immune system⁸². Among the target cells with IL-21R on their surface are NK, B and CD8⁺ T cells⁸³. Expression of the receptor on the surface of T cells is low but can be induced via T cell receptor engagement or IL-21⁸⁴. Monogenic defects in the IL-21R gene demonstrated impaired functionality of B, T and NK cells⁸⁵, thus confirming the essential role of the interaction between IL-21 and its receptor for both innate and adaptive immunity. Additionally, IL-21 plays a prominent role in the development of the pro-inflammatory Th17 cells via an autocrine mechanism⁸⁶. Moreover, it can limit functionality of regulatory T cells⁸⁷ and plays an important role in B cell development⁸⁸ and IgG antibody production⁸⁹.

Of interest in the setting of cancer and chronic viral infection are the various effects of IL-21 on CD8⁺ cytotoxic lymphocytes, as T cell exhaustion is a major impediment to disease clearance and overcoming it a major challenge⁹⁰. On its own, interleukin-21 seems to act in a context-dependent and distinct manner on the development of CD8⁺ T cells, as there have been conflicting reports on the fate of cytotoxic lymphocytes after their exposure to IL-21. Even though no apparent benefit to T effector function was mediated by IL-21 in vitro, adoptive transfer of IL-21-primed cells led to a more robust immune response in a preclinical murine melanoma model⁹¹. In a lymphoma model with adoptive transfer of anti-CD19 CAR T cells overexpressing the common gamma chain cytokines, overexpression of IL-7 and IL-21 led to increased tumor eradication and long-term survival when compared to anti-CD19 CAR T cells only or with the additional overexpression of IL-2 and IL-15⁹².

Several studies have focused on the induction of a memory phenotype via IL-21. A report on the formation of a distinct memory phenotype demonstrated that reconstitution of IL-21 in an IL-21 knock-out murine model of chronic viral infection re-introduced a less terminally differentiated but functionally active population of CD8⁺ T cells⁹³. Overexpression of the ligand in transgenic mice also drove the differentiation of naïve CD8⁺ cells to a massively increased niche of CD62L^{high}CD44^{high} memory cells in vivo, which showed a proliferative advantage after TCR engagement⁹⁴. Moreover, IL-21 signaling was indispensable for antigen-dependent CD8⁺ T proliferation in models of chronic viral infection and cancer^{95,96,97}. Synergy with either of two other common gamma chain cytokines, IL-7 and IL-15, increased proliferative capacity of CD8⁺ cells and promoted the development of a CD62L^{high}CD44^{high} memory phenotype⁹⁸. In a human clinical trial with antigen-specific cytotoxic lymphocytes, expansion with IL-21 ex vivo induced a long-lasting memory phenotype after adoptive cell therapy⁹⁹. Consistent in these reports is the key role of the IL-21/IL-21R interaction for sustained activity of a non-exhausted memory CD8⁺ population, which denotes the prospective advantages of interleukin 21 and its receptor in cancer immunotherapy.

Of the different signal transduction pathways mediating the effects of IL-21 on innate and adaptive immunity, the JAK-STAT pathway is documented best. The common γ chain within the IL-21 receptor complex enables phosphorylation of both Janus-kinase 1 (JAK1) and JAK3. They in turn activate the transcription factors Signal Transducer and Activator of Transcription 1 (STAT1) and STAT3¹⁰⁰. Even though IL-21 can bind to the IL-21R alpha chain on its own, the common γ_c is required for effective signal transduction¹⁰¹. STAT3 has been implicated in fostering T cell proliferation and differentiation of naïve into T_{CM} cells¹⁰². Binding of IL-21 to its receptor complex induces proliferation in a STAT3-dependent manner¹⁰³. Moreover, the transcription factor has been shown to induce CD8⁺ T cell memory formation,

especially in response to IL-21 in conjunction with IL-10 in a murine model of acute and chronic infection¹⁰⁴.

Despite the described beneficial effects of IL-21 on the immune system, the cytokine has also been implicated in a variety of autoimmune and inflammatory diseases owing to its pleiotropic effects^{82,105}. In a preclinical model of systemic lupus erythematosus (SLE), IL-21 was shown to drive expansion of autoreactive B cells and serum levels of IL-21 were predictive of disease severity¹⁰⁶. Moreover, blocking the IL-21/IL-21R pathway led to clinical improvement in the animals¹⁰⁷. High levels of IL-21 can also lead to the development of rheumatoid arthritis (RA), as the cytokine benefits the expansion of IL-17 producing Th17 pro-inflammatory cells¹⁰⁸. Administration of the IL-6R antagonist tocilizumab in RA patients not only mitigated disease severity, but also reduced IL-21 production¹⁰⁹. Furthermore, IL-21 can act as a growth factor in multiple myeloma¹¹⁰ and Hodgkin's lymphoma¹¹¹. This makes clinical use of the interaction between interleukin-21 and its receptor a challenge¹¹², as response to the cytokine seems to be context-dependent. Nevertheless, IL-21 can be used in cancer immunotherapy to induce a robust immune response and foster the development of a less differentiated memory phenotype, which could improve in vivo persistence of adoptively transferred T cells.

3 Hypothesis and aims of the study

Acute lymphoblastic leukemia (ALL) is the most common pediatric malignancy and a leading cause of non-violent death in childhood². The advent of antibody- and T cell-based immunotherapy has revolutionized the treatment of relapsed and/or refractory B-cell precursor (BCP) ALL. Adoptive cell therapy with anti-CD19 chimeric antigen receptor (CAR) T cells allows for MHC-independent targeting and destruction of CD19⁺ leukemic blasts of B-cell origin²⁴. Despite high initial remission rates after immunotherapy, about 30% to 50% of pediatric patients relapse within 2 years³⁵. One of the main mechanisms responsible for treatment failure is the lack of long-time persistence of the infused CAR T cells, a common cause of which is T cell exhaustion⁴⁷.

Research from our group has shown that T cells in bone marrow samples of pediatric patients with leukemia exhibit a more differentiated phenotype and express co-inhibitory markers¹¹³, which are hallmarks of T cell exhaustion. Moreover, bone marrow CD8⁺ T cells have a reduced expression of the interleukin-21 receptor (IL-21R) in comparison to healthy donors (unpublished data). The respective ligand, interleukin-21 (IL-21) belongs to the common cytokine receptor gamma chain family and is produced by a variety of immune cells, such as CD4⁺ T cells⁷⁹. The ligand-receptor interaction has been implicated in the development of a distinct and functional memory phenotype in CD8⁺ T cells⁹⁵, which can then persist *in vivo* and eradicate malignant cells. With this in mind, we hypothesized that expression of IL-21R is of vital importance for the long-term functionality and proliferation of cytotoxic lymphocytes and may improve long-term persistence of adoptive cell therapy.

The aim of this project is to investigate the effect of IL-21R alpha chain expression on CD8⁺ T cell functionality *in vitro* via genomic CRISPR/Cas9 knock-out and retroviral overexpression of the receptor. A special focus lies on the interaction between IL-21 and its receptor and how altered expression of IL-21R may impact signal transduction via STAT3. Furthermore, the antileukemic potency of first- and second-generation anti-CD19 CAR T cells with IL-21R genomic knock-out and overexpression is to be characterized in a co-culture setting. The interaction between IL-21-producing CD4⁺ CAR T cells and IL-21R-expressing CD8⁺ T cells will be mimicked in analogy to physiology. The long-term goal of the project is to improve long-term persistence of CAR T cells in pediatric patients with advanced BCP-ALL.

4 Materials

4.1 Equipment and software

| Equipment/software | Name, Manufacturer |
|---------------------------|---|
| Autoclaves | VX-55, VX-150, DX-65, Systec, Linden, Germany |
| Cell counting auxiliaries | Cell Counting Chamber Neubauer, Chamber Depth 0.1 mm, Paul Marienfeld, Lauda-Königshofen, Germany |
| Centrifuges | Multifuge X3R and Mini Centrifuge Fresco 17, Heraeus, Hanau, Germany |
| Cleaner Box | UVC/T-M-AR, DNA-/RNA UV-cleaner box, Biosan, Riga, Latvia |
| Cooling units | Cooler (4 °C) Comfort No Frost, Liebherr, Biberach an der Riß, Germany |
| | Cryogenic Freezer MVE 600 Series, Chart, Luxemburg |
| | Freezer (-20 °C) Premium No Frost, Liebherr, Biberach an der Riß, Germany |
| | Freezer (-86 °C) HERAfreeze HFC Series, Heraeus, Hanau, Germany |
| | Freezer (-86 °C) HERAfreeze HFU T Series, Heraeus, Hanau, Germany |
| | Thermo Scientific Cryo 200 liquid nitrogen dewar, Thermo Fisher Scientific, Waltham, Massachusetts, USA |
| Flow cytometer | BD LSRFortessa Cell Analyzer, BD, Franklin Lakes, New Jersey, USA |
| | MACSQuant Analyzer 10, Miltenyi Biotec, Bergisch Gladbach, Germany |
| Freezing container | Nalgene Mr. Frosty, Thermo Fisher Scientific, Waltham, Massachusetts, USA |
| Gel Imager | Gel iX20 Imager, Intas Science Imaging, Göttingen, Germany |
| Heat block | Eppendorf ThermoMixer comfort, Eppendorf, Hamburg, Germany |
| Incubator | HERAcell 240, 150i CO ₂ Incubator, Thermo Fisher, Waltham, Massachusetts, USA |
| Laminar flow hood | HERAsafe, Thermo Fisher, Waltham, Massachusetts, USA |
| | Uniflow KR130, Uniequip, Planegg, Germany |
| Magnetic cell separator | EasyEight EasySep Magnet, Stemcell Technologies, Vancouver, British Columbia, Canada |
| | EasySep Magnet, Stemcell Technologies, Vancouver, British Columbia, Canada |
| | MACS MultiStand, Miltenyi Biotec, Bergisch Gladbach, Germany |
| | MidiMACS Separator, Miltenyi Biotec, Bergisch Gladbach, Germany |
| | QuadroMACS Separator, Miltenyi Biotec, Bergisch Gladbach, Germany |

| | |
|-----------------------|--|
| Microscope | Axiovert 25, Carls Zeiss Microscopy, Jena, Germany |
| | Leica DM IL, Leica Microsysteme, Wetzlar, Germany |
| Spectrophotometer | Nanodrop ND-1000 spectrophotometer, Nanodrop Technologies, Wilmington, Delaware, USA |
| Pipettes (electrical) | Easypet 3, Eppendorf, Hamburg, Germany |
| Pipettes (manual) | 2.5 µl, 20 µl, 200 µl, 1000 µl Eppendorf Research, Eppendorf, Hamburg, Germany |
| Power Supply | Biorad Power Pac 200, Biorad, Hercules, California, USA |
| Scale | R 200 D, Sartorius AG, Göttingen, Germany |
| Software | FlowJo 10.0.7r2, Ashland, Oregon, USA |
| | Gel iX20 Imager Windows Version, Intas Science Imaging, Göttingen, Germany |
| | GraphPad PRISM 8.4, La Jolla, California, USA |
| | Microsoft Office 2016, Redmond, Washington, USA |
| | LEGENDplex Software 8, San Diego, California, United States |
| | Biorender, Toronto, Ontario, Canada |
| Thermocycler | peqSTAR 96 Universal Gradient, Isogen, Utrecht, Netherlands |
| Transfection device | Amaxa Nucleofector II, Lonza Bioscience, Morrisville, North Carolina, United States |
| Water bath | LAUDA Aqualine AL 18, LAUDA-Brinkmann, Delran, New Jersey, USA |

4.2 Solutions, media and sera for cell culture

| Solution/ Medium/ Serum | Order number | Manufacturer |
|--|--------------|--|
| 100 bp DNA Ladder Ready to Load | 01-11-00050 | Solis BioDyne, Tartu, Estonia |
| Agarose | 50004 | Seakem Le Agarose, DMA, Rockland, Maine, USA |
| Albiomin 5 % infusion solution human albumin (HSA) | 623 050 | Biotest, Dreieich, Germany |
| Alt-R Cas9 Electroporation Enhancer | 1075915 | Integrated DNA Technologies, Coralville, Iowa, USA |
| Alt-R CRISPR-Cas9 Negative Control crRNA #1 | 1072544 | Integrated DNA Technologies, Coralville, Iowa, USA |

| | | |
|--|-----------------------------|--|
| Alt-R CRISPR-Cas9 IL-21R crRNA | - | Integrated DNA Technologies, Coralville, Iowa, USA |
| Alt-R CRISPR-Cas9 tracrRNA | 1072533 | Integrated DNA Technologies, Coralville, Iowa, USA |
| Alt-R S.p. Cas9 Nuclease 3NLS | 1081058 | Integrated DNA Technologies, Coralville, Iowa, USA |
| Biocoll separating solution | L6115 | Biochrom, Berlin, Germany |
| BLINCYTO® (Blinatumomab) | - | Amgen, Thousand Oaks, California, USA |
| Brefeldin A | 5936 | Sigma-Aldrich, Steinheim, Germany |
| CellTrace Violet Proliferation Kit | C34557 | Invitrogen, Thermo Fisher Scientific, Life Technologies Cooperation, Eugene, Oregon, USA |
| Compensation beads | 552843 | BD Biosciences, San Diego, California, USA |
| | 130-097-900, 130-104-693 | MACS Comp Bead Kit anti mouse/anti REA, Miltenyi Biotec, Bergisch Gladbach, Germany |
| Dimethylsulfoxid | D5879 | Honeywell, Seelze, Germany |
| | 4720.4 | Carl Roth, Karlsruhe, Germany |
| DMEM | FG1445 | Biochrom, Berlin, Germany |
| DNA Clean & Concentrator -5 | D4014 | Zymo Research, Irvine, California, USA |
| DNeasy Blood & Tissue Kit | 69504 | QIAGEN, Hilden, Germany |
| DNA Gel Loading Dye (6X) | R0611 | Thermo Fisher Scientific, Waltham, Massachusetts, USA |
| Dulbecco's phosphate buffered saline (PBS) | 14190-250 | Gibco, Life Technologies, Darmstadt, Germany |
| EasySep Human CD4+ T Cell Isolation Kit | 17952 | Stemcell Technologies, Vancouver, British Columbia, Canada |
| EasySep Human CD8+ T Cell Isolation Kit | 17953 | Stemcell Technologies, Vancouver, British Columbia, Canada |
| EasySep Human T Cell Enrichment Kit | 19051 | Stemcell Technologies, Vancouver, British Columbia, Canada |

| | | |
|---|---|--|
| Ethidium bromide | 2218.1 | Roth, Karlsruhe, Germany |
| Fetal Bovine Serum | F0804 | Sigma-Aldrich CHEMIE, Steinheim, Germany |
| Fix & Perm Cell Permeabilization Kit | GAS004 | Life Technologies, Frederick, Maryland, USA |
| Heparin sodium 25,000 I.U./5ml | | Ratiopharm, Ulm, Germany |
| HEPES-Buffer (1M) | L 1613 | Biochrom, Berlin, Germany |
| Human AB serum | | Human AB serum was kindly provided by Prof. R. Lotfi, University Hospital Ulm, Institute for Transfusion Medicine and German Red Cross Blood Services Baden-Württemberg—Hessen, Institute for Clinical Transfusion Medicine and Immunogenetics, both from Ulm, Germany |
| IL-2, IL-7, IL-15, IL-21 (human, premium grade) | 130-097-745 130-95-363 130-095-764 130-095-784 | Miltenyi Biotec, Bergisch Gladbach, Germany |
| L-Glutamine 200 mM | K 0283 | Biochrom, Berlin, Germany |
| Methanol | 34860 | Sigma-Aldrich CHEMIE, Steinheim, Germany |
| MicroBeads (CD4, CD8, CD56) | 130-045-101, 130-045-201, 130-050-401 | Miltenyi Biotec, Bergisch Gladbach, Germany |
| Non-Essential Amino Acids | 11140-035 | Gibco, Life Technologies, Darmstadt, Germany |
| Penicillin/Streptomycin | 15140-122 | Gibco, Life Technologies, Darmstadt, Germany |
| Protamine sulfate | P3369 | Sigma-Aldrich CHEMIE, Steinheim, Germany |
| Q5 High-Fidelity DNA Polymerase | M0491S | New England BioLabs, Frankfurt am Main, Germany |
| RetroNectin Reagent | T100A | Takara, Saint-Germain-en-Laye, France |
| Sodium pyruvate | 11360-039 | Gibco, Life Technologies, Darmstadt, Germany |

| | | |
|----------------------------------|-------------|---|
| Staphylococcal enterotoxin B | 4881 | Sigma-Aldrich CHEMIE, Steinheim, Germany |
| TAE Buffer | A4686 | TAE buffer (50x), Applichem, Darmstadt, Germany |
| TexMACS GMP Medium | 170-076-307 | Miltenyi Biotec, Bergisch Gladbach, Germany |
| T cell TransAct, human | 130-111-160 | Miltenyi Biotec, Bergisch Gladbach, Germany |
| TransIT-293 Transfection Reagent | Mirumir2704 | Mirus Bio LLC, Madison, Wisconsin, USA |
| Trypan blue | 15250-061 | Gibco, Life Technologies, Darmstadt, Germany |
| Tween 20 | 9127.1 | Carl Roth, Karlsruhe, Germany |
| VLE RPMI 1640 Medium | F1415 | Biochrom, Berlin, Germany |

4.3 Consumables

| Consumable | Order number | Name, Manufacturer |
|---|---------------------------------------|---|
| Cannula | 851.638.235 | Safety-Multifly-Needle, Sarstedt, Nümbrecht, Germany |
| Cell culture dish | 664 160 | Cellstar Greiner Labortechnik, Kremsmünster, Austria |
| Cell culture flasks with ventilation caps | 83.3910.002, 83.3911.002, 83.3912.002 | T25, T75, T175, Sarstedt, Nümbrecht, Germany |
| Cell culture multiwell plates, 6 well | 657160 | Cellstar Greiner Labortechnik, Kremsmünster, Austria |
| Cell culture multiwell plates, 24 well | 3524 | Costar Corning Incorporated, Corning, New York, USA |
| Cell culture multiwell plates, 48 well | 3548 | Costar Corning Incorporated, Corning, New York, USA |
| Cell culture multiwell plates, 96 well | 163320 | Nunclon Delta Surface, Thermo Fisher Scientific, Waltham, Massachusetts, USA |
| Compresses | 18507 | Gauze Compresses 10 x 10 cm, Nobamed Paul Danz, Wetter, Germany |
| Cover slips | C10143263NR1 | Menzel-Gläser 20 x 20 mm, Gerhard Menzel, Braunschweig, Germany |
| FACS buffers and solutions | 130-092-747, 130-092-748, 130-092-749 | Running Buffer, Storage Solution, Washing Solution, Miltenyi Biotec, Bergisch Gladbach, Germany |
| | 340345, 340346, 342003 | FACS clean/rinse/flow, Becton, Dickinson and Company (BD), Franklin Lakes, New Jersey, USA |
| Freezing tubes | 72.379 | Cryo Pure Gefäß 1.8 ml, Sarstedt, Nümbrecht, Germany |
| Magnetic separation columns | 130-042-401, 130-042-901 | LS Columns, LD Columns, Miltenyi Biotec, Bergisch Gladbach, Germany |
| Pasteur pipettes | 747720 | Glass Pasteur Pipettes 230 mm, Brand, Wertheim, Germany |

| | | |
|--|--|---|
| Pipette tips | 70.1130.217, 70.760.213, 70.760.212, 70.762.211 | 0.1-2.5 µl, 10 µl, 20 µl, 100 µl, 2-200 µl, 1000 µl, Sarstedt, Nümbrecht, Germany |
| Reaction vessels | 62.554.502 | 15 ml, Sarstedt, Nümbrecht, Germany |
| | 4440100 | 50 ml, Orange Scientific, Braine-l'Alleud, Belgium |
| | 72.690.550 | 1.5 ml, Sarstedt, Nümbrecht, Germany |
| Round bottom tubes with cell strainer snap cap | 352235 | 5 ml Polystyrene Round Bottom Tube, Falcon, Corning Science, Taunusipilas, Mexico |
| Safety gloves | 9209817 | Vaso Nitril Blue, B. Braun Melsungen, Melsungen, Germany |
| Serological pipettes | 86.1685.001, 86.1253.001, 86.1254.001 | 5 ml, 10 ml, 25ml Serological Pipette, Sarstedt, Nümbrecht, Germany |
| Skin disinfectant | 975512, 306650 | Sterilium Classic Pure, Sterilium Virugard, Hartmann, Heidenheim, Germany |
| Sterile filters | SE2M229104, SE2M230104 | 0.2µm, 0.45µm, Carl Roth, Karlsruhe, Germany |
| Surface disinfectant | CLN-1006.5000 | Ethanol 80 % MEK/Bitrex, CLN, Niederhummel, Germany |
| Syringe | 309658 | 3ml, Becton, Dickinson and Company (BD), Franklin Lakes, New Jersey, USA |
| | 4606728V | 10ml, B. Braun Melsungen, Melsungen, Germany |
| | 4617509F | 50ml, Omnifix, B. Braun Melsungen, Melsungen, Germany |

4.4 Antibodies

| Fluorochrome | Antigen | Clone | Order number | Manufacturer |
|---------------|---------------|-----------------|--------------|---|
| 7AAD | Viability dye | | 420404 | Biologend, San Diego, California, USA |
| APC-eFluor780 | Viability dye | | 65-2860-40 | ThermoFisher Scientific, Waltham, Massachusetts, U.S. |
| AF647 | Anti-STAT3 | Clone 4/P-STAT3 | 557815 | Becton, Dickinson and Company (BD), Franklin Lakes, New Jersey, USA |
| APC | CCR4 | L291H4 | 359407 | Biologend, San Diego, California, USA |
| APC | CD107a | H4A3 | 328619 | Biologend, San Diego, California, USA |
| APC | CD8 | SK1 | 556414 | Becton, Dickinson and Company (BD), Franklin Lakes, New Jersey, USA |
| APC | CD14 | TÜK4 | 130-115-559 | Miltenyi Biotec, Bergisch Gladbach, Germany |
| APC | CD95 | DX2 | 130-092-417 | Miltenyi Biotec, Bergisch Gladbach, Germany |

| | | | | |
|--------------|---------------|----------|-------------|---|
| APC | CD137 | REA765 | 130-110-764 | Miltenyi Biotec, Bergisch Gladbach, Germany |
| APC | IL-2 | 5344.111 | 341116 | Becton, Dickinson and Company (BD), Franklin Lakes, New Jersey, USA |
| APC | PD-1 | A17188B | 621609 | Biologend, San Diego, California, USA |
| APC-Vio770 | CD3 | REA613 | 130-113-136 | Miltenyi Biotec, Bergisch Gladbach, Germany |
| APC-Vio770 | CD8 | REA734 | 130-110-681 | Miltenyi Biotec, Bergisch Gladbach, Germany |
| BB515 | CCR6 | 11A9 | 564479 | Becton, Dickinson and Company (BD), Franklin Lakes, New Jersey, USA |
| BB515 | TIM-3 | 7D3 | 565568 | Becton, Dickinson and Company (BD), Franklin Lakes, New Jersey, USA |
| BV421 | CD56 | HCD56 | 318328 | Biologend, San Diego, California, USA |
| BV421 | IL-21R | 17A12 | 563728 | Biologend, San Diego, California, USA |
| BV421 | TIM-3 | F38-2E2 | 345008 | Biologend, San Diego, California, USA |
| BV650 | CD62L | DREG-56 | 563808 | Becton, Dickinson and Company (BD), Franklin Lakes, New Jersey, USA |
| BV785 | CD127 | A7R34 | 135037 | Biologend, San Diego, California, USA |
| BUV395 | CD45RO | UCHL1 | 564292 | Becton, Dickinson and Company (BD), Franklin Lakes, New Jersey, USA |
| BUV496 | CD4 | SK3 | CD4 | Becton, Dickinson and Company (BD), Franklin Lakes, New Jersey, USA |
| BUV737 | CD3 | SK7 | CD3 | Becton, Dickinson and Company (BD), Franklin Lakes, New Jersey, USA |
| FITC | Anti-c-myc | 14D3 | 130-116-485 | Miltenyi Biotec, Bergisch Gladbach, Germany |
| FITC | CD62L | MEL-14 | 104405 | Biologend, San Diego, California, USA |
| Pacific Blue | TNF- α | MAb11 | 502920 | Biologend, San Diego, California, USA |
| PE | CD19 | LT19 | 130-113-169 | Miltenyi Biotec, Bergisch Gladbach, Germany |
| PE | CD132 | AG184 | 555900 | Becton, Dickinson and Company (BD), Franklin Lakes, New Jersey, USA |
| PE | CD25 | REA570 | 130-113-286 | Miltenyi Biotec, Bergisch Gladbach, Germany |
| PE | CD45RO | UCHL1 | 304206 | Biologend, San Diego, California, USA |

| | | | | |
|-------------|---------------|----------|-------------|---|
| PE | CD56 | REA196 | 130-113-312 | Miltenyi Biotec, Bergisch Gladbach, Germany |
| PE | IFN- γ | 25723.11 | 340452 | Becton, Dickinson and Company (BD), Franklin Lakes, New Jersey, USA |
| PE | IL-21R | 4A9 | 131905 | Biologend, San Diego, California, USA |
| PE-CF594 | CXCR3 | 1C6 | 562451 | Becton, Dickinson and Company (BD), Franklin Lakes, New Jersey, USA |
| PE-Cy7 | CD3 | SK7 | 344815 | Biologend, San Diego, California, USA |
| PE-Cy7 | IL-21R | 17A12 | 359513 | Biologend, San Diego, California, USA |
| PE-Vio770 | CD3 | REA613 | 130-113-140 | Miltenyi Biotec, Bergisch Gladbach, Germany |
| PE-Vio770 | CD19 | REA675 | 130-113-647 | Miltenyi Biotec, Bergisch Gladbach, Germany |
| PE-Vio770 | CD45RO | REA611 | 130-113-560 | Miltenyi Biotec, Bergisch Gladbach, Germany |
| PE-Vio770 | CD69 | REA824 | 130-112-615 | Miltenyi Biotec, Bergisch Gladbach, Germany |
| PE-Vio770 | CD95 | REA738 | 130-113-004 | Miltenyi Biotec, Bergisch Gladbach, Germany |
| PerCP-Cy5.5 | CD8 | SK1 | 344709 | Biologend, San Diego, California, USA |
| VioBlue | CD62L | 145/15 | 130-098-699 | Miltenyi Biotec, Bergisch Gladbach, Germany |
| VioGreen | CD4 | REA623 | 130-113-230 | Miltenyi Biotec, Bergisch Gladbach, Germany |

5 Methods

Parts from sections 5.1 to 5.2 were adapted from the dissertation of Antonia Apfelbeck: Generation and Characterization of CD19 CAR T cells with PD-1_CD28 fusion receptor as they were performed in the course of this project (Ludwig-Maximilian-University, Munich).

5.1 Genomic modification of primary T cells

5.1.1 PBMCs and T cell isolation. Primary T cell activation

Experiments were performed with cells isolated from healthy donors. Peripheral blood mononuclear cells (PBMCs) were harvested via density gradient centrifugation, as described below. 50-100 ml blood was collected in EDTA tubes and diluted with the same amount of cold PBS within 2 hours of collection. The blood was then carefully layered on Biocoll and centrifuged at 800 g for 30 minutes at 20 °C without brake. After removal of part of the plasma, PBMCs were aspirated and washed twice with cold PBS.

For experiments with bulk T cells, the EasySep Human T Cell Enrichment Kit was used on PBMCs according to the manufacturer's instructions. For isolation of separate populations of either CD4⁺ or CD8⁺ T⁺ cells, EasySep Human CD4⁺ T Cell Isolation Kit and EasySep Human CD8⁺ T Cell Isolation Kit were utilized, respectively. All populations were then cultured at a density of 1 million cells per ml in TexMACS research grade medium, supplemented with 2.5% human AB serum. Bulk and CD4⁺ T cells also received 12.5 ng/ml IL-7 and 12.5 ng/ml IL-15, whereas CD8⁺ T cells were expanded with 30 U/ml IL-2 and 12.5 ng/ml IL-15. For activation, T Cell TransAct (anti-CD3 and anti-CD28) was added and primary T cells were cultured for two days.

5.1.2 Generation of retroviral vector particles

A packaging cell line (293Vec-RD114) producing retroviral vectors was generated for all constructs according to published literature¹¹⁴. Viral supernatants were collected 24 hours and 48 hours after producer cells reached about 90% confluency. After removal of debris via centrifugation at 400 g for 4 minutes at 20 °C, supernatants were filtered through a 0.45 µm filter and stored at -80 °C. Construct sequences are shown in the supplements.

5.1.3 Retroviral T cell transduction

Retroviral transduction was performed two days after activation of primary T cells. 24-well plates were coated with 2.5 µg RetroNectin reagent per well either overnight at 4 °C or for 2 hours at 37 °C. Wells were blocked with 2% Albumin Fraction V in PBS for 30 minutes at room temperature and afterwards washed with a 1:40 dilution of HEPES 1M in PBS. Both solutions were sterile filtrated beforehand through a 0.20 µm filter. 1 ml of either thawed virus supernatant or PBS for untransduced controls was centrifuged on coated wells at 3000 g for 90 minutes at 32 °C. Supernatants were then aspirated and 1 million activated T cells in TexMACS medium supplemented with 2.5% human AB serum, 12.5 ng/ml IL-7 and IL-15, and 2 µg/ml protamine sulfate were added per well. After centrifugation at 400 g for 10 minutes at 32 °C, T cells were expanded for either 14 days (IL-21R alpha chain and common gamma chain overexpressing T cells) or 10 days (CAR T cells). To remove the virus, transduced T cells were washed either on day 2 after transduction or on day 3 in case CRISPR/Cas9 knock-out was performed on CAR T cells on the same day. Cells were counted every two to three days under light microscope after diluting them 1:2 with trypan blue to determine their expansion rate. After counting, TexMACS + 2.5% human AB serum + 12.5 ng/ml of IL-7 and IL-15 were added to keep the T cell concentration at 1 million cells per ml.

5.1.4 IL-21 Receptor knock-out with CRISPR/Cas9

CRISPR/Cas9 genomic knock-out of the IL-21R gene was performed via Integrated DNA Technologies two-part guide RNA (gRNA) system according to the manufacturer's protocol. IL-21R gRNA had the following sequence: ACGACATTTTCAGTGTCAA. gRNA was generated by heating the 1:1 mixture of CRISPR RNA (crRNA) and transactivating crRNA (tracrRNA) at 95 °C for 5 minutes. Cas9 endonuclease and Cas9 Electroporation Enhancer were added, and a functional ribonucleoprotein complex (RNP) was formed after incubation for 15 minutes at room temperature. Genome editing was performed on activated primary T cells or retrovirally transduced CAR T cells. After resuspension in buffer 1 M¹¹⁵, the RNP complex was added to each sample. For electroporation, Amaxa Nucleofector II Device was used according to the manufacturer's instructions. Negative control gRNA from the manufacturer was used to perform the same procedure on (CAR) T cells serving as control to the IL-21R knock-out. After electroporation, fresh medium was immediately added, and cells expanded according to the protocol in 5.1.3.

The CRISPR/Cas9 knock-out was verified via PCR and Sanger sequencing. For this purpose, genomic DNA was isolated from both knock-out and control cells with the DNeasy Blood and Tissue Kit and amplified via the Q5 High-Fidelity DNA Polymerase reaction according to the following PCR reaction cycle: denaturation at 98 °C for 30 seconds, 35 cycles at 98 °C for 10 seconds, 65 °C for 20 seconds and 72 °C for 60 seconds, 72 °C for 2 minutes. The electrophoresis 1.5% agarose gel was loaded with the PCR products after mixing them with DNA Gel Loading Dye (6X). Bands were visualized with the iX20 Imager, excised and sent for Sanger sequencing (Genewiz) after extraction via Gel DNA Recovery kit. Primer sequences are shown in the supplements.

5.1.5 Characterization of the T cell product after genetic modification

On the last day of expansion, genetically modified T cells were characterized via flow cytometry based on their phenotype, cellular composition and surface expression of IL-21R, CD132 and c-myc as marker for CAR molecule expression. Staining for CD3, CD4, CD8, 7-AAD, c-myc, IL-21R, CD62L, CD45RO, CD95, CD19, CD56 and CD14 was performed. During analysis, the phenotype of the T cell product was defined as follows: naïve (T_N) CD62L⁺CD45RO⁻CD95⁻, stem cell-like memory (T_{SCM}) CD62L⁺CD45RO⁻CD95⁺, central memory (T_{CM}) CD62L⁺CD45RO⁺CD95⁺, effector memory (T_{EM}) CD62L⁻CD45RO⁺CD95⁺ and effector T cells (T_{EFF}) CD62L⁻CD45RO⁻CD95⁺. Cellular composition was characterized as follows: Monocytes CD14⁺, Natural killer (NK) cells CD14⁻CD3⁻CD56⁺, NK T cells CD14⁻CD3⁺CD56⁺, bulk T cells CD14⁻CD3⁺CD56⁻, CD4⁺ T cells CD3⁺CD4⁺, CD8⁺ T cells CD3⁺CD8⁺, CD4⁺CD8⁺ T cells CD3⁺CD4⁺CD8⁺, CD4⁻CD8⁻ T cells CD3⁺CD4⁻CD8⁻, B cells CD14⁻CD3⁻CD56⁻CD19⁺.

5.2 Functionality assays with genetically modified T cells

For functionality assays, fully expanded T cells were frozen, thawed and left overnight to rest at 37 °C in TexMACS research grade medium supplemented with 2.5% human AB serum, 12.5 ng/ml IL-7 and IL-15. For CAR T cells, the lowest CAR transduction rate within *all* donors was determined and used as baseline to adjust transduction rates of all constructs by adding untransduced control cells. The number of effector cells reflects the number of bulk T cells used in the assays. The same holds true for experiments with non-CAR T cells (e.g., IL-21R transduced and IL-21R knock-out T cells). The target cell line used in all experiments was Nalm6, a CD19⁺ BCP-ALL cell line. Prior to plating, T cells and targets were washed and resuspended in TexMACS GMP medium. T cells cultured without targets and T cells stimulated with 2 μl TransAct served as negative and positive controls, respectively. T cells isolated from at least two healthy donors were used for all experiments and any condition was measured in technical duplicates, unless otherwise specified.

5.2.1 IL-21R surface expression induction

Thawed genetically modified T cells were activated with 2 µl TransAct, and IL-21R surface expression was measured via flow cytometry at 0h, 24h, 48h and 72h after staining for CD3, CD4, CD8, 7-AAD and IL-21R.

5.2.2 Co-culture with blinatumomab

The bispecific T cell engager (BiTE) blinatumomab was used in all co-culture assays with non-CAR T cells at a concentration of 1 ng/ml with the aim of establishing contact between CD3⁺ T cells and CD19⁺ tumor cell lines. Negative co-culture controls without blinatumomab were also included to exclude unspecific activation of T cells.

5.2.3 Co-culture with interleukin-21

To examine the effect of this common gamma chain cytokine, all functionality assays included a condition where IL-21 was added at a concentration of 100 ng/ml to the co-culture of T cells and Nalm6 cells.

5.2.4 Cytotoxicity assay

After resting, the T cell product was depleted of NK (T) cells by negative selection using magnetic separation of CD56-labeled cells according to the supplier's information. In experiments with CAR T cells, post-depletion CAR transduction rate was re-evaluated in a FITC c-myc single stain and if necessary, adjusted to the lowest transduction rate within all donors as described. Nalm6 target cells were labeled with CellTrace Violet (CTV) Cell Proliferation Kit and co-cultured with T cells at different effector-to-target ratios. Target-cell killing was then evaluated via flow cytometry after 24 hours for CAR T cells or 48 hours for non-CAR T cells. The killing rate was calculated by setting the absolute cell count of CTV-positive cells into relation to the count of CTV-positive targets only. The following formula was used:

$$\% \text{ Killing} = 100 - \left(100 \times \frac{\text{Targets only}}{\text{Targets in co - culture}} \right)$$

5.2.5 CD107a degranulation assay

A degranulation assay was conducted in some instances to measure CD107a expression on CD8⁺ T cells. Immediately after co-culture of T cells with the same amount of CD19⁺ target cells, 1 µl of CD107a antibody was added to each condition. After 3 hours, cells were washed and stained for CD107a, CD3, CD4, CD8, 7-AAD and IL-21R. CD107a degranulation was then measured via flow cytometry.

5.2.6 Intracellular cytokine staining (ICS)

After resting, T cells were co-cultured with Nalm6 cells at a 1:1 ratio for 24 hours. 10 µg/ml Brefeldin A was then added for two hours to block protein transport inside the cell. Cells were washed with cold PBS and stained extracellularly for CD3, CD4, CD8, 7-AAD, IL-21R and c-myc to distinguish between T cell populations. Intracellular staining for IL-2, IFN-γ and TNF-α was performed with the Fix & Perm Cell Fixation & Permeabilization Kit according to the supplier's information.

5.2.7 Proliferation assay

To examine cell proliferation, T cells were labeled with the CellTrace Violet (CTV) Cell Proliferation Kit for 5 minutes and then the reaction was stopped by adding human AB serum and TexMACS GMP medium. After counting, cells were washed twice and seeded for 48 or 72 hours in a co-culture setting with Nalm6 target cells. Prior to flow cytometry, cells were stained for CD3, CD4, CD8 and 7-AAD.

5.2.8 Phenotype, activation and exhaustion markers

3h, 6h or 24 hours after co-culture of T cells with CD19⁺ target cells at a 1:1 ratio, these were stained for the activation markers CD69 and CD25, the exhaustion markers PD-1 and TIM-3, the maturity markers CD62L, CD45RO, CD95, CXCR3, CCR6 and CCR4, as well as CD3, CD4, CD8, 7-AAD, IL-21R and c-myc.

The CAR T helper phenotype was characterized via the markers CXCR3, CCR6 and CCR4. Naïve CD4⁺ were defined as CD45RO⁻CD95⁻, with Th0 cells from this population being negative for all three markers. In contrast, mature CD4⁺ T cells were positive for CD45RO and CD95 and could be differentiated into these populations: Th1Th17 CCR4⁻CCR6⁺CXCR3⁺, CCR6⁺ only CCR4⁻CCR6⁺CXCR3⁻, Th17 CCR4⁺CCR6⁺CXCR3⁻, CXCR3⁺Th17 CCR4⁺CCR6⁺CXCR3⁺, Th2 CCR4⁺CCR6⁻CXCR3⁻, CXCR3⁺ Th2 CCR4⁺CCR6⁻CXCR3⁺ and Th1 CCR4⁻CCR6⁻ CXCR3⁺ cells.

5.2.9 Measurement of STAT3 phosphorylation

Frozen T cells were thawed, washed and resuspended in RPMI medium. IL-21 was added to all conditions at a concentration of 100 ng/ml and after 5 min on ice, the samples were transferred to a shaker at 37 °C for 15 min. No interleukin was added in the negative control samples. For positive control, 1 mM Na₃VO₄ as a general phosphatase inhibitor¹¹⁶ was freshly prepared and added to samples for 5 min. Medium A from the Fix & Perm Cell Fixation & Permeabilization Kit was used to fix the cells, followed by ice-cold 100% methanol for 10 min to allow for permeabilization. Cells were stained for CD4, CD8 and pSTAT3 (pY705) and STAT3 phosphorylation status measured via FACS.

5.2.10 Bead-based multiplex immunoassay

CAR T cells were co-cultured with the same amount of Nalm6 target cells for 24 hours and centrifuged at 400 g for 4 minutes at 20 °C. Co-culture supernatants from two donors were then frozen and stored at -80 °C. The LEGENDplex Human CD8/NK Panel, a bead-based multiplex assay measured via flow cytometry, was performed according to the manufacturer's instructions with the thawed supernatants. These were measured in a 1/4 and 1/200 final dilution. Standard curves for all measured cytokines were generated by measuring eight standards with decreasing bead concentration.

5.3 IL-10 and IL-21 Enzyme-linked immunosorbent assay (ELISA)

24h after co-culture of CAR T and Nalm6 cells at a 1:1 E:T ratio, supernatants were frozen and stored at -80 °C. Measurement of IL-10 concentration was performed via the IL-10 ELISA MAX Deluxe kit with thawed supernatants from three donors according to the manufacturer's instructions. The IL-21 ELISA MAX Deluxe kit was utilized to verify IL-21 overexpression by IL-21 overexpressing CAR T cells, with untransduced cells serving as negative control. Measurement of both IL-10 and IL-21 was performed by reading the absorbance at 450 nm via the FLUOstar Omega microplate reader.

5.4 General cell culture

Cells were cultured at 37 °C with 5% CO₂. CD19⁺ cell lines were cultured in RPMI + 10% fetal bovine serum (FBS) + 1% penicillin/streptomycin + 1% L glutamine and splitted every three to five days. Cell lines were frozen in RPMI + 20% fetal bovine serum (FBS) + 1% penicillin/streptomycin + 1% L glutamine containing 10% dimethyl sulfoxide (DMSO). Primary T cells were frozen in 5% human serum albumin (HSA) containing 10% DMSO. After freezing -80 °C overnight, cells were transferred to liquid nitrogen (-179° C) for long-term preservation. For thawing, cells were rapidly warmed in a water bath, transferred and washed in TexMACS research grade medium.

5.5 Flow cytometry

Antibodies for flow cytometry staining were titrated prior to use. PBS and 1% fetal bovine serum (FBS) were used as FACS buffer for staining and washing. Cells were centrifuged at 400 g for 4 minutes at 20

°C, supernatant was removed and 50 µl of the antibody staining solution was added to each sample. Cells were then stained for 15 minutes at room temperature in the dark and washed once. In some instances, cells were fixed with 2% paraformaldehyde at 4 °C after staining. These were then washed twice and resuspended in 200 µl FACS buffer. Flow cytometric measurements were performed on MACSQuant Analyzer 10 or LSR Fortessa.

5.6 Software

Flow cytometric data was analysed using FlowJo 10. Schematic illustrations were created with BioRender, graphs with GraphPad Prism 8.4. The CAR cytokine profile was calculated with LEGENDplex Software 8. The InDel frequency of the CRISPR/Cas9 knock-out was calculated via the webtool TIDE, based on sequence trace decomposition¹¹⁷.

5.7 Statistical analysis

All data are given as mean ± standard deviation (SD), unless otherwise indicated. Normal distribution of the data was tested via the Shapiro-Wilk test. When comparing two groups, the unpaired Student's t-test was used. The one-way and two-way ANOVA tests followed by Tukey's multiple comparisons test as post hoc test were used if ≥3 groups were compared. A p value of <0.05 indicates significant (*), <0.01 very significant (**), and <0.001 extremely significant (***) differences. Calculations were performed with GraphPad Prism 8.4.

6 Results

6.1 CRISPR/Cas9 genomic knock-out and retroviral transduction of IL-21R in primary T cells

6.1.1 Generation of IL-21R overexpressing and CRISPR/Cas9 knock-out T cells

To elucidate the effect of the IL-21 receptor on T cell characteristics, CRISPR/Cas9 genomic knock-out ($_{CR}IL-21R^{KO}$) and retroviral overexpression of the receptor alpha chain ($_{RV}IL-21R^{OE}$) in human primary T cells were performed. A schematic drawing of the CRISPR/Cas9 knock-out with the respective crRNA binding site of the IL-21R alpha chain gene can be seen in Figure 6.1.A. To control for the effects of the manipulation itself, untransduced (UT) and electroporated with non-targeting crRNA control ($_{CR}Control$) cells were expanded alongside the $_{RV}IL-21R^{OE}$ and $_{CR}IL-21R^{KO}$ cells and used in all experiments (Figure 6.1.B).

On the last day of expansion after CRISPR/Cas9 knock-out and retroviral transduction of IL-21R, surface expression of the receptor was determined via flow cytometry. Exemplary FACS plots in Figure 6.1.C show increased surface expression of IL-21R after IL-21R transduction in CD8⁺ T cells. Mean transduction rate in $_{RV}IL-21R^{OE}$ was 24.1% (range 16% to 32.6%), whereas almost no IL-21R could be detected in the other three conditions.

To validate the genomic knock-out, DNA from both $_{CR}IL-21R^{KO}$ and $_{CR}Control$ cells was isolated at the end of expansion and the PCR product covering the CRISPR cut site analyzed via Sanger sequencing. To evaluate knock-out efficiency, the webtool TIDE was used to compare knock-out and CRISPR control samples in terms of InDel frequency (crRNA binding site shown in Figure 6.1.A). The genomic knock-out was furthermore confirmed on a protein level via FACS staining of the IL-21 receptor 72 hours after stimulation of cells from all four conditions (Figure 6.1.D). Mean surface expression of IL-21R in $_{CR}IL-21R^{KO}$ cells was 2% after induction, whereas both control cell conditions reached similar levels of expression (mean 27.5% in UT and 22.7% in $_{CR}Control$). This experiment also confirmed the high surface expression of IL-21R after retroviral transduction, which could be further increased with an appropriate stimulus (mean of 58.98%, range 50.9% to 66.8%). More than a 2.5-fold expression induction was achieved after engagement of the receptor compared to unstimulated $_{RV}IL-21R^{OE}$ cells at the end of expansion.

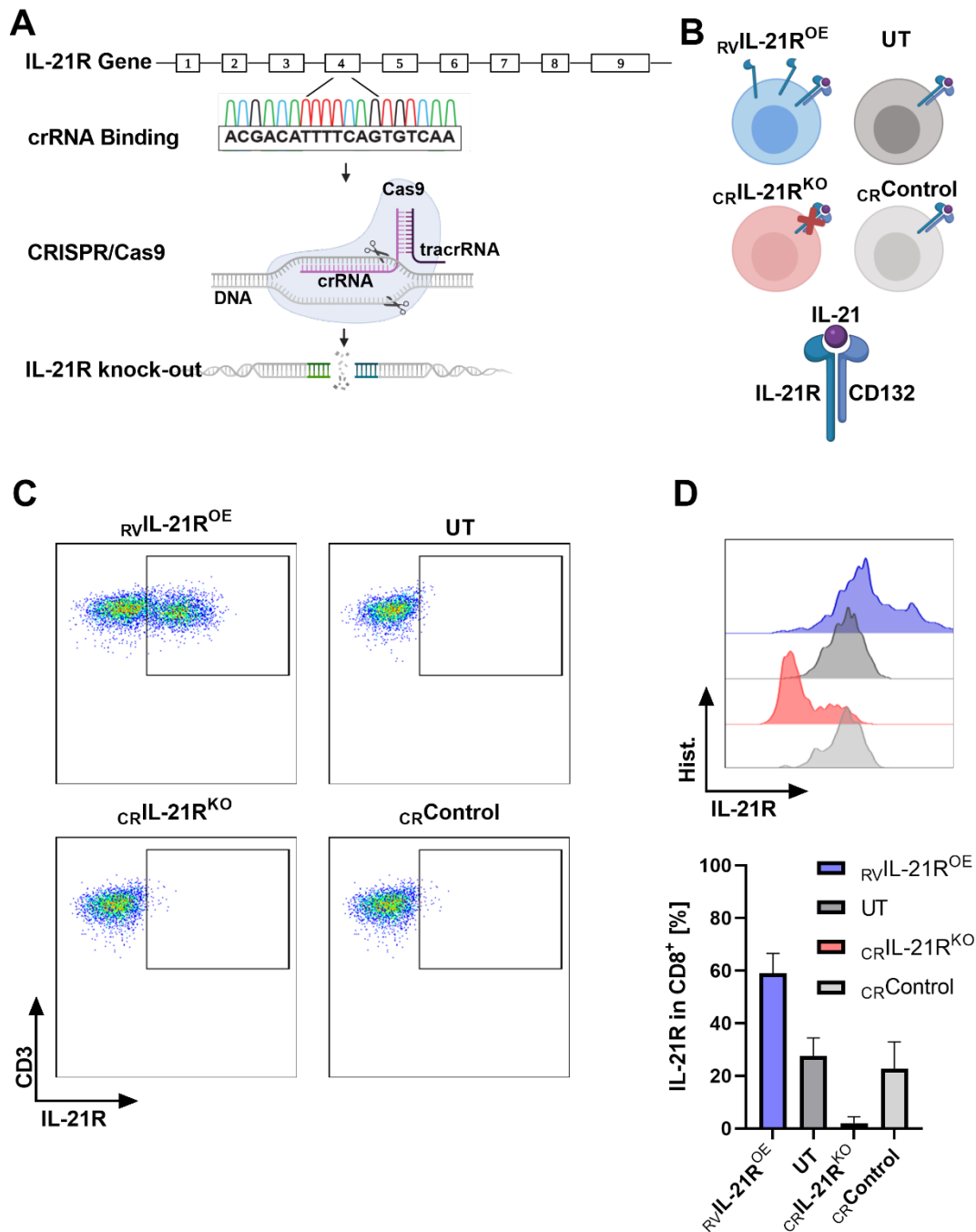


Figure 6.1 Generation of IL-21R overexpressing and CRISPR/Cas9 knock-out T cells

IL-21R surface expression was measured via flow cytometry. **A.** Schematic drawing of the IL-21R gene with its exons (1 - 9), as well as the working mechanism of the CRISPR/Cas9 system. crRNA IL-21R can bind to the base sequence in exon 4, thus leading to a double-strand break via the tracrRNA:crRNA-directed Cas9 protein. The chromatogram was obtained via Sanger sequencing. **B.** Schematic drawing of the tested constructs. IL-21R alpha chain was overexpressed in *RVIL-21R^{OE}* cells and a genomic knock-out was performed in *CRIL-21R^{KO}* cells. Untransduced (UT) and electroporated control cells (*CRControl*) were expanded alongside the other conditions. The structure of the receptor with the IL-21R chain and the common gamma chain (CD132) is also shown. **C.** Exemplary FACS plots of IL-21R surface expression in CD8⁺ T cells on day 12 of expansion, proving successful transduction in *RVIL-21R^{OE}* cells. The basal expression of the receptor in the other tested cells was negligible. **D.** Surface expression of IL-21R 72h after stimulation with anti-CD3 and anti-CD28 antibodies was highly upregulated in *RVIL-21R^{OE}* cells. Control cells demonstrated a similar percentage of IL-21R⁺ CD8⁺ cells, whereas less than 5%

surface expression was noted in $_{CR}IL-21R^{KO}$ cells. Data is representative of three donors and shown as mean \pm SD. RV: retroviral, OE: overexpression, CR: electroporation, KO: CRISPR/Cas9 genomic knock-out, Hist.: histogram.

T cells were expanded for fourteen days after genomic manipulation. $_{RV}IL-21R^{OE}$ T cells showed a significantly reduced expansion rate compared to UT cells on day eight and twelve with more than a 3-fold lower cell count (day eight mean 6.5×10^6 vs. 20.5×10^6 cells, $p=0.001$, day twelve mean 10.7×10^6 vs. 44.2×10^6 cells, $p=0.012$), as seen in Figure 6.2.A. No statistical difference in expansion was noted between $_{CR}Control$ and $_{CR}IL-21R^{KO}$ cells. At the end of expansion, phenotype analysis showed predominantly central memory and effector memory $CD8^+$ T cells among all conditions except in $_{RV}IL-21R^{OE}$ cells. IL-21R overexpressing cells had a mean of 36.5% stem cell-like memory, 20.5% central memory, 27.5% effector memory and 15.4% effector T cells, thus a tendency towards a less differentiated phenotype with a higher frequency of stem cell-like memory and central memory T cells was observed when compared to untransduced controls (mean sum 56.9% in $_{RV}IL-21R^{OE}$ vs. 42.4% in UT, $p=0.097$) (Figure 6.2.B). Differences in T cell differentiation in electroporated T cells were negligible, since $_{CR}Control$ showed a similar phenotype to $_{CR}IL-21R^{KO}$ cells (mean of sum of T_{SCM} and T_{CM} 40.1% vs. 42.4%, $p=0.825$). Similar results were observed in $CD4^+$ T cells, since no statistical difference in T cell populations among the tested conditions was found (data not shown).

To further study the differences in IL-21R expression after genomic manipulation, on the one hand, and broadly compare functionality between $_{RV}IL-21R^{OE}$ and UT cells, on the other, phosphorylation of STAT3 on addition of IL-21 was evaluated via flow cytometry. After binding of IL-21 to the IL-21R alpha chain, the common gamma chain is recruited, which leads to phosphorylation of STAT3 (Figure 6.2.C). Thus, levels of phosphorylated STAT3 (pSTAT3) can indirectly demonstrate if signal transduction takes place effectively after interaction between IL-21 and its receptor. As seen in Figure 6.2.D, the lack of the IL-21R alpha chain in the CRISPR/Cas9 knock-out led to a low percentage of pSTAT3 with a mean of 8.9%, confirming the high efficiency of the knock-out. No significant difference in mean phosphorylation of STAT3 between $_{RV}IL-21R^{OE}$ and UT cells was observed (mean 51.1% vs. 42.9%, $p=0.618$), despite marked differences in IL-21R surface expression. Exemplary FACS plots of one donor show the effect of IL-21 on STAT3 phosphorylation, with unstimulated cells used to define the appropriate gate.

The generation of IL-21R overexpressing and CRISPR/Cas9 knock-out T cells proved to be feasible and was validated with different methods. $_{RV}IL-21R^{OE}$ T cells showed a tendency towards a less differentiated phenotype and expanded less vigorously than control cells. Genomic knock-out of the IL-21R alpha chain did not impair cell viability, as expansion rate was comparable to that of $_{CR}Control$, but STAT3 phosphorylation was highly reduced after contact with IL-21.

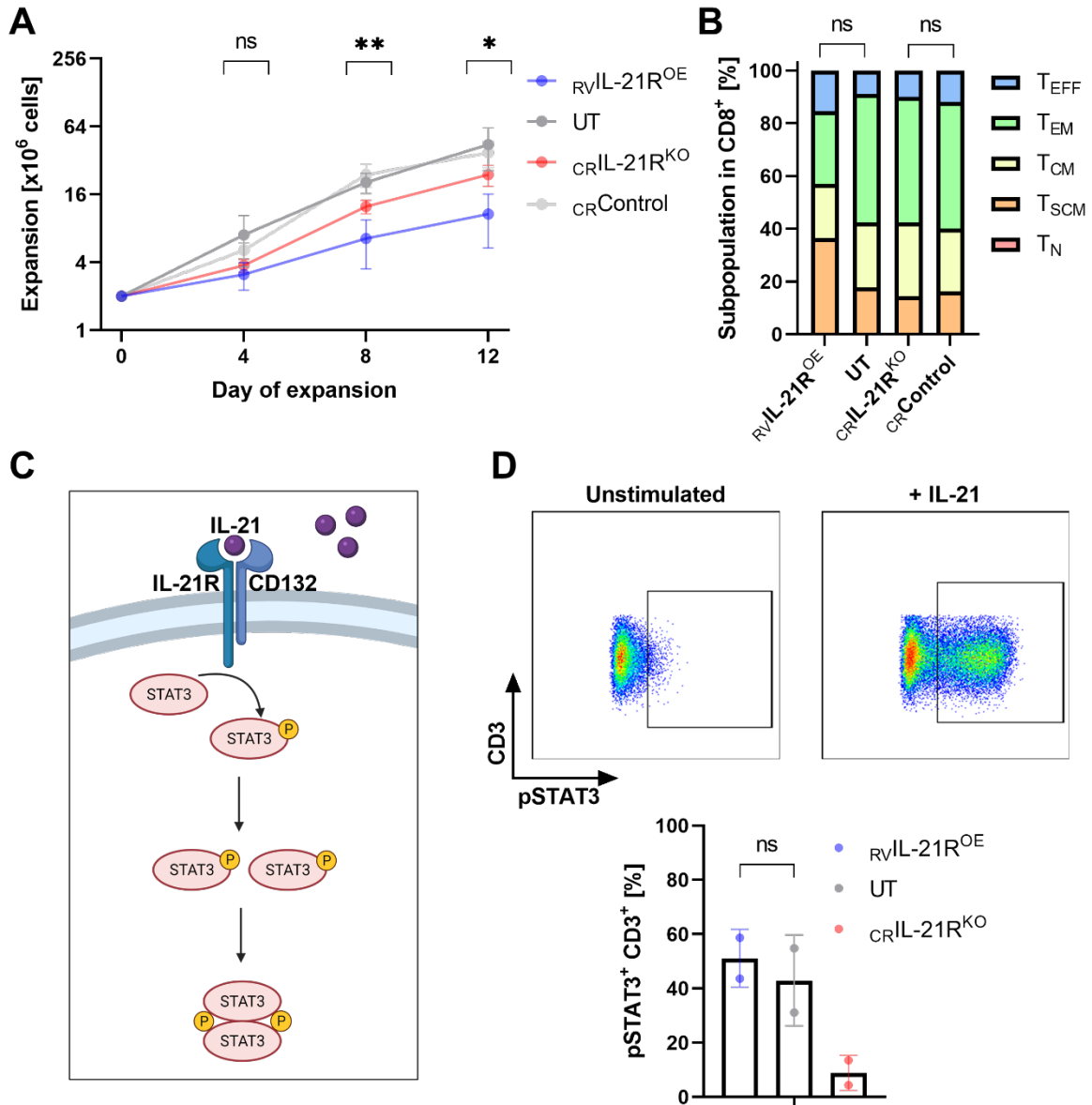


Figure 6.2 Characterization of the final cell product and measurement of signal transduction via pSTAT3 in IL-21R overexpressing and CRISPR/Cas9 knock-out T cells

Phenotype and pSTAT% were measured via flow cytometry. **A.** Expansion rate of the tested conditions was determined every two to three days by counting cells diluted 1:2 with trypan blue and is shown for twelve days after retroviral transduction and genomic knock-out of the IL-21 receptor. Expansion of $RVIL-21R^{OE}$ was significantly lower compared to UT cells. **B.** CD8⁺ cells on the last day of expansion show a predominantly central memory and effector memory phenotype. No significant difference in the sum of T_{SCM} and T_{CM} between IL-21R overexpressing or knock-out T cells and their respective controls could be demonstrated. However, $RVIL-21R^{OE}$ cells trended towards a less differentiated phenotype. Data in A. and B. is representative of three donors and shown as mean (± SD). **C.** A schematic drawing of the signal transduction cascade taking place after IL-21 binds to the IL-21R. IL-21-induced phosphorylation of STAT3 (pSTAT3) leads to dimerization and impacts transcription. **D.** Percentage of pSTAT3 measured in CD3⁺ T cells. FACS plots show pSTAT3% in $RVIL-21R^{OE}$ cells, either unstimulated or after addition of IL-21. Phosphorylation status was low in $CRIL-21R^{KO}$ cells, whereas no difference was measured between $RVIL-21R^{OE}$ and UT cells. Data is representative of two donors and shown as mean ± SD. A two-tailed, unpaired Student's t-test was used to compare groups. T_N: naïve T cells, T_{SCM}: stem cell-like memory T cells, T_{CM}: central memory T cells, T_{EM}: effector memory T cells, T_{EFF}: effector T cells. NK cells: natural killer cells, NK T cells: natural killer T cells, STAT: signal transducer and activator of transcription.

6.1.2 Functionality of IL-21R overexpressing and CRISPR/Cas9 knock-out T cells

To further investigate the role of the IL-21 receptor on CD8⁺ T cell functionality, co-culture assays were performed with CD19⁺ Nalm6 cells with the addition of blinatumomab to enable an interaction between T cells and target cells. To mimic the ligand/receptor interaction, experiments were performed in parallel either without or in the presence of IL-21. A schematic overview of the following experiments can be seen in Figure 6.3.A.

Direct cytotoxicity was evaluated by co-culturing T cells of all four conditions with Nalm6 target cells at three different E:T ratios for 48 hours, prior to flow cytometry. In general, T cells with IL-21R alpha chain overexpression (Figure 6.3.B) and CRISPR/Cas9 knock-out (Figure 6.3.C), as well as their respective controls exhibited dose-dependent killing of the CD19⁺ target cells upon addition of blinatumomab. A condition without blinatumomab served as negative control and showed unspecific cell killing, which at the 1:1 E:T ratio was two- to three-fold lower compared to T cells with blinatumomab in the co-culture (data not shown). Cytotoxic potential of all tested cells at the 1:1 E:T ratio is seen in Figure 6.3.D. $_{CR}IL-21R^{KO}$ cells demonstrated the highest cytotoxic potential on addition of blinatumomab (mean 56.1%, range 42.6% to 70.2% vs. mean 39.2%, range 26.5% to 50.8% in $_{CR}Control$, $p=0.046$). Mean values between IL-21R overexpressing T cells and untransduced control cells were similar (mean 44.5%, range 19.8% to 59.4% in $_{RV}IL-21R^{OE}$ vs. mean 47.4%, range 7.3% to 75.9% in UT, $p=0.696$), with high interdonor variation in cytotoxicity. At the highest 5:1 ratio, a mean cytotoxicity of 71.2% (range 66% to 72.4%) was reached among all tested T cell conditions. Even though at the 1:1 ratio IL-21 increased cytotoxicity in $_{RV}IL-21R^{OE}$ cells by 22% (mean 44.5% vs. mean 54.4%, $p=0.216$), a similar, but slightly less pronounced effect could be seen in UT (mean 47.4% vs. mean 52.9%, $p=0.718$) and $_{CR}Control$ cells (mean 39.2% vs. mean 45%, $p=0.283$). Addition of the ligand led to almost no change in the cytotoxic potential of $_{CR}IL-21R^{KO}$ cells (mean 56.1% without IL-21 vs. mean 56.6% with IL-21, $p=0.957$).

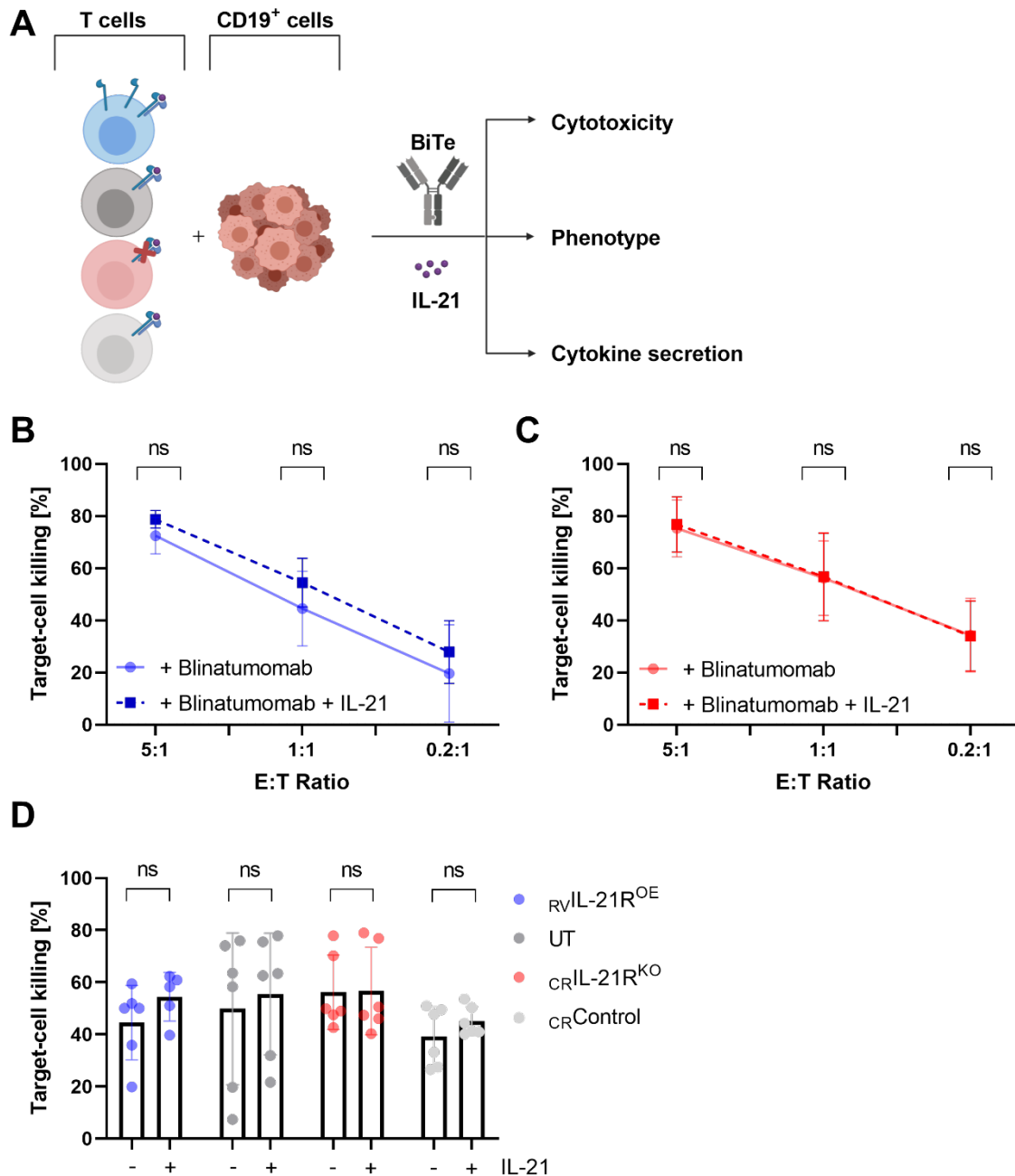


Figure 6.3 Overview of functionality assays and CD19-specific cytotoxicity of IL-21R overexpressing and CRISPR/Cas9 knock-out T cells

A. Schematic drawing of the functionality assay setup. The bispecific antibody blinatumomab was added in a co-culture of T cells and CD19⁺ Nalm6 cells at different E:T ratios to enable their interaction. After 48 hours of co-culture, cytotoxicity was measured via flow cytometry at three E:T ratios and the effect of IL-21 on **B.** $_{RV}IL-21R^{OE}$, and **C.** $_{CR}IL-21R^{KO}$ was investigated. **D.** Comparison of target-cell killing between tested cells at the 1:1 E:T ratio. Addition of IL-21 slightly increased cytotoxicity of $_{RV}IL-21R^{OE}$, UT and $_{CR}Control$ cells. No such effect was observed in IL-21R knock-out cells. Data is representative of three donors and experiments were performed in technical duplicates. Data is shown as mean \pm SD. The two-tailed, unpaired Student's t-test was used to compare every separate group. BiTe: bispecific antibody (blinatumomab), E:T ratio: effector-to-target ratio.

As an indirect parameter of cytotoxicity, CD107a degranulation of CD8⁺ T cells was measured after three hours in co-culture with CD19⁺ target cells. Exemplary FACS plots showing the effect of blinatumomab and IL-21 on CD107a degranulation can be seen in Figure 6.4.A. Mean percentage of CD107a⁺ CD8⁺ T

cells did not differ significantly between $_{RV}IL-21R^{OE}$ (mean 51.8%, range 36.9% to 63.5%) and UT (mean 54%, range 49.2% to 64.7%, $p=0.772$). Addition of IL-21 to the co-culture increased degranulation by less than 5% in IL-21R overexpressing cells, thus no difference between conditions was seen (mean 53.7% vs. mean 51.2% in UT, $p=0.623$). $_{CR}IL-21R^{KO}$ and $_{CR}Control$ cells both performed similarly and no disadvantage regarding degranulation was demonstrated by the IL-21R knock-out cells (Figure 6.4.B).

Furthermore, phenotype of the generated T cells was re-evaluated after 6 hours in co-culture to examine eventual short-term phenotypic changes on contact with target cells, as seen in Figure 6.4.C. In contrast to phenotype at the end of expansion, there was a shift to an effector memory- and effector-predominant phenotype among all tested $CD8^+$ T cells, with their mean frequency comprising more than 50% in all conditions. $_{RV}IL-21R^{OE}$ exhibited a mean of 30.5% effector, 31.3% effector memory, 7.7% central memory, 27% stem cell-like memory and 3.3% naïve T cells. Although less than 1% naïve cells were seen in the remaining conditions, phenotypic distribution was mostly consistent between genetically modified cells and their respective controls. The mean sum of T_{SCM} and T_{CM} cells was slightly lower in electroporated (mean 30.8%, range 27.1% to 33.5% in $_{CR}IL-21R^{KO}$ vs. mean 26.5%, range 18.9% to 33.5% in $_{CR}Control$, $p=0.405$) compared to IL-21R overexpressing and untransduced T cells (mean 34.7%, range 22.5% to 43.7% in $_{RV}IL-21R^{OE}$ vs. mean 41.8%, range 38.2% to 44.3% in UT, $p=0.339$). The addition of IL-21 to the co-culture did not significantly alter the phenotype, as there was a less than 5% mean increase in less differentiated T cells among all tested T cell conditions. Similar results were achieved after measurement of phenotype after 24 and 48 hours (data not shown).

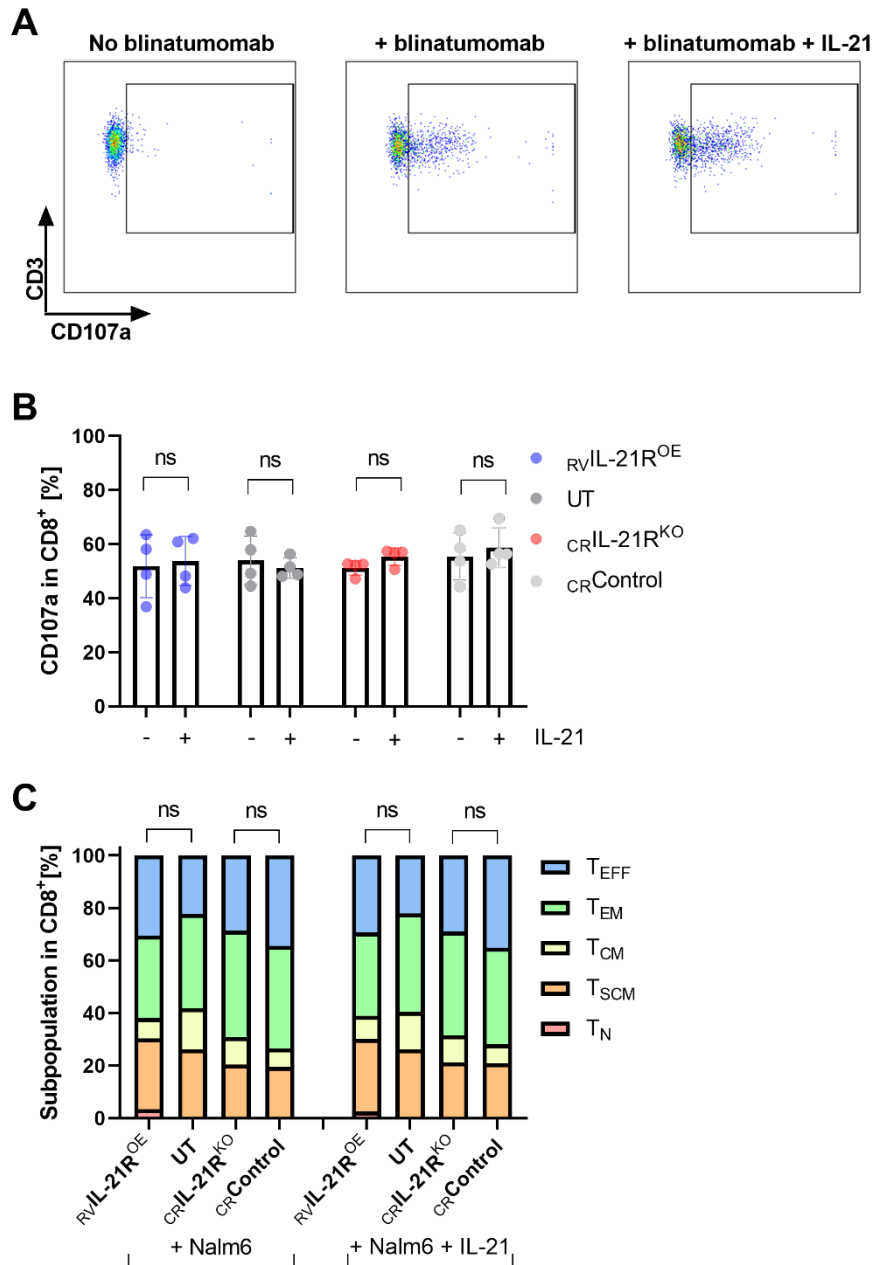


Figure 6.4 CD19-specific CD107a degranulation and phenotype of IL-21 overexpressing and CRISPR/Cas9 knock-out T cells

CD107a degranulation of CD8⁺ T cells was measured via flow cytometry 3 hours after co-culture with Nalm6 target cells on addition of blinatumomab ± IL-21. Conditions without blinatumomab served as negative control. The phenotype of CD8⁺ T cells was measured via FACS 6 hours after contact with CD19⁺ target cells. **A.** FACS plots show CD107a⁺ CD8⁺ cells in one donor, with the appropriate gate set according to the condition without blinatumomab. **B.** No difference was noted between cells regarding CD107a degranulation, even after addition of IL-21 to the co-culture. Data is representative of at least three donors. **C.** More than half of the T cells in all conditions had either effector memory or effector phenotype, with the percentage of central memory T cells declining in the co-culture setting compared to the end of expansion. Addition of IL-21 did not significantly change phenotypic differentiation. Data is representative of three donors and shown as mean. A two-tailed, unpaired Student's t-test was used to compare groups. T_N: naïve T cells, T_{SCM}: stem cell-like memory T cells, T_{CM}: central memory T cells, T_{EM}: effector memory T cells, T_{EFF}: effector T cells. NK cells: natural killer cells, NK T cells: natural killer T cells.

Next, cytokine secretion was assessed after 24 hours in the co-culture setting by intracellular staining of IFN-γ and TNF-α, followed by flow cytometric analysis (Figure 6.5). A mean of 8.1% of RVIL-21R^{OE} and

9.5% of untransduced CD8⁺ TNF- α ⁺ cells were detectable (range 5.2% to 10.2% vs. range 7.5% to 12.6%, p=0.556). Electroporated T cells demonstrated higher basal TNF- α secretion (mean 15.8%, range 10.1% to 26.5% in $_{CR}IL-21R^{KO}$ vs. mean 13.4%, range 6.7% to 20% in $_{CR}Control$, p=0.7341). IL-21 in the co-culture led to a 1.7-fold increase in TNF- α ⁺ $_{CR}Control$ cells (mean 23.1%, range 21.6% to 25.7%, p=0.073 vs. condition without IL-21), whereas a 26% decrease in secretion was observed in the $_{CR}IL-21R^{KO}$ cells (mean 11.6%, range 10.6% to 12.5%, p=0.478 vs. condition without IL-21). There was a 32% increase in cytokine secretion in the IL-21R overexpressing construct (mean 10.8%, range 10.3% to 11.9%, vs. condition without IL-21, p=0.165), but no statistical difference in TNF- α secretion between $_{RV}IL-21R^{OE}$ and UT cells was seen after addition of IL-21, as seen in Figure 6.5.B.

Moreover, IFN- γ level was lowest in $_{RV}IL-21R^{OE}$ (mean 6.2%, range 4.4% to 8.5% vs. mean 14.5%, range 8.3% to 22% in UT, p=0.114), when no IL-21 was added to the co-culture (Figure 6.5.C). In contrast, the ligand increased secretion in both conditions by a mean of 90%. Nevertheless, owing to the higher secretion at baseline, UT cells showed a two-fold higher percentage of CD8⁺ IFN- γ ⁺ cells (mean 26.6%, range 16.4% to 42.6%) compared to $_{RV}IL-21R^{OE}$ (mean 12.8%, range 5.9% to 20.4%, p=0.201) after IL-21 was added (Figure 6.5.D). The ligand did not improve cytokine secretion in $_{CR}IL-21R^{KO}$ cells and even lessened it by a mean of 17% (mean 16.4% without IL-21 vs. mean 13.6% with IL-21, p=0.613), which was not the case in $_{CR}Control$ cells (mean 13% without IL-21 vs. mean 35.9% with IL-21, p=0.006).

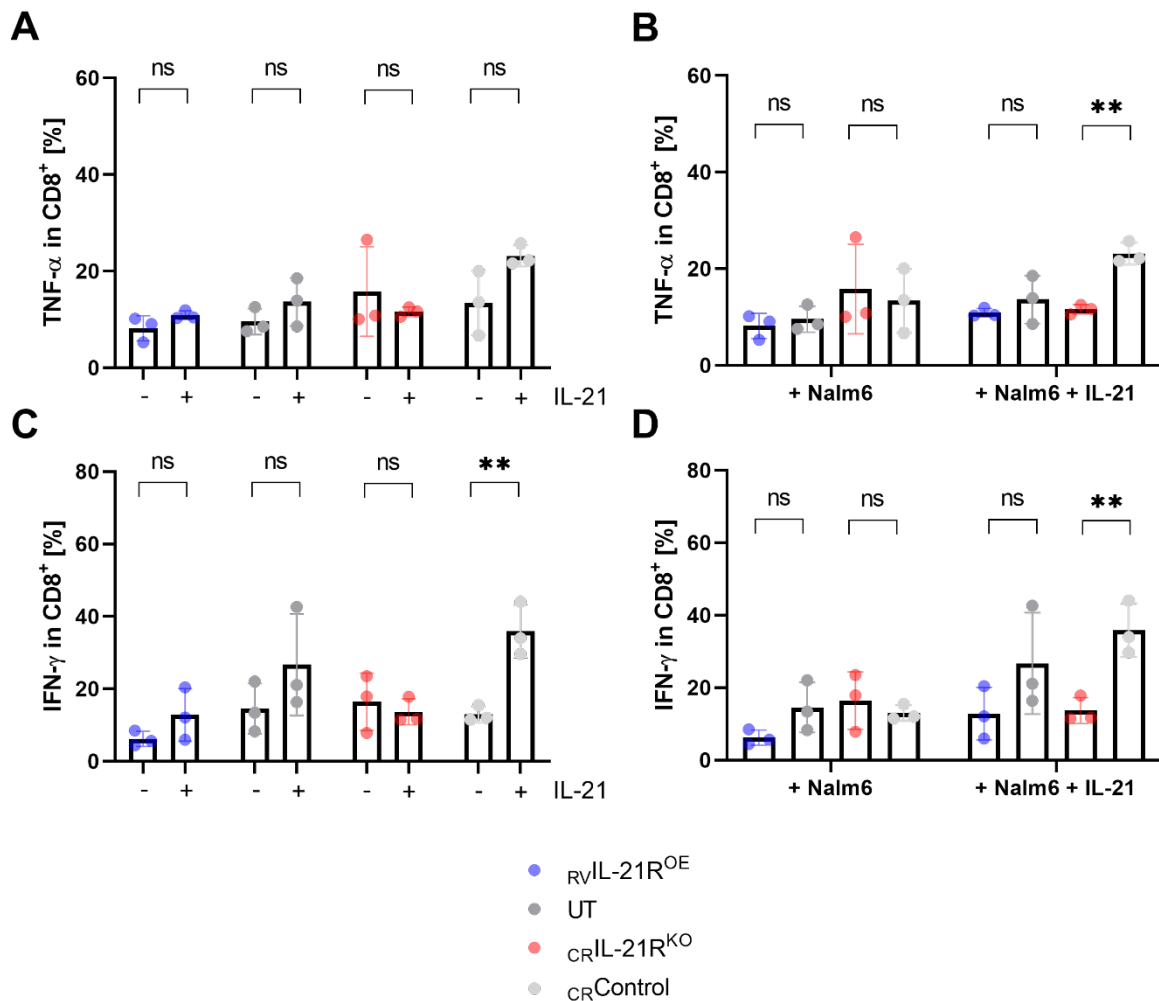


Figure 6.5 Intracellular cytokine staining of IL-21R overexpressing and CRISPR/Cas9 knock-out T cells

T cells were co-cultured with CD19⁺ targets ± IL-21 for 24h. After addition of Brefeldin A for 2 hours, cells were fixed, permeabilized and stained, and intracellular cytokine secretion was determined via flow cytometry. Cytokine secretion is shown as percentage in the CD8⁺ T cells in the co-culture. The upper two plots (A. and B.) visualize TNF- α secretion, whereas the lower two plots (C. and D.) demonstrate IFN- γ secretion in the IL-21R overexpressing and CRISPR/Cas9 knock-out T cells and their respective controls. The effect of IL-21 addition to the co-culture is demonstrated on the left, while on the right the focus is on cytokine secretion of the different conditions. A. and C. Effect of IL-21 on cytokine secretion was evaluated within each construct separately regarding the presence of IL-21. TNF- α secretion was lowest in $_{RV}IL-21R^{OE}$ cells but increased to a level comparable to UT cells after addition of IL-21. The percentage of IFN- γ^+ in UT cells was twice as high as in $_{RV}IL-21R^{OE}$ cells, even after IL-21 was added. B. and D. Comparison between IL-21R overexpressing or CRISPR/Cas9 knock-out T cells and their respective controls. Addition of IL-21 to the co-culture slightly decreased cytokine secretion in $_{CR}IL-21R^{KO}$ cells. Data is representative of three donors and shown as mean \pm SD. The two-tailed, unpaired Student's t-test was used to compare every separate group. TNF- α : tumor necrosis factor alpha, IFN- γ : interferon gamma.

In summary, functionality of T cells after IL-21R overexpression or CRISPR/Cas9 knock-out was comparable to their respective controls. The addition of IL-21 to the co-culture led to a slight, non-significant increase in directly measured cytotoxicity in conditions with normal or increased IL-21R expression. CD107a degranulation of T cells was not altered upon addition of IL-21 independent of IL-21R expression status. Phenotype was comparable among tested T cells after 14 days of expansion and no IL-21 dependent effect on phenotype was seen after 6 hours. $_{RV}IL-21R^{OE}$ cells demonstrated decreased cytokine secretion, which was only in part rescued by addition of IL-21 to the co-culture of T cells and CD19⁺ target cell line Nalm6.

6.2 Retroviral transduction of IL-21R and common gamma chain in primary T cells

6.2.1 Generation of IL-21R and common gamma chain overexpressing T cells

Based on the results in 6.1.2, overexpressing only the IL-21R alpha chain in T cells led to no marked differences in functionality compared to untransduced control cells. Since the common gamma chain cytokine receptor IL-21R is made up of two subunits, IL-21R and CD132 (common gamma chain, γ_C), we decided to examine the effect of the common gamma chain on T cell characteristics. Human primary T cells were retrovirally transduced with the construct CD132 ($_{RV}CD132^{OE}$) and a bicistronic construct ($_{RV}IL-21R_CD132^{OE}$), which allowed for equimolar translation of both the IL-21R alpha and the common gamma chain via an F2A linker. The aim was to compare these two conditions to $_{RV}IL-21R^{OE}$ cells in terms of functionality. Untransduced T cells (UT) served as negative control. A schematic drawing of the constructs is shown in Figure 6.6.A.

T cells were transduced and expanded for fourteen days as described in 5.1.3. Mean surface expression of IL-21R was 58.2% in $_{RV}IL-21R^{OE}$, 55.2% in $_{RV}IL-21R_CD132^{OE}$, 7.4% in $_{RV}CD132^{OE}$, and 2.4% in UT cells. CD132 was expressed in 55.2% of $_{RV}CD132^{OE}$ cells and 6.6% of $_{RV}IL-21R_CD132^{OE}$ (exemplary FACS plots can be seen in Figure 6.6.B). The low surface expression of the common γ_C in the bicistronic construct was probably due to the construct structure with IL-21R coming before the F2A-linked CD132. In both UT and $_{RV}IL-21R^{OE}$ cells surface expression of the common gamma chain was negligible.

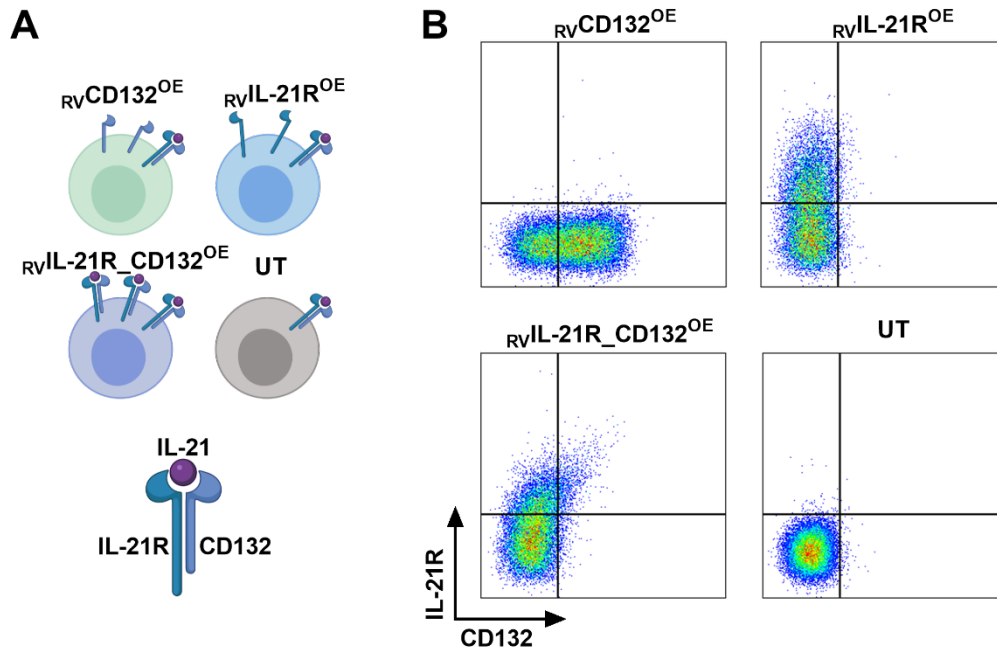


Figure 6.6 Generation of IL-21R and common gamma chain overexpressing T cells

CD132 surface expression was measured via flow cytometry. **A.** A schematic drawing of the tested constructs. The common gamma chain (CD132) was overexpressed in $RVCD132^{OE}$ cells and compared to T cells overexpressing the IL-21R alpha chain ($RVIL-21R^{OE}$) and a bicistronic construct with both chains of the cytokine receptor ($RVIL-21R_CD132^{OE}$). Untransduced (UT) cells were expanded alongside the other conditions and served as control. The structure of the IL-21 receptor with the IL-21R chain and the common gamma chain is also shown. **B.** Exemplary FACS plots of CD132 and IL-21R surface expression in $CD3^+$ T cells on day 12 of expansion, thus showing successful transduction in $RVCD132^{OE}$ and $RVIL-21R_CD132^{OE}$ cells, compared to the low basal surface expression of the common gamma chain in UT and $RVIL-21R^{OE}$ cells. Co-expression of IL-21R and CD132 in $RVIL-21R_CD132^{OE}$ T cells can also be seen. Data is representative of two donors. RV: retroviral, OE: overexpression.

Fold expansion was comparable among constructs (Figure 6.7.A). The following analyses were performed with bulk $CD8^+$ T cells to avoid bias when comparing to UT cells. Moreover, gating on the double-positive population in the $RVIL-21R_CD132^{OE}$ condition yielded a low cell count, which made comparison to other conditions challenging. Phenotypic analysis of $CD8^+$ cells on the last day of expansion showed predominance of stem cell-like memory and central memory T cells with the mean percentage T_{SCM} 46.5% (range 45.4% to 47.4%) among tested conditions. No differences in differentiation were measured between tested cells, as seen in Figure 6.7.B. The transduction process itself did not seem to influence T cell differentiation, as untransduced T cells showed a similar phenotype.

Next, signal transduction via STAT3 phosphorylation on addition of IL-21 was examined (Figure 6.7.C). Independent of the level of surface expression of either CD132 or IL-21R alpha chain, all constructs reached a similar pSTAT3 percentage after addition of IL-21, with $RVIL-21R^{OE}$ cells showing the highest (mean 51.4%, range 49.2% to 53.7%) and UT control cells the lowest level of phosphorylation (mean 42.2%, range 37.5% to 47%, $p=0.491$). However, no significant difference in phosphorylation status was established. These results are consistent with data from previous experiment (Figure 6.2).

The generation of CD132 and IL-21R overexpressing T cells was feasible and no disadvantage in cellular expansion and phenotype was observed. The phosphorylation of STAT3 after binding of the ligand IL-21 was comparable among all conditions, which indicates that a basal surface expression of IL-21R is sufficient for signal transduction to occur efficiently. Overexpression of the common gamma chain alone or in conjunction with the IL-21R alpha chain did not increase phosphorylation.

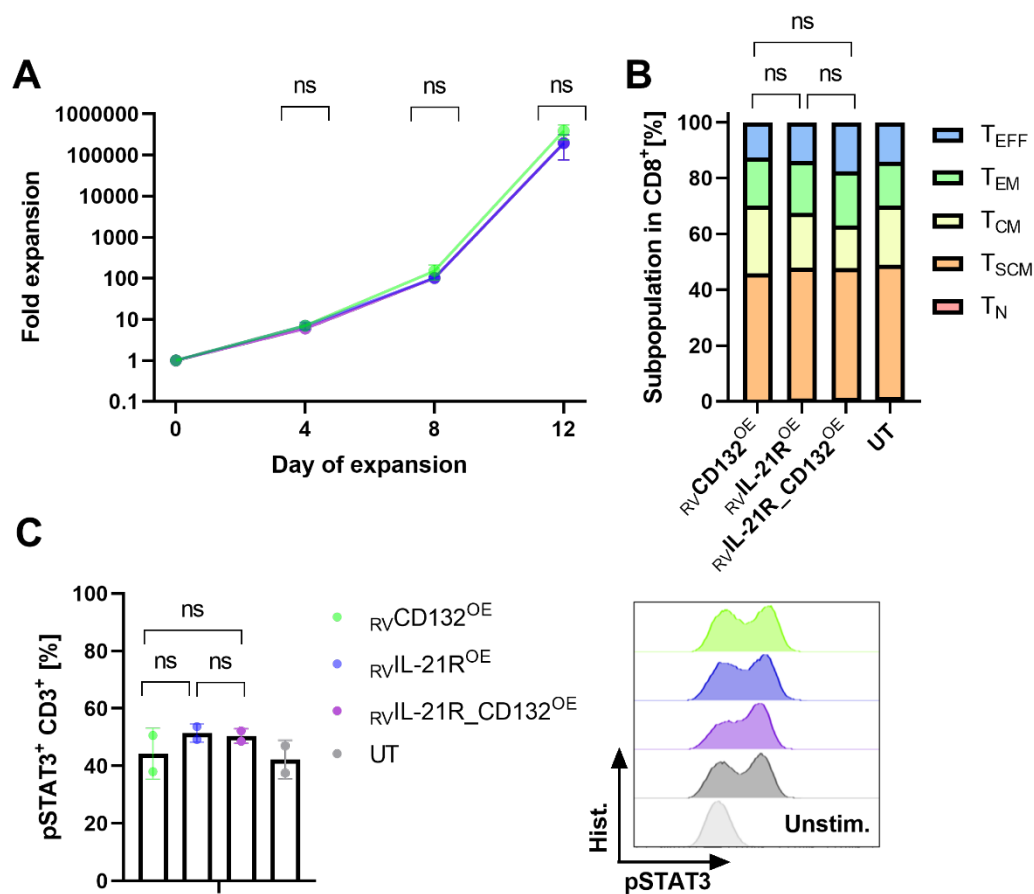


Figure 6.7 Characterization of the final cell product and measurement of pSTAT3 in IL-21R and common gamma chain overexpressing T cells

Phenotype and pSTAT3% were measured via FACS. **A.** Expansion rate of the tested conditions was determined every two to three days via cell counting after staining with trypan blue. Fold expansion is relative to the number of cells used for transduction. Expansion did not differ among the constructs overexpressing IL-21R alpha chain and/or CD132. **B.** CD8⁺ cells on the last day of expansion showed a predominantly stem cell-like memory and central memory phenotype. No significant difference in the sum of T_{SCM} and T_{CM} was seen. **C.** Percentage of pSTAT3 measured in CD3⁺ T cells. The histogram shows pSTAT3 in the tested cells, either unstimulated or after addition of IL-21. Phosphorylation status was comparable between constructs. Data is representative of two donors and shown as mean ± SD. One-way ANOVA was used to compare groups. T_N: naïve T cells, T_{SCM}: stem cell-like memory T cells, T_{CM}: central memory T cells, T_{EM}: effector memory T cells, T_{EFF}: effector T cells. NK cells: natural killer cells, NK T cells: natural killer T cells, STAT: signal transducer and activator of transcription.

6.2.2 Functionality of IL-21R and common gamma chain overexpressing T cells

The generated constructs were then functionally tested in a co-culture setting with CD19⁺ Nalm6 target cells. Blinatumomab was added to ensure interaction between T cells and tumor cells. Experiments without and with IL-21 were performed in parallel to further examine effects of the ligand-receptor interaction on T cell function. The experimental setup and measurement of the different assays correspond to conditions in previous experiments. A schematic drawing of the setup is seen in Figure 6.8.A.

To investigate direct anti-CD19 cytotoxicity, all four conditions were co-cultured with Nalm6 cells at three E:T ratios for 48 hours (Figure 6.8.B). In a setting without IL-21, all T cells killed in an E:T ratio-

dependent manner with the highest lysis demonstrated by $_{RV}CD132^{OE}$ cells (mean 51.1%) at the 1:1 E:T ratio. The other two constructs overexpressing IL-21R showed a similar cytotoxic potency (mean 36 % in $_{RV}IL-21R^{OE}$ vs. 39.1% in $_{RV}IL-21R_CD132^{OE}$, $p=0.957$) to UT control cells (vs. mean 37.4%, $p=0.996$ and $p=0.991$, respectively). About a 15% increase in lytic potential was achieved in $_{RV}IL-21R^{OE}$ cells on addition of IL-21 (mean 51.9%) at 1:1 E:T ratio, which was comparable to the effect of the ligand to $_{RV}IL-21R_CD132^{OE}$ (mean 56.1%, $p=0.6$) and UT cells (mean 57.6%, $p=0.359$) (Figure 6.8.C). IL-21 had almost no effect on cytotoxicity when only the common gamma chain was overexpressed (mean 51.1% vs. 52.1%). Mean unspecific killing without blinatumomab at the 1:1 E:T ratio among all conditions was 25.27% (data not shown).

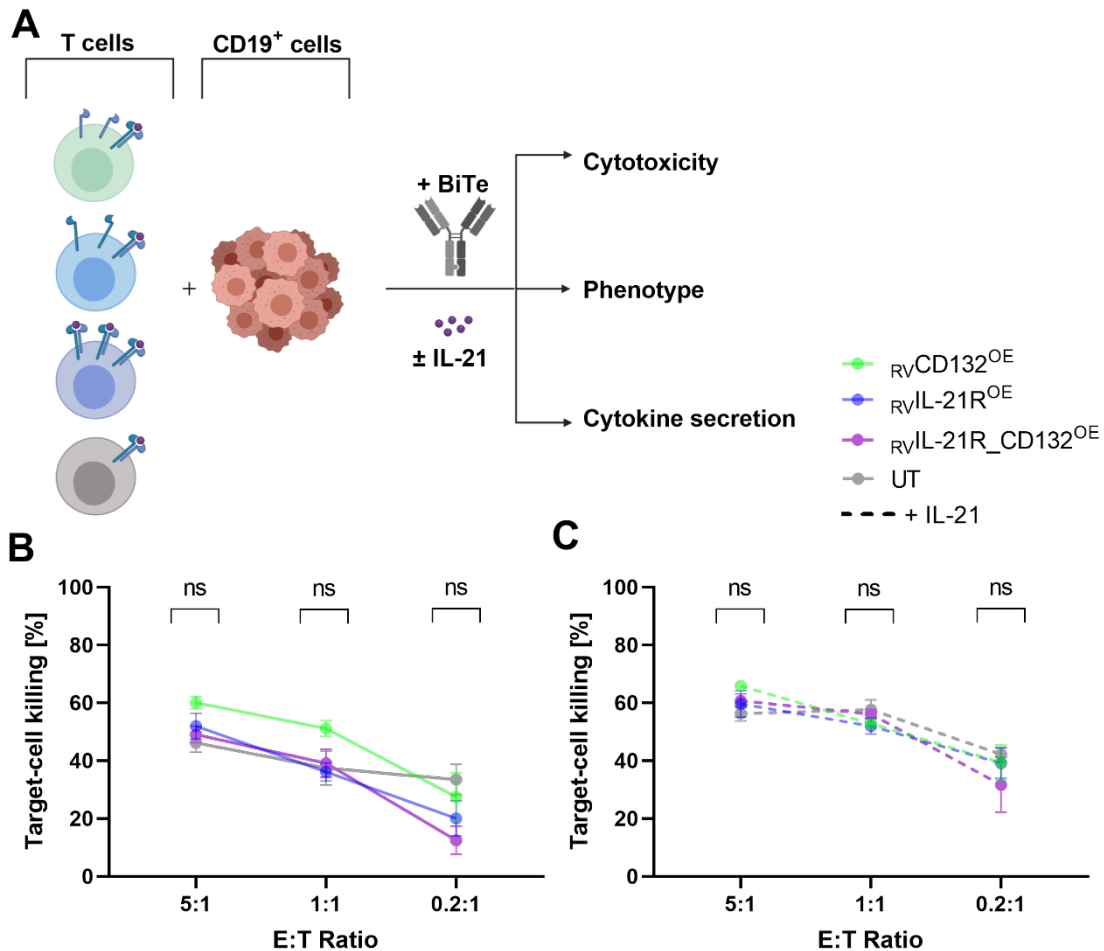


Figure 6.8 Overview of functionality assays and CD19-specific cytotoxicity of IL-21R and common gamma chain overexpressing T cells

A. Schematic drawing of the functionality assay setup. To ensure interaction, the bispecific antibody blinatumomab was added in the co-culture of T cells and CD19⁺ Nalm6 cells at different E:T ratios. **B.** After 48 hours of co-culture, cytotoxicity was measured via flow cytometry at three E:T ratios. Target-cell killing was highest in $_{RV}CD132^{OE}$ cells, but comparison to the other constructs yielded no statistical significance. **C.** The effect of IL-21 on the tested cells was investigated by adding it to the co-culture conditions. The ligand increased cytotoxicity in $_{RV}IL-21R^{OE}$, UT and $_{RV}IL-21R_CD132^{OE}$ cells. Data is representative of two donors and experiments were performed in technical duplicates. Data is shown as mean \pm SD. One-way ANOVA was used to compare groups at every E:T ratio. BiTe: bispecific antibody (blinatumomab), E:T ratio: effector-to-target ratio, RV: retroviral, OE: overexpression.

In a further experiment, the ability of the constructs to secrete cytokines was examined via intracellular staining of IFN- γ and TNF- α after 24 hours in a co-culture with Nalm6 cells, followed by FACS analysis of the CD8⁺ fraction. A mean of 12.6% of $_{RV}IL-21R^{OE}$ and 12.1% of $_{RV}IL-21R_CD132^{OE}$ TNF- α ⁺ cells were

detectable. Both constructs demonstrated a significantly higher TNF- α secretion than $_{RV}CD132^{OE}$ cells (mean 9.3%, $p=0.001$ and $p=0.006$, respectively). This effect remained after introduction of IL-21 to the co-culture, despite a 10-20% drop in absolute cytokine secretion among all constructs. In both co-culture conditions, the percentage of TNF- α^+ UT control cells was comparable to that of constructs overexpressing IL-21R, as seen in Figure 6.9.A.

Similar results were obtained regarding CD8⁺ IFN- γ^+ cells (Figure 6.9.B). Secretion was lowest in $_{RV}CD132^{OE}$ T cells compared to both constructs overexpressing the IL-21R alpha chain (mean 4.71% in $_{RV}CD132^{OE}$ vs. mean 7.03% in $_{RV}IL-21R^{OE}$ and mean 7.31% in $_{RV}IL-21R_CD132^{OE}$, $p=0.058$ and $p=0.048$, respectively). This effect was even more pronounced on addition of IL-21 to the co-culture, as both $_{RV}IL-21R^{OE}$ and $_{RV}IL-21R_CD132^{OE}$ secreted significantly more IFN- γ than the CD132 overexpressing construct (at least a 1.7-fold increase compared to $_{RV}CD132^{OE}$), which remained the least secreting construct despite presence of IL-21. There was, however, no significant difference in IFN- γ secretion between the constructs overexpressing IL-21R (mean 11.7% in $_{RV}IL-21R^{OE}$, mean 13% in $_{RV}IL-21R_CD132^{OE}$, $p=0.771$) and both were comparable to UT control cells.

In a final experiment phenotypic differentiation of the constructs was examined after 6 hours in co-culture conditions (Figure 6.9.C). $_{RV}CD132^{OE}$ T cells exhibited a stem cell-like memory- and central memory-predominant phenotype with a frequency of less than 1% naïve, 43.3% stem cell-like memory, 11.2% central memory, 18.9% effector memory and 25.5% effector T cells. The sum of stem cell-like memory and central memory cells in the common gamma chain overexpressing condition was significantly higher than in the two IL-21R overexpressing constructs (vs. mean 38.9% in $_{RV}IL-21R^{OE}$, $p=0.039$, vs. mean 37.8% in $_{RV}IL-21R_CD132^{OE}$, $p=0.026$), which had a higher frequency of T_{EM} and T_{EFF} cells. On addition of IL-21 to the co-culture, central memory and stem cell-like memory T cells rose in a range from 7.2% to 42.5% in $_{RV}IL-21R^{OE}$ and $_{RV}IL-21R_CD132^{OE}$ cells. Nevertheless, $_{RV}CD132^{OE}$ T cells still showed a significantly higher mean percentage of T_{SCM} and T_{CM} . The phenotype of UT control cells demonstrated a mean of 1.5% naïve, 36.6% stem cell-like memory, 7% central memory, 22.3% effector memory and 32.3% effector T cells without IL-21 in the co-culture. UT T cells showed an increase in immature T cell phenotypes upon addition of IL21 into the co-culture, too.

In summary, all constructs demonstrated an E:T ratio-dependent cell lysis. A marked increase in cytotoxicity was seen on addition of IL-21 to the co-culture, except for $_{RV}CD132^{OE}$ T cells, which reached high lytic potential independent of ligand presence, especially in the higher E:T ratios. In general, IL-21 had hardly any effect on the functionality of $_{RV}CD132^{OE}$ cells, as neither cytokine secretion nor phenotype changed significantly after introduction of IL-21 to the co-culture. This was not the case in constructs overexpressing the IL-21R alpha chain, as a rise in both lytic potential and IFN- γ secretion could be observed. Phenotype 6h after co-culture was less strongly influenced by the ligand, as a more differentiated phenotype was observed in $_{RV}IL-21R^{OE}$ and $_{RV}IL-21R_CD132^{OE}$ than in $_{RV}CD132^{OE}$ T cells.

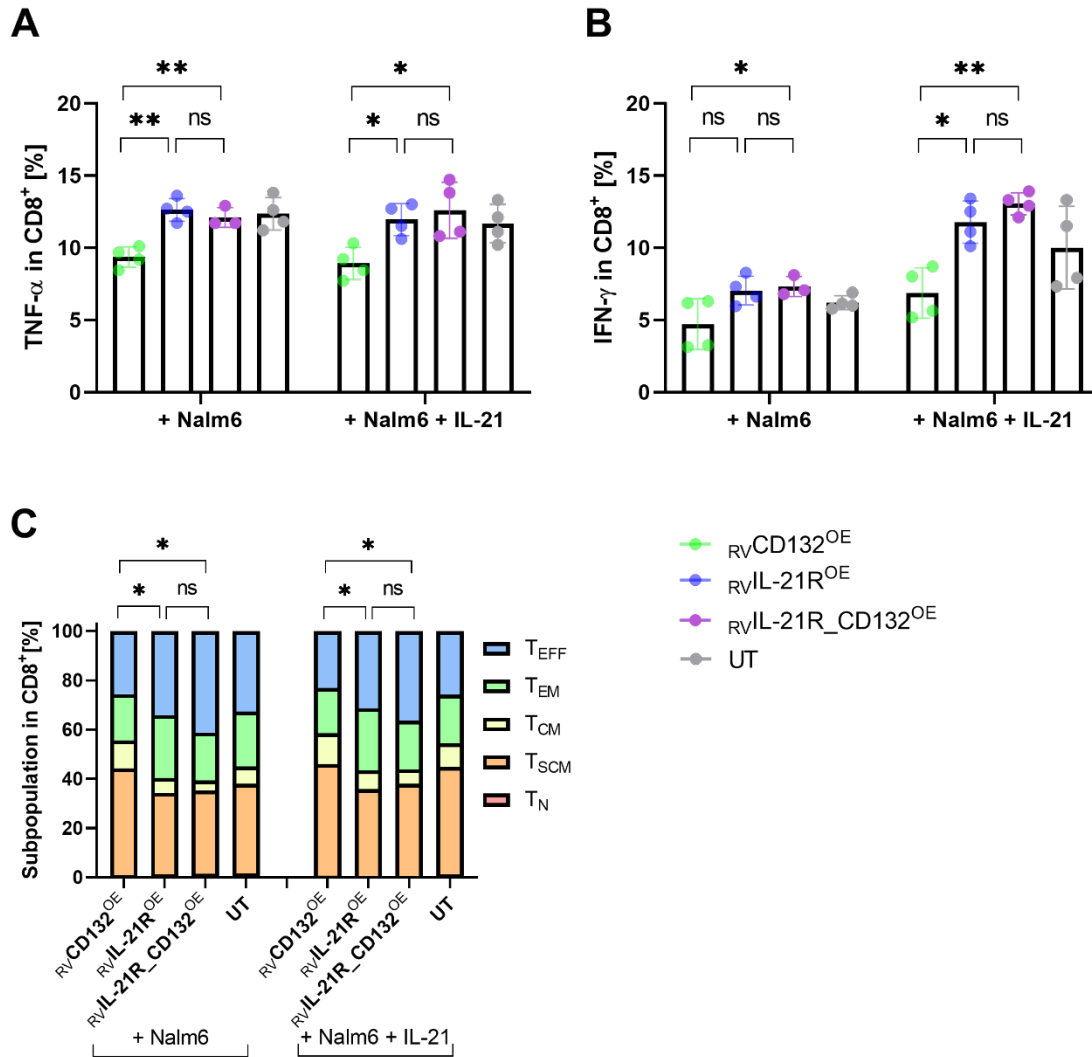


Figure 6.9 Intracellular cytokine staining and phenotype of IL-21R and common gamma chain overexpressing T cells

For intracellular cytokine staining, T cells were co-cultured with CD19⁺ targets \pm IL-21 for 24h. After addition of Brefeldin A for 2 hours, cells were fixed, permeabilized and stained, and cytokine secretion was measured via FACS and is shown as percentage in the CD8⁺ T cells. Phenotype of CD8⁺ T cells was measured via FACS 6 hours after contact with CD19⁺ target cells. **A.** TNF- α secretion was highest in RVIL-21R^{OE} and RVIL-21R_CD132^{OE}, whereas RVCD132^{OE} cells demonstrated a significantly lower percentage of TNF- α ⁺ cells. UT cells were comparable to both constructs with IL-21R alpha chain overexpression. The effect remained after addition of IL-21 to the co-culture. **B.** IFN- γ secretion was lowest in RVCD132^{OE} cells. IL-21 led to a pronounced increase in IFN- γ ⁺ cells in RVIL-21R^{OE} and the bicistronic construct. **C.** CD8⁺ RVCD132^{OE} cells demonstrated a significantly less mature phenotype compared to the constructs overexpressing IL-21R, with stem cell-like memory and central memory T cells being predominant. IL-21 did not reverse this effect. Data is representative of two donors, shown as mean (\pm SD) and experiments were performed in technical duplicates. Groups were compared via one-way ANOVA. TNF- α : tumor necrosis factor alfa, IFN- γ : interferon gamma, T_N: naïve T cells, T_{SCM}: stem cell-like memory T cells, T_{CM}: central memory T cells, T_{EM}: effector memory T cells, T_{EFF}: effector T cells. NK cells: natural killer cells, NK T cells: natural killer T cells.

Basal expression of the IL-21R alpha chain was shown to be sufficient for interaction between the receptor and its ligand. RVIL-21R^{OE} was non-inferior to the bicistronic construct RVIL-21R_CD132^{OE} in terms of expansion, signal transduction, phenotype, cytotoxicity, and cytokine secretion. Thus, co-expression of the common gamma chain was discontinued in the further study the IL-21R/IL-21 interaction in anti-CD19 CAR T cells.

6.3 CRISPR/Cas9 knock-out and retroviral transduction of IL-21R in anti-CD19 CAR T cells

6.3.1 Generation of first- and second-generation anti-CD19 CAR T cells overexpressing IL-21R

To examine whether the IL-21/IL-21R interaction is beneficial in a CAR context, three bicistronic constructs were designed with an F2A linker in order to achieve equimolar translation of both proteins (CAR and IL-21R alpha chain). As seen in Figure 6.10.A, the first-generation CAR construct ($_{RV19z_IL-21R^{OE}}$) consisted of an anti-CD19 single chain variable fragment, a c-myc tag for detection of the CAR protein via flow cytometry, a CD8 extracellular and transmembrane domain and an intracellular CD3 ζ chain. Second-generation CAR constructs ($_{RV19-BBz_IL-21R^{OE}}$ and $_{RV19-28z_IL-21R^{OE}}$) additionally contained either intracellular 4-1BB or CD28 costimulatory domains. Three conventional CAR constructs without F2A linker and IL-21R ($_{RV19z}$, $_{RV19-BBz}$, $_{RV19-28z}$) were used as controls in all experiments, together with untransduced (UT) cells.

As described in 5.1.2 and 5.1.3, activated primary T cells were transduced with six CAR constructs designed in our laboratory and expanded for ten days. On the last day of expansion, CAR surface expression was analyzed to ensure sufficient transduction rate, as seen in Figure 6.10.B. In general, IL-21R overexpressing CAR T cells had a consistently lower transduction rate compared to conventional CAR T cells, as both $_{RV19z}$ (mean 79.5%, range 75.4% to 85.3%) and $_{RV19-BBz}$ (mean 62%, range 58.7% to 68%) exhibited a significantly higher frequency of CAR⁺ cells compared to $_{RV19z_IL-21R^{OE}}$ (vs. mean 59.7%, range 47.6% to 68.8%, $p=0.046$) and $_{RV19-BBz_IL-21R^{OE}}$ (vs. mean 48%, range 46% to 49.8%, $p=0.012$). Surface expression of IL-21R was also determined and co-expression of both receptors validated, as seen in the exemplary plots in Figure 6.10.D. Endogenous expression of IL-21R in control CAR T cells was just as low as in UT control cells (data not shown). The three IL-21R alpha chain overexpressing constructs demonstrated a significantly increased percentage of IL-21R⁺ cells when compared to UT cells (vs. mean 46% in $_{RV19z_IL-21R^{OE}}$, $p=0.0003$, vs. mean of 30.7% in $_{RV19-BBz_IL-21R^{OE}}$, $p=0.003$, vs. mean 43.1% in $_{RV19-28z_IL-21R^{OE}}$, $p=0.0004$) (Figure 6.10.C).

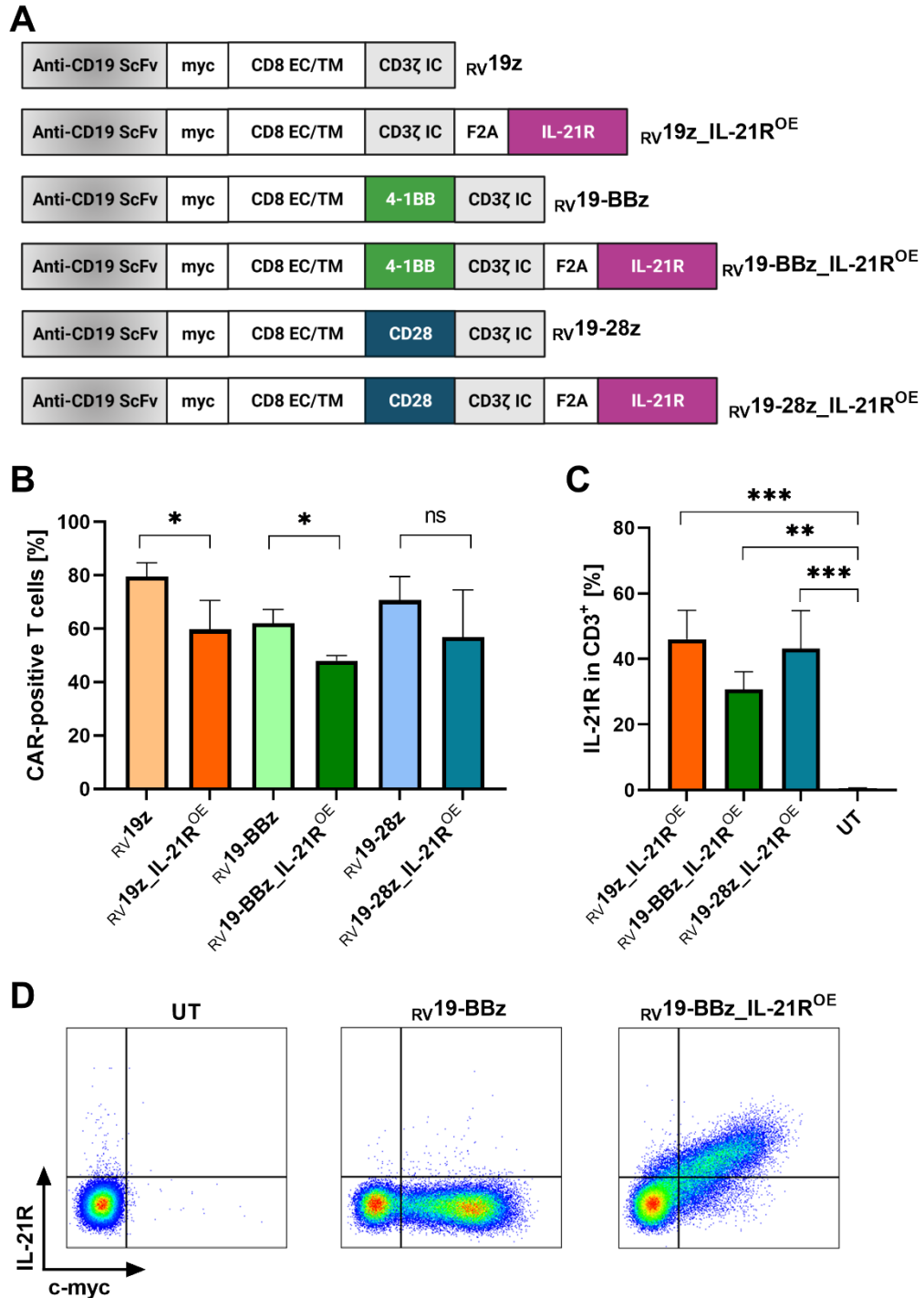


Figure 6.10 Generation of first- and second-generation anti-CD19 CAR T cells overexpressing IL-21R

A. Schematic drawing of the three bicistronic constructs with an F2A linker for equimolar translation of both CAR and IL-21R and controls. **B.** and **C.** Surface expression of CAR and IL-21R in first- and second-generation CAR T cells was determined via flow cytometry on day 10 of expansion. Data is representative of three donors and shown as mean \pm SD. The two-tailed, unpaired Student's t-test was used to compare CAR expression between every separate group. One-way ANOVA was performed for statistical testing to compare IL-21R surface expression between untransduced controls and IL-21R overexpressing CAR T cells. **D.** Exemplary FACS plots of $RV19-BBz_IL-21R^{OE}$ and controls proving simultaneous expression of the two receptors. ScFv: single chain variable fragment, EC: extracellular, TM: transmembrane, IC: intracellular, RV: retroviral, OE: overexpression.

Expansion rate did not differ significantly between the IL-21R overexpressing constructs and the corresponding conventional CAR T cells. On day ten after transduction (Figure 6.11.B), constructs with either a 4-1BB or CD28 co-stimulatory domain demonstrated a 29.6- to 36.7-fold expansion and IL-21R co-expression led to no disadvantage in the expansion numbers. Although the lowest expansion rate was noted in first-generation constructs (mean 17-fold, range 12- to 30-fold in $_{RV19z}$ vs. mean 20-fold, range 6- to 25-fold in $_{RV19z_IL-21R^{OE}}$, $p=0.719$), high cell numbers could be reached in all constructs just after ten days of expansion.

To monitor for slight changes due to IL-21R overexpression, the final T cell product was characterized on the last day of expansion. The phenotype of all tested constructs was skewed towards a less mature differentiation stage with stem cell-like memory and central memory cells being predominant. The mean sum of these varied between 85.2% and 90% among constructs, with no significant differences between IL-21R overexpressing and corresponding conventional CAR T cells (Figure 6.11.C). Frequency of naïve T cells was below 1% in all conditions. An exemplary comparison of $_{RV19z}$ and $_{RV19z_IL-21R^{OE}}$ yielded no significant difference in the mean percentage of central memory (68.1% vs. 53.1%, $p=0.259$), effector memory (13.5% vs. 8.2%, $p=0.214$) and effector (1.1% vs. 3.5%, $p=0.188$) T cells. Even though a higher percentage of stem cell-like memory T cells could be seen in the IL-21R overexpressing construct (35% vs. 17.1%, $p=0.1374$), this difference did not reach statistical significance. The same trend was observed in $_{RV19-BBz_IL-21R^{OE}}$ and $_{RV19-28z_IL-21R^{OE}}$ CAR T cells.

After the expansion period, cellular composition of the different constructs was analyzed on the last day of expansion to establish the purity of the T cell product (Figure 6.11.D). A mean range of 91.4% to 94.4% of T cells was seen in all tested CAR T cells. A small percentage of NK T cells (mean range of 3.7% to 5.3%) could be observed, as the culture medium facilitated their growth. Across all constructs, a high CD4/CD8 ratio of 1.9 was achieved, with a mean of 57.5% CD4⁺ T cells. An exemplary cellular composition of $_{RV19z_IL-21R^{OE}}$ was as follows: a mean of 36.4% CD8⁺, 50.1% CD4⁺, 5% NK T, 1.3% CD4⁺CD8⁺, 4% CD4⁻CD8⁻ T cells, and less of 1% of monocytes, NK, B cells and others. No significant differences in cellular composition were noted among CAR constructs.

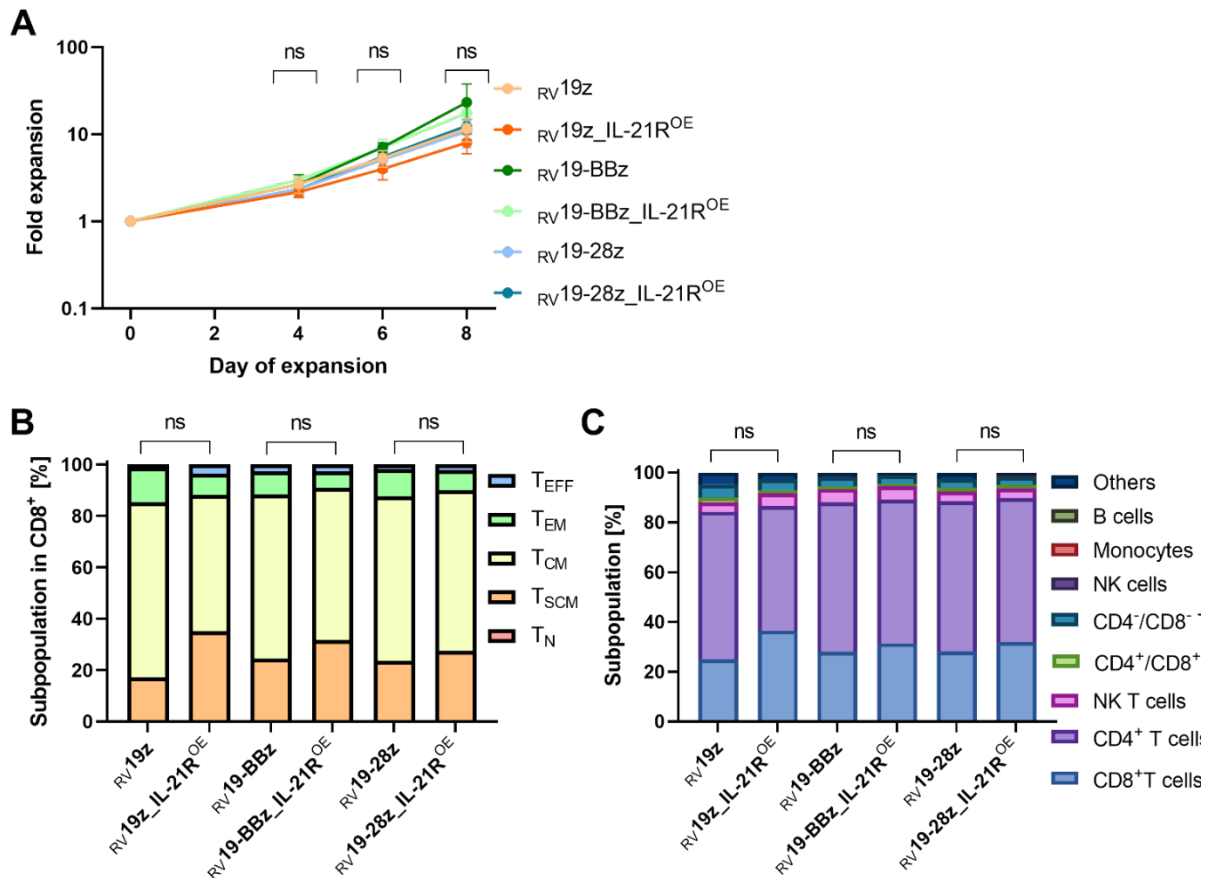


Figure 6.11 Characterization of the final CAR T cell product

Expansion rate was determined every two to three days during expansion by counting cells diluted 1:2 with trypan blue. Phenotype and cellular composition were measured via flow cytometry. **A.** High cell numbers could be reached after ten days of expansion with no difference in expansion rate between CAR constructs. **B.** CD8⁺ cells on day 10 of expansion show a predominantly memory phenotype with mostly T_{SCM} and T_{CM}, the latter reaching a mean of 62% among all constructs and donors. No significant difference in the sum of T_{SCM} and T_{CM} was seen between IL-21R overexpressing CAR T cells and their respective control. **C.** CD4⁺ cells made up the bulk of the final CAR T cell product on the last day of expansion with no significant difference between constructs. Groups of IL-21R overexpressing CAR and their respective first- or second-generation control were tested via the two-tailed, unpaired Student's t-test. Two-way ANOVA was used to compare cellular composition of the CAR constructs. Data is representative of three donors and shown as mean ± SD. T_N: naïve T cells, T_{SCM}: stem cell-like memory T cells, T_{CM}: central memory T cells, T_{EM}: effector memory T cells, T_{EFF}: effector T cells. NK cells: natural killer cells, NK T cells: natural killer T cells.

These results prove that the generation of IL-21R overexpressing anti-CD19 CAR T cells is feasible using bicistronic CAR constructs, with high transduction rates among the tested CAR T cells. Moreover, no disadvantage in expansion rate, phenotype or cellular composition was detectable on the last day of expansion, compared to conventional CAR T cells, despite the unphysiologically high surface expression of the IL-21R alpha chain. A predominantly stem cell-like memory- and central memory phenotype was observed among all tested constructs, with a high percentage of CD4⁺ T cells in the final product. Albeit insignificant, a trend towards a higher CD8 frequency and a higher CD8 T_{scm} frequency could be observed in first generation anti-CD19 CAR T cells and both second generation anti-CD19 CAR T cells overexpressing IL-21R.

6.3.2 Functionality of first- and second-generation IL-21R overexpressing anti-CD19 CAR T cells

To test the functionality of the IL-21R overexpressing anti-CD19 CAR T cells, the first- ($_{RV19z_IL-21R^{OE}}$) and the second-generation construct with a CD28 co-stimulatory domain ($_{RV19-28z_IL-21R^{OE}}$) were compared to the respective conventional CAR T cells in a co-culture setting with CD19⁺ Nalm6 target cells. As in previous experiments, IL-21 was added to the co-culture to enable interaction with the interleukin receptor. Figure 6.12.A illustrates the set-up of co-culture assays.

As a first-line functionality screening, direct cytotoxicity of anti-CD19 CAR T cells was examined at different effector-to-target (E:T) ratios, as described in 5.2.4. Untransduced cells were used to control for unspecific killing and showed a 30% lower mean killing rate at the 1:1 E:T ratio after 24 hours of co-culture (data not shown) compared to all tested CAR constructs. An E:T ratio-dependent target-cell killing was observed in all CAR constructs documenting CD19-specificity of anti-CD19 CAR T cells (Figure 6.12.B and C). At a 1:1 E:T ratio, mean cytotoxicity of $_{RV19z_IL-21R^{OE}}$ was similar to $_{RV19z}$ (mean 72.4% vs. 71.7%, $p=0.879$). Comparable results were obtained for the second-generation CAR construct (mean 71.4% in $_{RV19-28z_IL-21R^{OE}}$ vs. 74.8% in $_{RV19-28z}$, $p=0.569$). In general, cytotoxic capacity without addition of IL-21 was only marginally lower in IL-21R overexpressing CAR T cells. On stimulation with the ligand IL-21, the mean cytotoxic effect (79.6% in first-generation and 81.2% in second-generation CAR constructs) was increased in all conditions irrespective of the IL-21R alpha chain expression level (mean 79.3% in $_{RV19z_IL-21R^{OE}}$ vs. 79.9% in $_{RV19z}$, $p=0.368$, mean 80.4% in $_{RV19-28z_IL-21R^{OE}}$ vs. 82% in $_{RV19-28z}$, $p=0.281$).

In a further experiment, proliferation after 48 hours was measured via the fraction of Cell Trace violet negative CD8⁺ T cells, as described in the methods section. In first-generation CAR T cells with IL-21R overexpression a mean of 21.6% (range 10.1% to 30.7%) of bulk CD8⁺ cells proliferated upon contact with CD19⁺ target cells, whereas 19.5% (range 7% to 34.4%, $p=0.782$) of the $_{RV19z}$ cells proliferated (Figure 6.12.D). Addition of IL-21 to the co-culture induced a 39.8% increase in proliferation of $_{RV19z_IL-21R^{OE}}$ and a 37.9% increase in proliferation of $_{RV19z}$ CAR T cells, with no significant difference between constructs ($p=0.509$). Almost half of conventional $_{RV19-28z}$ cells (mean 49.1%, range 43% to 55.9%) proliferated in co-culture with Nalm6 target cells, whereas $_{RV19-28z_IL-21R^{OE}}$ demonstrated a slightly higher mean proliferation (mean 53%, range 45.1% to 58.2%, $p=0.283$). Contact with IL-21 did not significantly change proliferation of the second-generation CAR constructs in contrast to both first-generation constructs. A higher mean proliferation rate could be observed when gating on CD8⁺ CAR⁺ T cells, but no significant differences could be established regardless of construct and experimental conditions (data not shown).

In Figure 6.12.E increased proliferation of the CAR constructs after contact with CD19⁺ target cells is shown as fold change, with mean fluorescence intensity of the respective unstimulated cells serving as control. All tested constructs showed a CD19-specific increase in proliferation on contact with CD19⁺ target cells. The two IL-21R alpha chain overexpressing constructs demonstrated a 2- to 2.4-fold rise in proliferative capacity upon contact with CD19⁺ tumor cells in comparison to UT control cells (mean fold change in UT 0.84, $p=0.001$ and $p=0.0001$ vs. FC in $_{RV19z_IL-21R^{OE}}$ and $_{RV19-28z_IL-21R^{OE}}$, respectively). This was seen as further confirmation of the anti-CD19 specificity of both constructs.

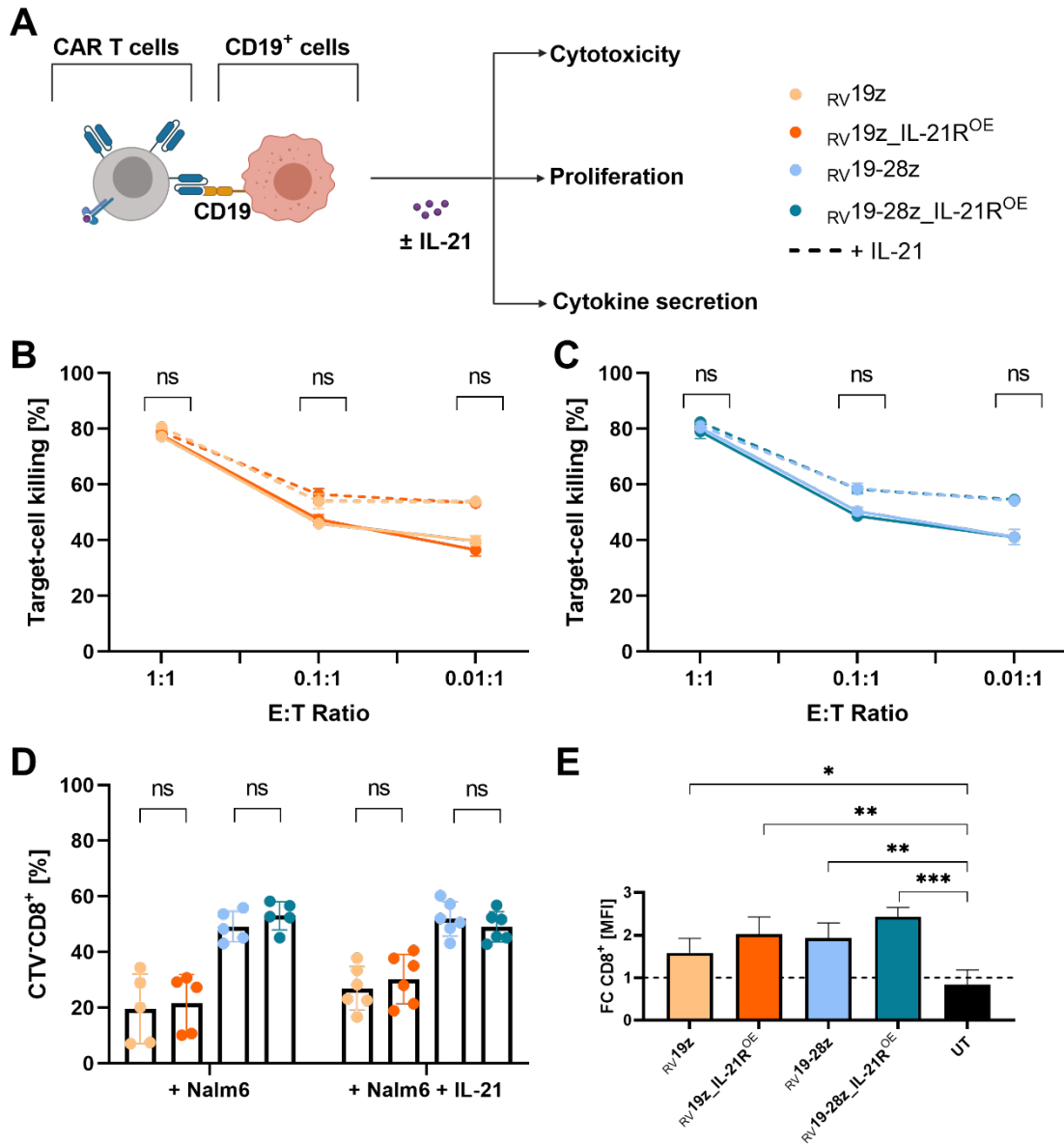


Figure 6.12 CD19-specific cytotoxicity and proliferation of IL-21R overexpressing CAR T cells

A. Schematic drawing showing the functionality assay setup. **B-C.** After 24 hours of co-culture with Nalm6 target cells, cytotoxicity was measured via flow cytometry at three E:T ratios and the effect of IL-21 investigated. A comparison is shown between the IL-21R overexpressing CAR T cells **B.** *RV19z_IL-21^{OE}*, **C.** *RV19-28z_IL-21^{OE}*, and the corresponding control CAR T cells. Upon addition of IL-21, no significant differences were detected between CAR constructs. Data is representative of two donors and experiments were performed in technical duplicates. **D.** Proliferation of IL-21R overexpressing CAR T cells and their respective controls after 48h of co-culture with Nalm6 target cells, shown for bulk CD8⁺ cells and examining the effect of IL-21 on addition to the co-culture. **E.** The increase in proliferation among the tested CAR T cells is demonstrated as fold change upon co-culture with Nalm6 cells, with the median fluorescence intensity of unstimulated CARs serving as baseline. Compared to the UT control cells, on average a 2-fold rise in proliferation could be observed among the different constructs, which demonstrated anti-CD19 specificity. Data in B-E. is representative of three donors and experiments were performed in technical duplicates. Data is shown as mean ± SD. The unpaired Student's t-test was used to compare every separate group and one-way ANOVA to perform multiple comparisons between IL-21R overexpressing CAR T cells and untransduced controls. MFI: median fluorescence intensity, FC: fold change, E:T ratio: effector-to-target ratio, CTV: cell-trace violet.

After 24 hours of co-culture with CD19⁺ targets, CD8⁺ CAR T cells were analyzed for INF- γ and TNF- α secretion. *RV19z_IL-21^{OE}* had a mean of 16.7% TNF- α ⁺ cells (range 5.3% to 25%) and *RV19z* 19.6% (range

17.3% to 25.6%, $p=0.416$). The second-generation construct with IL-21R overexpression also demonstrated a slightly lower secretion (mean 25%, range 13.8% to 42.4%) compared to the conventional control (mean 27%, range 20.2% to 30.4%, $p=0.710$). No significant difference was noted when the IL-21R overexpressing constructs were compared to conventional CAR T cells (mean 20.5% in $_{RV19z_IL-21R^{OE}}$ vs. mean 20.5% in $_{RV19z}$, $p=0.991$, mean 31.1% in $_{RV19-28z_IL-21R^{OE}}$ vs. mean 30% in $_{RV19-28z}$, $p=0.839$). Addition of IL-21 to the co-culture increased the mean percentage of $TNF-\alpha^+$ cells by 20.5% ($_{RV19z_IL-21R^{OE}}$) and 24.7% ($_{RV19-28z_IL-21R^{OE}}$). In general, $TNF-\alpha$ secretion did not differ significantly between IL-21R overexpressing CAR T cells and their conventional controls and IL-21 led to no significant increase in the mean frequency of $TNF-\alpha^+$ cells (Figure 6.13.A and B).

In contrast, when no IL-21 was added to the co-culture, $INF-\gamma$ secretion was significantly lower in $_{RV19z_IL-21R^{OE}}$ (mean 29.8%, range 17.5% to 42.6%) and $_{RV19-28z_IL-21R^{OE}}$ (mean 36.6%, range 24.3% to 44.5%) compared to conventional CAR T cells (vs. mean 44.7% in $_{RV19z}$, $p=0.014$, vs. mean 55.1% in $_{RV19-28z}$, $p=0.002$). This effect could, however, be partially reversed by adding IL-21 to the co-culture with IL-21R overexpressing CAR T cells, since a significant increase of $INF-\gamma^+$ cells could be observed in $_{RV19z_IL-21R^{OE}}$ (mean increase of 11.2%, $p=0.030$) and $_{RV19-28z_IL-21R^{OE}}$ cells (mean increase of 17.2%, $p=0.003$). This IL-21/IL-21R interaction was less pronounced in conventional CAR T cells and did not reach statistical significance (Figure 6.12.C and D).

In summary, the anti-CD19 specificity of both $_{RV19z_IL-21R^{OE}}$ and $_{RV19-28z_IL-21R^{OE}}$ CAR constructs was demonstrated in terms of direct cytotoxicity, proliferation and pro-inflammatory cytokine secretion. Most functional features of IL-21R overexpressing anti-CD19 CAR T cells were comparable to their IL-21R wild-type counterparts. However, a significantly reduced secretion of $INF-\gamma$ in co-culture when compared to the respective conventional CAR T cells stood out. Interestingly, addition of IL-21 to the co-culture led to a significant rise in $CD8^+ INF-\gamma^+$ CAR T cells in IL-21R OE anti-CD19 CAR T cells only.

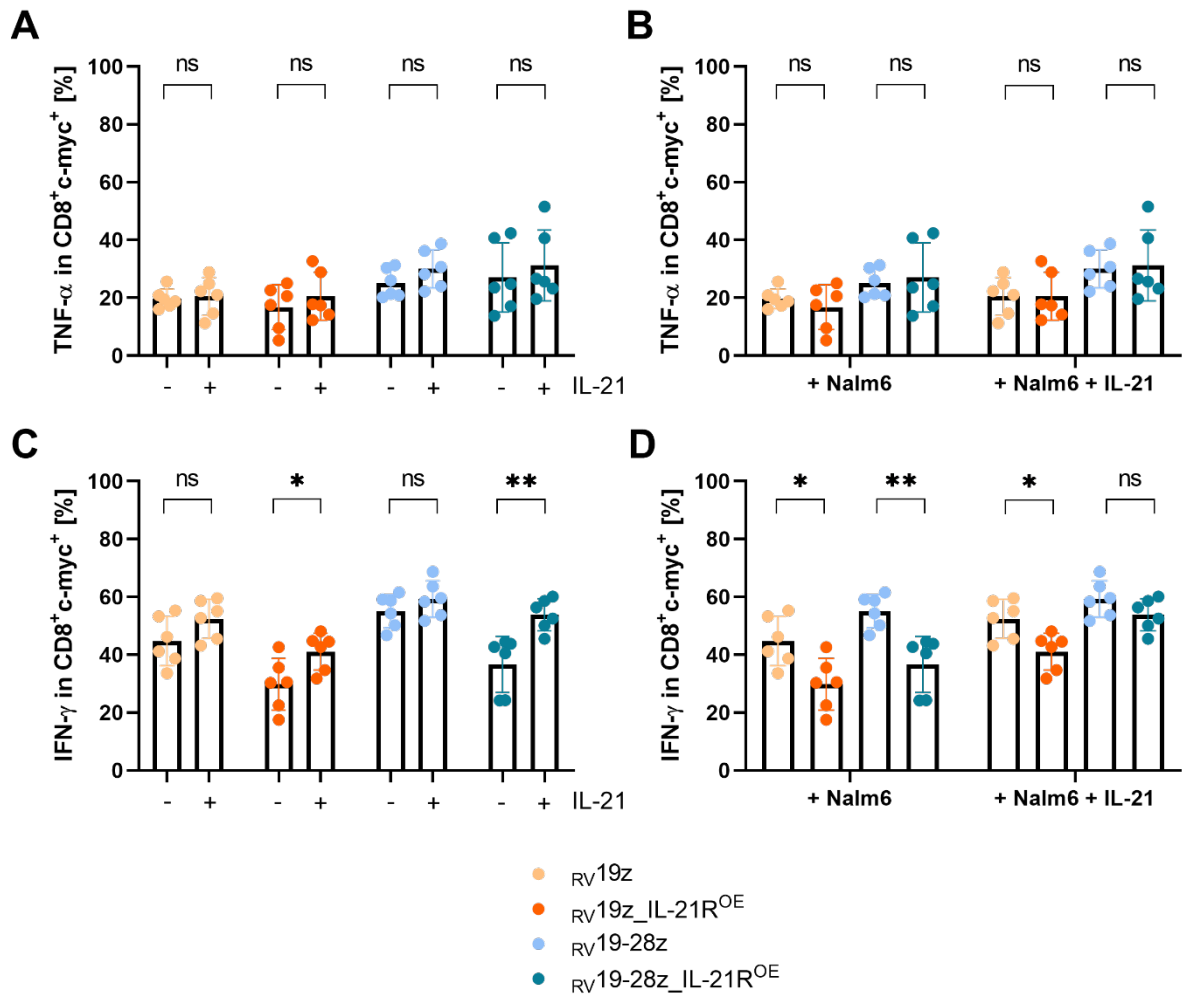


Figure 6.13 Intracellular cytokine staining of IL-21R overexpressing CAR T cells

CAR T cells were co-cultured with CD19⁺ targets \pm IL-21 for 24h. After addition of Brefeldin A for 2 hours, cells were fixed, permeabilized and stained, and intracellular cytokine secretion was determined via flow cytometry. Cytokine secretion is shown as percentage of CD8⁺ c-myc⁺ CAR T cells in the co-culture. **A.** and **B.** Comparison of TNF- α secretion and **C.** and **D.** IFN- γ secretion in the IL-21R overexpressing CAR constructs *RV19z_IL-21R^{OE}* and *RV19-28z_IL-21R^{OE}* and their controls. **A.** and **C.** Effect of IL-21 on cytokine secretion was evaluated within each construct separately. Despite similar TNF- α secretion of all constructs, a significant increase in IFN- γ levels was reached in the two constructs overexpressing the IL-21 receptor alpha chain. **B.** and **D.** Cytokine secretion between IL-21R overexpressing and conventional CAR was compared and showed significantly lower levels of IFN- γ in both *RV19z_IL-21R^{OE}* and *RV19-28z_IL-21R^{OE}* when no IL-21 was added. By adding IL-21 to the co-culture, IFN- γ secretion of the IL-21R overexpressing CARs reached the levels in conventional CAR T cells. Data is representative of three donors and experiments were performed in technical duplicates. Data is shown as mean \pm SD. The unpaired Student's t-test was used to compare every separate group. TNF- α : tumor necrosis factor alpha, IFN- γ : interferon gamma.

6.3.3 Generation of IL-21R CRISPR/Cas9 knock-out in second-generation anti-CD19 CAR T cells

After proving the general functionality of anti-CD19 CAR T cells overexpressing the IL-21 receptor alpha chain, further experiments focused on second-generation constructs with a 4-1BB costimulatory domain, reflecting the wide-spread clinical use of such constructs. A CRISPR/Cas9 genomic knock-out was performed on the third day after transduction of a second-generation conventional CAR construct with a 4-1BB costimulatory domain (*RV19-BBz_{CR}IL-21R^{KO}*), as described in 5.1.4. Negative control CAR T cells were electroporated with non-targeting crRNA instead of IL-21R gRNA (*RV19-BBz_{CR}Control*). To verify the genomic knock-out, DNA from both CAR T constructs was analyzed via Sanger sequencing and

compared via the webtool TIDE to determine knock-out efficiency, since flow-cytometric analysis of the IL-21R surface expression could not differentiate between the two CAR constructs (data not shown).

These two electroporated conditions were expanded alongside conventional CAR T cells ($_{RV19-BBz}$), as well as IL-21R overexpressing CAR T cells ($_{RV19-BBz_IL-21R^{OE}}$), both with a 4-1BB co-stimulatory domain. A schematic drawing of the four different conditions can be seen in Figure 6.14.A. CAR T cells were expanded for ten days following transduction of the CAR construct. Expansion was only compared between $_{RV19-BBz}$ and $_{RV19-BBz_IL-21R^{OE}}$, and similar rates to those shown in Figure 6.11.B were demonstrated. Since the electroporation procedure necessary for CRISPR/Cas9 genomic knock-out reduced expansion, no comparisons to non-electroporated CAR T cells were performed. $_{RV19-BBz_{CR}IL-21R^{KO}}$ and $_{RV19-BBz_{CR}Control}$ both expanded in a similar way, although the final total cell count was considerably lower than that of the non-electroporated $_{RV19-BBz}$ and $_{RV19-BBz_IL-21R^{OE}}$ (data not shown).

On the last day of expansion, phenotype and cellular composition of the final T cell product was characterized. Effector memory T cells predominated (mean 38.6%, range 37.8% to 41.9% among all constructs), even though some donor-specific variations were observed (Figure 6.14.B). Less than 1% naïve T cells remained after expansion. The mean sum of less differentiated cells (stem cell-like memory and central memory T cells) was highest among $_{RV19-BBz_IL-21R^{OE}}$ CAR T cells (mean 35.2%, range 32.4% to 37.1%). However, no statistical difference was observed in comparison to conventional CAR T cells (mean 25.9%, range 14.8% to 38.6%, $p=0.259$). The electroporated CAR T cells demonstrated comparable mean sum of T_{SCM} and T_{CM} (mean 27.1% in $_{RV19-BBz_{CR}IL-21R^{KO}}$ vs. 29.3% in $_{RV19-BBz_{CR}Control}$, $p=0.879$). In general, all tested constructs had a similar phenotypic differentiation, despite the slight tendency of IL-21R overexpressing CAR T cells towards a higher percentage of stem cell-like memory and central memory T cells.

In terms of cellular composition, the final product was pure with a T cell fraction of almost 90% (mean 88.6%, range 87.7% to 89.7%) among all tested constructs, as can be seen in Figure 6.14.C. The CD4/CD8 ratio ranged from 1.4 to 1.8 and was thus skewed towards a higher percentage of CD4⁺ T cells. Development of NK T cells (mean 7.2%) was facilitated by the culture medium. Cellular composition of $_{RV19-BBz_{CR}IL-21R^{KO}}$ was 28.2% CD8⁺, 53% CD4⁺, 2.6% CD4⁺CD8⁺, 3.8% CD4⁻CD8⁻ T cells, 7.3% NK T cells, and less than 1% of NK cells, monocytes, and other cell types. No significant differences in cellular composition were noted between constructs.

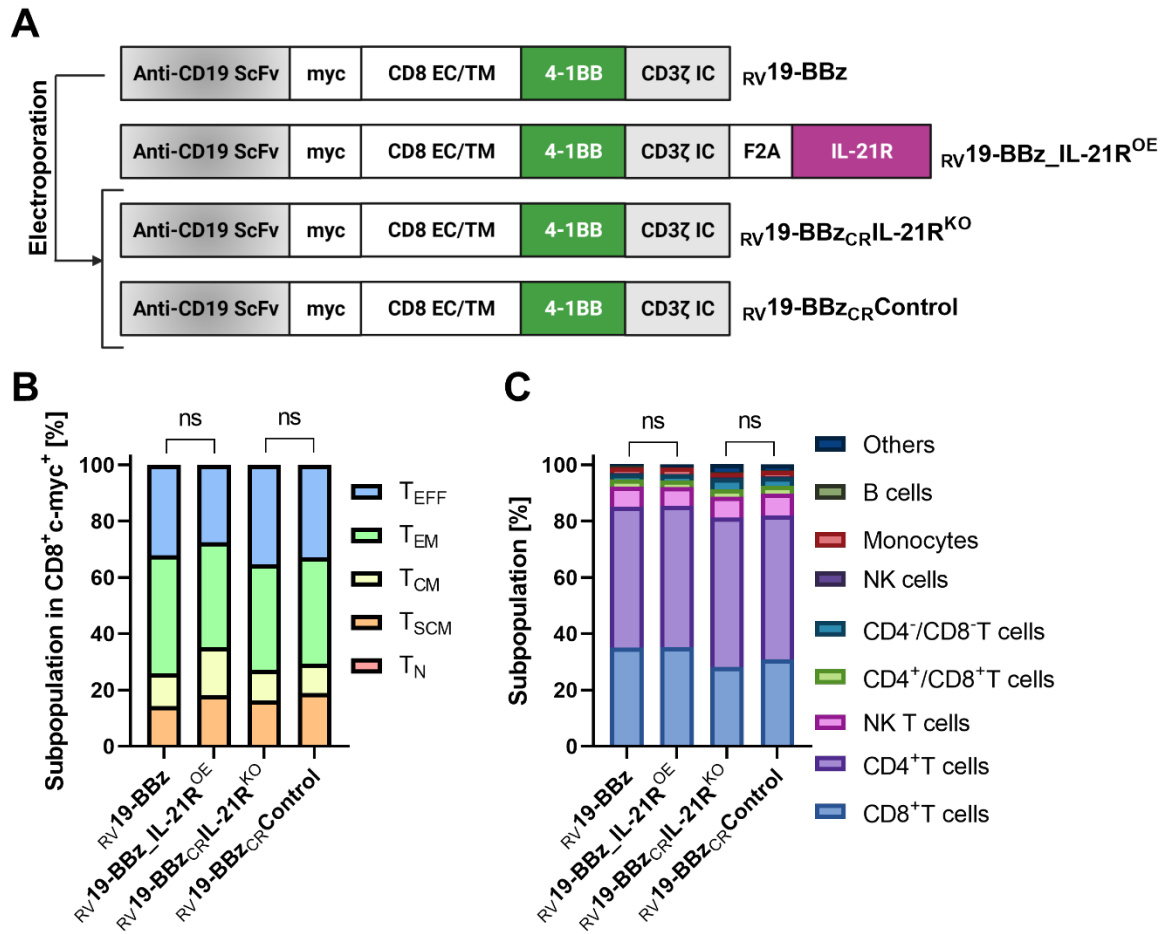


Figure 6.14 Generation of IL-21R CRISPR/Cas9 knock-out and overexpressing second-generation CAR T cells and characterization of the final cell product

A. Schematic drawing of the conventional CAR construct $_{RV19-BBz}$, the CRISPR/Cas9 knock-out $_{RV19-BBz_{CR}IL-21R^{KO}}$, the negative CRISPR/Cas9 control $_{RV19-BBz_{CR}Control}$ and the IL-21R alpha chain overexpressing CAR construct $_{RV19-BBz_IL-21R^{OE}}$. **B.** $CD8^+ c-myc^+$ cells on last day of expansion. Mean sum of T_{SCM} and T_{CM} was highest in $_{RV19-BBz_IL-21R^{OE}}$, but no statistical significance was reached. **C.** Cellular composition on day 10 of expansion. $CD4^+$ cells made up the bulk of the final CAR T cell product on the last day of expansion with no significant difference between constructs. Data is representative of three donors and shown as mean \pm SD. The unpaired Student's t-test was used to compare each separate group. Two-way ANOVA was used to compare cellular composition of the CAR constructs. ScFv: single chain variable fragment, EC: extracellular, TM: transmembrane, IC: intracellular, RV: retroviral, OE: overexpression, CR: electroporated cells, KO: CRISPR/Cas9 knock-out, T_N : naïve T cells, T_{SCM} : stem cell-like memory T cells, T_{CM} : central memory T cells, T_{EM} : effector memory T cells, T_{EFF} : effector T cells, NK cells: natural killer cells, NK T cells: natural killer T cells.

In summary, genomic knock-out of the IL-21R in second-generation CAR T cells with a 4-1BB costimulatory domain was feasible and the generated cells were as viable as control cells. Despite undergoing retroviral transduction followed by a CRISPR/Cas9 genomic knock-out, $_{RV19-BBz_{CR}IL-21R^{KO}}$ CAR T cells demonstrated similar phenotype and cellular composition at the end of expansion to electroporated controls, as well as to a conventional and an IL-21R alpha chain overexpressing CAR construct. The CRISPR/Cas9 genomic knock-out of IL-21R was not detrimental for the development of CAR T cells, which is consistent with results generated in primary T cells.

6.3.4 Functionality of IL-21R overexpressing and knock-out anti-CD19 CAR T cells

After generating viable second-generation CAR T cells, which either lacked or overexpressed the IL-21 receptor alpha chain, CD19-specific functionality was tested in a co-culture setting with CD19⁺ Nalm6 target cells. An overview of the assays can be seen in Figure 6.15.A.

As a first test of functionality, direct cytotoxicity was measured after 24 hours in co-culture at three E:T ratios via FACS. All CAR T cells demonstrated an E:T ratio-dependent target-cell killing and thus proved CD19-specific (Figure 6.15.B). Mean cytotoxicity of *RV19-BBz_IL-21R^{OE}* was comparable to the conventional CAR construct (mean 53.6% vs. 54.7%, $p=0.913$). Both electroporated constructs demonstrated a slightly elevated cytotoxicity by a few percentage points (mean 57.8% in *RV19-BBz_CRIL-21R^{KO}* vs. 57.6% in *RV19-BBz_{CR}Control*, $p=0.987$). However, the cytotoxic potential at the 1:1 E:T ratio was remarkably consistent among all constructs, independent of the level of IL-21R surface expression and genomic manipulation. When IL-21 was added to the co-culture (Figure 6.15.C), cell lysis was increased at the 1:1 E:T ratio by a mean of 9.1% in the IL-21R overexpressing and by 4.4% in the conventional CAR T cells (mean cytotoxicity 58.5% in *RV19-BBz_IL-21R^{OE}* vs. 57.1% in *RV19-BBz*, $p=0.830$). This effect, however, reached no significance when compared to the co-culture conditions without IL-21. In electroporated constructs, cytotoxic activity on IL-21 addition was slightly reduced, especially in the IL-21R knock-out CAR T cells by 10.9% (mean cytotoxicity 51.4% in *RV19-BBz_CRIL-21R^{KO}* vs. 54.1% in *RV19-BBz_{CR}Control*, $p=0.779$).

Next, CAR T cell proliferation was explored after 48 hours in co-culture with Nalm6 cells via the CTV method (Figure 6.15.D). IL-21R overexpressing CAR T cells demonstrated the highest proliferative capacity even without the addition of IL-21 (mean in CD8⁺c-myc⁺ cells 73.3% vs. 64.7% in *RV19-BBz*, $p=0.255$), whereas the electroporated CAR T cells had a minimum of 10% lower proliferation rate compared to the conventional construct (56.8% in *RV19-BBz_CRIL-21R^{KO}* vs. 58.1% in *RV19-BBz_{CR}Control*, $p=0.789$). The IL-21R knock-out cells consistently demonstrated the lowest percentage of proliferating cells, and this remained in effect on addition of IL-21 to the co-culture. While electroporated CAR T cells in general retained their baseline proliferative rate, *RV19-BBz_IL-21R^{OE}* cells reached a mean 16.7% increase to baseline and a significantly higher proliferation rate than the conventional CAR T cells (mean 85.6% in IL-21R overexpressing vs. 59.8% in *RV19-BBz* CAR T cells, $p=0.0015$).

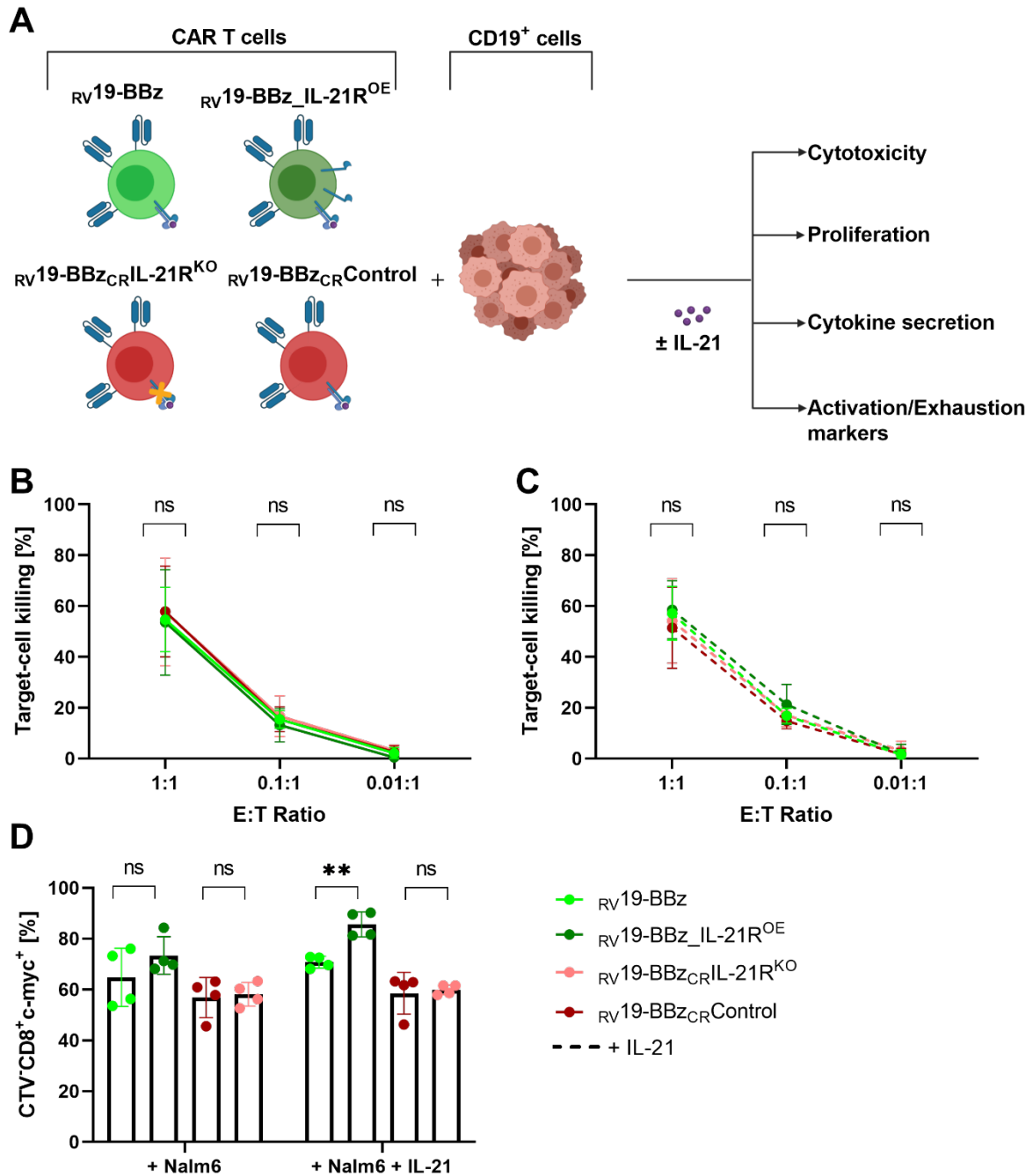


Figure 6.15 CD19-specific cytotoxicity and proliferation of IL-21R knock-out and overexpressing CAR T cells

A. Schematic drawing showing the functionality assay setup. **B.** After 24 hours of co-culture with Nalm6 target cells, cytotoxicity was measured via flow cytometry at three E:T ratios. **C.** Investigation of the effect of IL-21 on CD19-specific cytotoxicity of the constructs. No differences could be detected between the corresponding CAR T cells, with the IL-21R knock-out cells being as functional as the CRISPR control cells. A slight increase in cytotoxicity could be measured in IL-21R overexpressing CAR T cells compared to control, however, no significance was reached. Data is representative of three donors and experiments were performed in technical duplicates. **D.** Proliferation of CAR T cells after 48h of co-culture with Nalm6 target cells, shown for CD8⁺ c-myc⁺ cells. No difference between the conditions was seen when no IL-21 was added to the co-culture. However, IL-21 significantly increased proliferation of IL-21R overexpressing RV19-BBz_IL-21R^{OE} compared to the conventional CARs. IL-21 had hardly any effect on proliferation of the conventional RV19-BBz and the electroporated CARs. Data is shown for two donors and experiments were performed in technical duplicates. Data on the third donor can be accessed in the supplements. Data is shown as mean \pm SD. The two-tailed,

unpaired Student's t-test was used to compare each separate group. E:T ratio: effector-to-target ratio, MFI: median fluorescence intensity, FC: fold change, CTV: cell-trace violet.

In a further experiment, secretion of the cytokines INF- γ and TNF- α after 24 hours of co-culture was evaluated in CD8⁺ CAR T cells (Figure 6.16). The second-generation construct with an IL-21R alpha chain knock-out demonstrated a higher secretion of TNF- α compared to electroporated control cells (mean 27.7% in *RV19-BBz_{CR}IL-21R^{KO}* vs. mean 21.5% in *RV19-BBz_{CR}Control*, $p=0.030$). IL-21R overexpressing CAR T cells had the lowest mean frequency of TNF- α ⁺ cells (16.6%, range 15.6% to 17.7%), which was at least 50% higher in conventional *RV19-BBz* cells (26%, range 16.5% to 32.2%, $p=0.006$). Addition of IL-21 to the co-culture had two effects on TNF- α secretion: first, the TNF- α ⁺ frequency of *RV19-BBz_{IL-21R^{OE}}* CAR T cells rose by approximately 70% (mean 28.2%, range 26.6% to 31.2%). Second, a decrease in TNF- α ⁺ cells in the IL-21R knock-out cells was noted (mean 23.9% with IL-21 vs. 27.7% without IL-21, $p=0.111$). Moreover, on addition of IL-21 electroporated control CAR T cells secreted significantly more TNF- α in comparison to the IL-21R knock-out condition (mean 26.8% vs. 23.9%, $p=0.049$). In general, when no IL-21 was added to the co-culture, TNF- α secretion was lowest in IL-21R overexpressing CAR T cells. The ligand, however, led to a significant increase in the mean percentage of TNF- α ⁺ cells (Figure 6.16.A and B). Among electroporated cells, levels of TNF- α secretion depended less on the presence of IL-21 and even decreased when a genomic knock-out of the receptor had taken place.

Similar results were seen regarding INF- γ secretion (Figure 6.16.C and D). Without IL-21 in the co-culture, the mean percentage of INF- γ ⁺ was 32.9% in conventional *RV19-BBz* cells (range 27.4% to 36.8%), and significantly lower in *RV19-BBz_{IL-21R^{OE}}* cells (mean 13.6%, range 8.4% to 19.4%, $p<0.0001$). However, this effect could be reversed via IL-21, since a significant 95% increase in INF- γ secretion was observed in the IL-21R overexpressing construct (mean 26.5%, range 18.2% to 40.8% with IL-21, $p=0.183$), although the absolute INF- γ secretion remained lower compared to conventional CAR T cells (vs. mean 37.2% in *RV19-BBz*, $p=0.053$). Mean values between the two electroporated constructs were comparable (mean 29.3%, range 17.9% to 40.4% in *RV19-BBz_{CR}IL-21R^{KO}* vs. mean 34.4%, range 27.9% to 43% in *RV19-BBz_{CR}Control*, $p=0.307$). On addition of IL-21 to the co-culture, INF- γ secretion in the electroporated CAR T cells increased non-significantly by a mean of 16.6% independent of IL-21R knockout.

Next, the effect of IL-21 on the surface expression of exhaustion markers in CD8⁺ CAR T cells was examined (Figure 6.16). The co-inhibitory markers TIM-3 and PD-1 were measured via flow cytometry 24 hours after contact with CD19⁺ target cells. Mean fluorescence intensity (MFI) was used as indicator for surface expression. Due to high interdonor variance in expression, fold change on addition of IL-21 was calculated relative to basal surface expression in unstimulated CAR T cells. Even though the interaction with IL-21 in a co-culture setting led to the upregulation of TIM-3 surface expression, no significant difference between IL-21R alpha chain overexpressing and conventional CAR T cells was noted (mean 10-fold vs. mean 8.3-fold in *RV19-BBz*, $p=0.367$), as seen in Figure 6.16.E. A similar effect was observed in regard to PD-1 surface expression, which was also comparable between the tested constructs (Figure 6.16.F).

These experiments proved that CD19-specific functionality was retained in the tested second-generation CAR constructs independent of the type of genetic manipulation. Moreover, a CRISPR/Cas9 genomic knock-out of the IL-21R led to no detrimental effects on CAR functionality. In general, addition of IL-21 to the co-culture with CD19⁺ target cells had a minimal effect on *RV19-BBz_{CR}IL-21R^{KO}* cells. Cytotoxicity was similar among constructs, whereas proliferation was markedly higher in *RV19-BBz_{IL-21R^{OE}}* cells, especially when IL-21 was added. Secretion of INF- γ and TNF- α did not change after knock-out of the IL-21R alpha chain, since both electroporated CAR constructs demonstrated a similar frequency of secreting cells. Interestingly, overexpressing the IL-21R alpha chain in a CAR setting led to a significant decrease in basal cytokine secretion. The addition of IL-21, however, partially reversed this effect. No marked short-term exhaustion was observed in the construct overexpressing the IL-21R alpha chain after contact with IL-21.

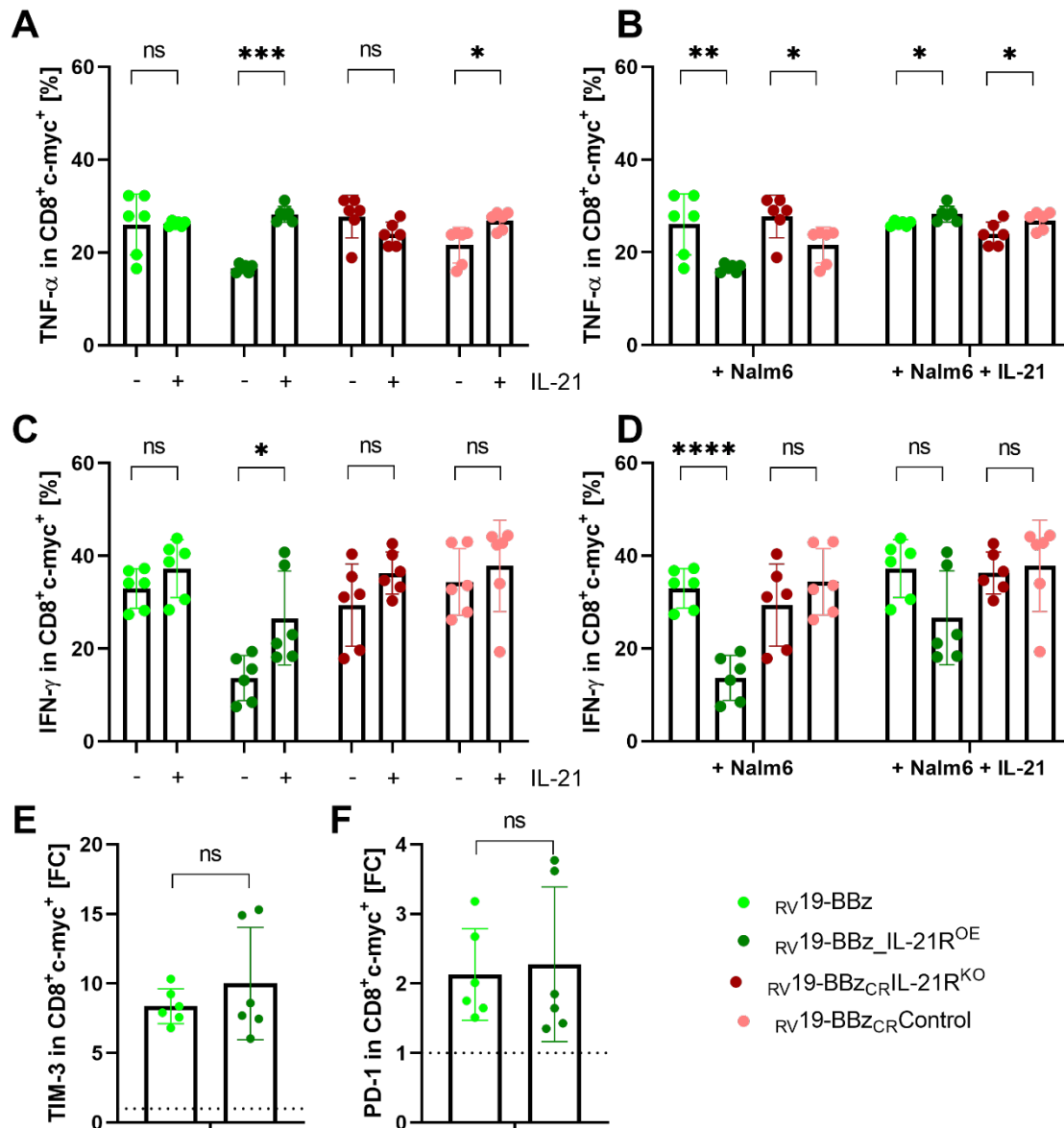


Figure 6.16 Intracellular cytokine staining and expression of co-inhibitory markers in IL-21R knock-out and overexpressing CAR T cells

CAR T cells were co-cultured with CD19⁺ targets ± IL-21 for 24h. For ICS, Brefeldin A was added for 2 hours, cells were fixed, permeabilized and stained, and intracellular cytokine secretion was determined via flow cytometry. Cytokine secretion is shown as percentage of CD8⁺ c-myc⁺ CAR T cells in the co-culture. Surface expression of the exhaustion markers TIM-3 and PD-1 was measured via FACS and the mean fluorescence intensity of the markers in CD8⁺ c-myc⁺ CAR T cells in co-culture with IL-21 was evaluated as fold change with the respective unstimulated CAR construct serving as baseline. **A.** and **B.** Comparison of TNF-α secretion and **C.** and **D.** IFN-γ secretion in the IL-21R overexpressing CAR construct *RV19-BBz_IL-21ROE*, the CRISPR/Cas9 IL-21R knock-out *RV19-BBzCR_IL-21KO* and their respective controls. **A.** and **C.** Effect of IL-21 on cytokine secretion was evaluated within each construct separately. **B.** and **D.** Cytokine secretion between IL-21R overexpressing and conventional CAR was compared and showed a consistently lower IFN-γ⁺ and TNF-α⁺ cells in *RV19-BBz_IL-21ROE* when no IL-21 was added. By adding IL-21 to the co-culture, this effect could be equalized and even reversed in terms of TNF-α secretion. Electroporation of the CAR T cells did not lead to a detrimental effect on cytokine secretion. **E.** The exhaustion markers TIM-3 and **F.** PD-1 are not significantly upregulated after contact of IL-21R alpha chain overexpressing CAR T cells with IL-21 in co-culture. Data is representative of three donors and experiments were performed in technical duplicates. Data is shown as mean ± SD. The two-tailed, unpaired Student's t-test was used to compare every separate group. TNF-α: tumor necrosis factor alpha, IFN-γ: interferon gamma, MFI: mean fluorescence intensity, FC: fold change.

6.3.5 Cytokine secretion and T helper phenotype of IL-21R overexpressing and knock-out anti-CD19 CAR T cells

Based on the results in 6.3.4, the lower percentage of cytokine secretion in $RV19-BBz_IL-21R^{OE}$ cells and the pronounced increase in this condition upon addition of IL-21, a cytokine profiling of the different CAR T cell constructs was performed via a bead-based immunoassay, as described in 5.2.10. The aim was to further characterize how the interaction between IL-21 and its receptor may change the functionality of the immune cells in a co-culture setting with $CD19^+$ target cells.

The heatmap in Figure 6.17.A shows the concentration of analyzed cytokines on addition of IL-21 to the co-culture, which was evaluated as fold change with the respective CAR construct in co-culture without IL-21 serving as baseline. This proved beneficial to visualize up- and downregulation of cytokine secretion depending on the presence of IL-21 in the four tested CAR T cell constructs. Thus, we aimed to identify cytokines specifically impacted by IL-21 signaling for further analysis.

Secretion of the cytokines IL-2 and IFN- γ was first evaluated, as both showed a distinct pattern. Concentration of IL-2 (Figure 6.17.B) was lowest in the IL-21R overexpressing CAR T cells (8.8 ng/ml, range 2.9 ng/ml to 15.5 ng/ml), which was only marginally higher in conventional $RV19-BBz$ cells (10.9 ng/ml, range 7.6 ng/ml to 14.3 ng/ml, $p=0.584$). Electroporated constructs demonstrated a higher basal secretion of IL-2 (mean 15.6 ng/ml in $RV19-BBz_CRIL-21R^{KO}$ vs. mean 24.2 ng/ml in $RV19-BBz_{CR}Control$, $p=0.271$) in a co-culture setting. Addition of the ligand led to a significant rise in IL-2 concentration in $RV19-BBz_IL-21R^{OE}$ cells (mean 17.5 ng/ml with IL-21 vs. mean 8.8 ng/ml without IL-21, $p=0.049$). At the same time, secretion of IL-2 by other tested CAR T cells was not influenced by IL-21, even slightly decreased on addition of the ligand. Therefore, an increase in IL-2 concentration could only be achieved if IL-21 interacted with its overexpressed receptor.

In contrast, IL-21 increased the concentration of IFN- γ in all constructs (Figure 6.17.C). IFN- γ rose more than 5-fold in $RV19-BBz_IL-21R^{OE}$ (mean 9765.6 ng/ml with IL-21 vs. mean 1660.6 ng/ml without IL-21, $p=0.0003$), 4-fold in $RV19-BBz$ (mean 5394.7 ng/ml with IL-21 vs. mean 1313.3 ng/ml without IL-21, $p=0.003$) and 3-fold in $RV19-BBz_{CR}Control$ cells (mean 12216.1 ng/ml with IL-21 vs. mean 3563.2 ng/ml without IL-21, $p=0.035$). This effect seemed to depend on the presence of IL-21R in the CAR T cells, as IFN- γ in $RV19-BBz_CRIL-21R^{KO}$ cells increased less than 1.5 times after addition of IL-21, with the lowest absolute concentration among all constructs (mean 4372 ng/ml with IL-21). Thus, disruption of the interaction between IL-21 and its receptor by IL-21R knock-out led to IL-21 having no effect on IFN- γ secretion in the presented co-culture setup. Moreover, even though basal expression of the IL-21 receptor alpha chain was associated with an increase in IFN- γ secretion after addition of IL-21 to the co-culture, the effect was most pronounced in anti-CD19 CAR T cells overexpressing the IL-21R (mean 5394.7 ng/ml in $RV19-BBz$ vs. mean 9765.6 ng/ml in $RV19-BBz_IL-21R^{OE}$, $p=0.0124$).

A marked effect of IL-21 on the IL-21R alpha chain overexpressing CAR T cells was observed regarding IL-10 concentration, which rose more than 80-fold on addition of IL-21 to the co-culture (mean 4.3 ng/ml without IL-21 vs. mean 359.6 ng/ml with IL-21, $p=0.005$), as can be seen in Figure 6.17.D. A less pronounced but significant increase in IL-10 secretion was observed in $RV19-BBz$ (mean 3 ng/ml without IL-21 vs. mean 31.7 ng/ml with IL-21, $p=0.021$) and $RV19-BBz_{CR}Control$ cells (mean 37.6 ng/ml without IL-21 vs. mean 164.7 ng/ml with IL-21, $p=0.029$). This was not the case in $RV19-BBz_CRIL-21R^{KO}$ cells, which mostly retained their baseline IL-10 concentration after IL-21 addition. Thus, Interaction of the ligand with its overexpressed receptor led to a remarkably increased production of IL-10. To verify these results, an IL-10 ELISA assay with the same co-culture conditions was performed (Figure 6.17.E), which showed consistent results.

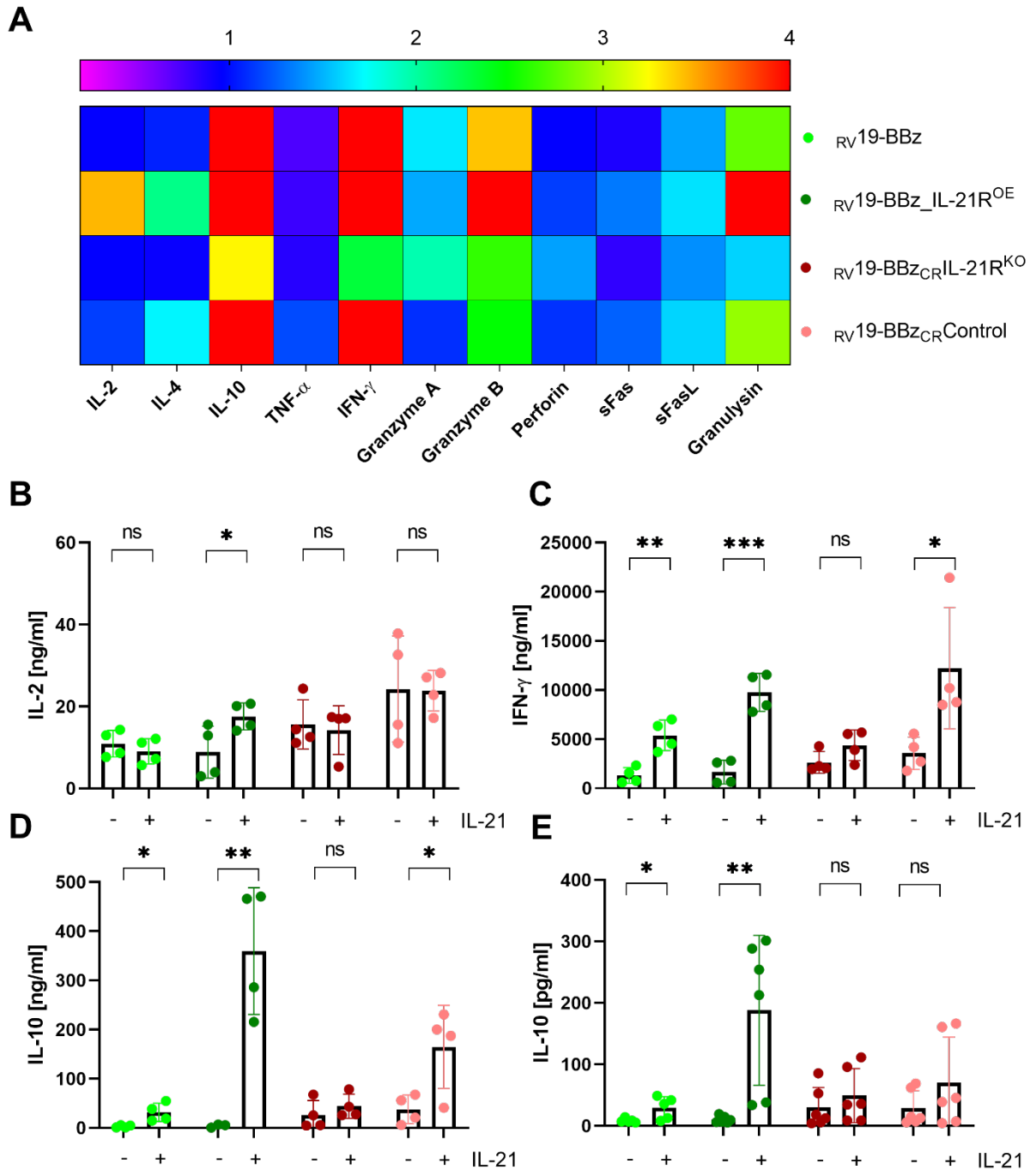


Figure 6.17 Cytokine profile of IL-21R overexpressing and knock-out anti-CD19 CAR T cells

A predefined bead-based assay for CD8⁺ T cells was used to simultaneously measure concentrations of different cytokines. CAR T cells were co-cultured with Nalm6 cells at a 1:1 E:T ratio \pm IL-21 for 24 hours and the supernatants were harvested and measured via FACS. **A.** A heatmap visualization of the cytokine profile of the four tested CAR T cell constructs. The cytokine concentration after addition of IL-21 to the co-culture was evaluated as fold change relative to the concentration in a co-culture setting without IL-21. **B.** IL-2 concentration was lowest in RV19-BBz_IL-21R^{OE} in co-culture without IL-21, but increased significantly when the ligand was added to the co-culture. Electroporated CAR T cells had a higher baseline IL-2 secretion. **C.** IFN- γ concentration rose significantly in all CAR T cells with normal surface expression of IL-21R or overexpressed receptor. This effect was less pronounced in RV19-BBz_{CR}IL-21R^{KO} cells. **D.** IL-10 concentration increased in the IL-21R overexpressing CAR T cells most after IL-21 was added to the co-culture. Data in A.-D. is shown for two donors and experiments were performed in technical duplicates. **E.** An IL-10 ELISA assay was performed to validate the effect of IL-21 on IL-10 secretion by RV19-BBz_IL-21R^{OE} cells. Data is shown for three donors

as mean \pm SD and experiments were performed in technical duplicates. The two-tailed, unpaired Student's t-test was used to compare each separate group. TNF- α : tumor necrosis factor alfa, IFN- γ : interferon gamma, sFasL: Fas ligand.

To better understand the significant increase in IL-10 concentration in $_{RV19-BBz_IL-21R^{OE}}$ cells after their interaction with IL-21 in a co-culture setting, the T helper phenotype of the tested CAR T cells was compared between four groups (CAR T cells only, CAR T cells on addition of IL-21, co-culture of CAR T cells with CD19⁺ targets, co-culture on addition of IL-21). The aim was to recognize a discrete T helper population in the IL-21R overexpressing CAR T cells which could account for the rise in IL-10 production.

The manually gated populations were analyzed according to 5.1.5 and 5.2.8 (Figure 6.18.A and .B). The condition consisting only of IL-21R alpha chain overexpressing CAR T cells showed many undifferentiated Th0 cells (mean 23.6%), followed by Th1 Th17 (mean 20.2%) and CCR6⁺ cells (mean 17%). The remaining CD4⁺ cells were distributed as follows: a mean of 8.5% CXCR3⁺ Th17, 14.3% Th17, 3.5% CXCR3⁺ Th2, 6.3% Th2 and 6.2% Th1 cells. Addition of the ligand IL-21 to the $_{RV19-BBz_IL-21R^{OE}}$ T cells led to no significant differences between the T helper subsets. As can be seen in the exemplary FACS plots, less naïve cells remained after contact of the CAR T cells with CD19⁺ Nalm6 target cells (mean 23.6% with CAR T cells only vs. mean 10.6%, $p=0.079$). A significant rise in CXCR3⁺ Th17 cells was observed (mean 8.5% with CAR T cells only vs. mean 23.1% in co-culture with Nalm6 cells, $p=0.039$). Distribution of the other T cell populations remained similar after co-culture. Addition of IL-21 to the co-culture had no significant impact on the phenotype of CAR T cells in co-culture.

In a further step, the T helper surface marker expression of the four anti-CD19 CAR constructs described in section 6.3.3 was compared in a co-culture setting with Nalm6 cells upon addition IL-21 and can be seen in Figure 6.18.C. However, no statistical difference between the Th populations of the tested constructs could be demonstrated which could have explained the increase of IL-10 secretion upon addition of IL-21 to the co-culture containing IL-21 receptor overexpressing CAR T cells.

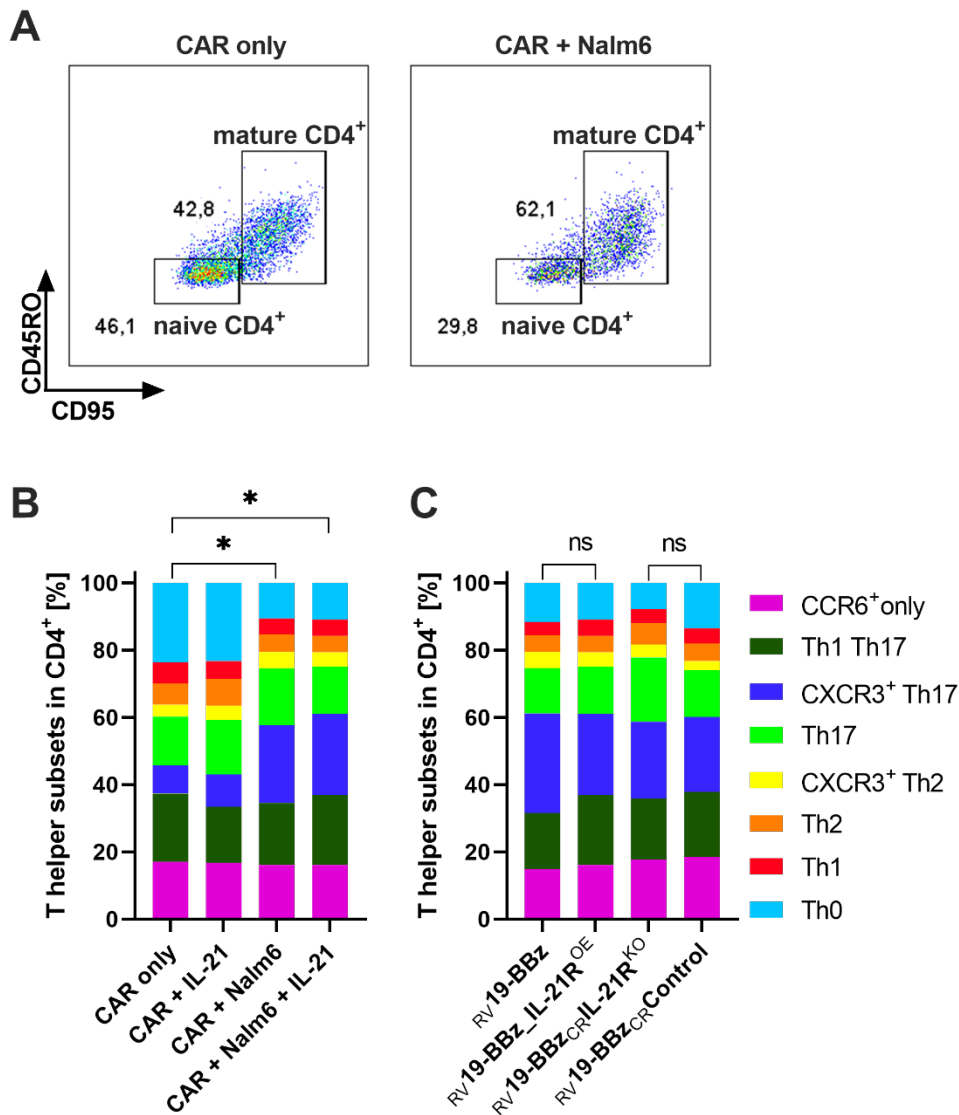


Figure 6.18 T helper phenotype of CD4⁺ IL-21R overexpressing and knock-out anti-CD19 CAR T cells

Phenotype was measured 24 hours after experimental setup via FACS. **A.** Exemplary FACS plots from one donor demonstrate the difference in the frequency of naïve and mature CD4⁺ IL-21R overexpressing CAR cells as defined by the surface expression of CD45RO and CD95, depending on the presence of CD19⁺ target cells. **B.** The T helper phenotype of CD4⁺ IL-21R overexpressing CAR T cells in four different culture conditions. A significant increase in the CXCR3⁺ Th17 population was observed after contact with Nalm6 target cells. Addition of IL-21 did not significantly change T helper subset frequency. **C.** The T helper phenotype of the four constructs (*RV19-BBz*, *RV19-BBz_IL-21R^{OE}*, *RV19-BBz_CRIL-21R^{KO}* and *RV19-BBz_CRControl*) was assessed 24 hours after co-culture with CD19⁺ target cells and IL-21. The ligand did not change the phenotypic distribution of CD4⁺ CAR T cells. This effect was not construct-dependent. Data is representative of three donors and shown as mean. Two-way ANOVA was performed to compare Th subsets. CAR only: only CAR T cells, CAR + IL-21: CAR T cells on addition of IL-21, CAR + Nalm6: co-culture of CAR T cells with Nalm6 target cells, CAR + Nalm6 + IL-21: addition of IL-21 to the co-culture, Th: T helper cells.

6.4 Retroviral transduction of IL-21R and IL-21 in purified CD4⁺ and CD8⁺ anti-CD19 CAR T cells

6.4.1 Generation of CD4⁺ and CD8⁺ anti-CD19 CAR T cells

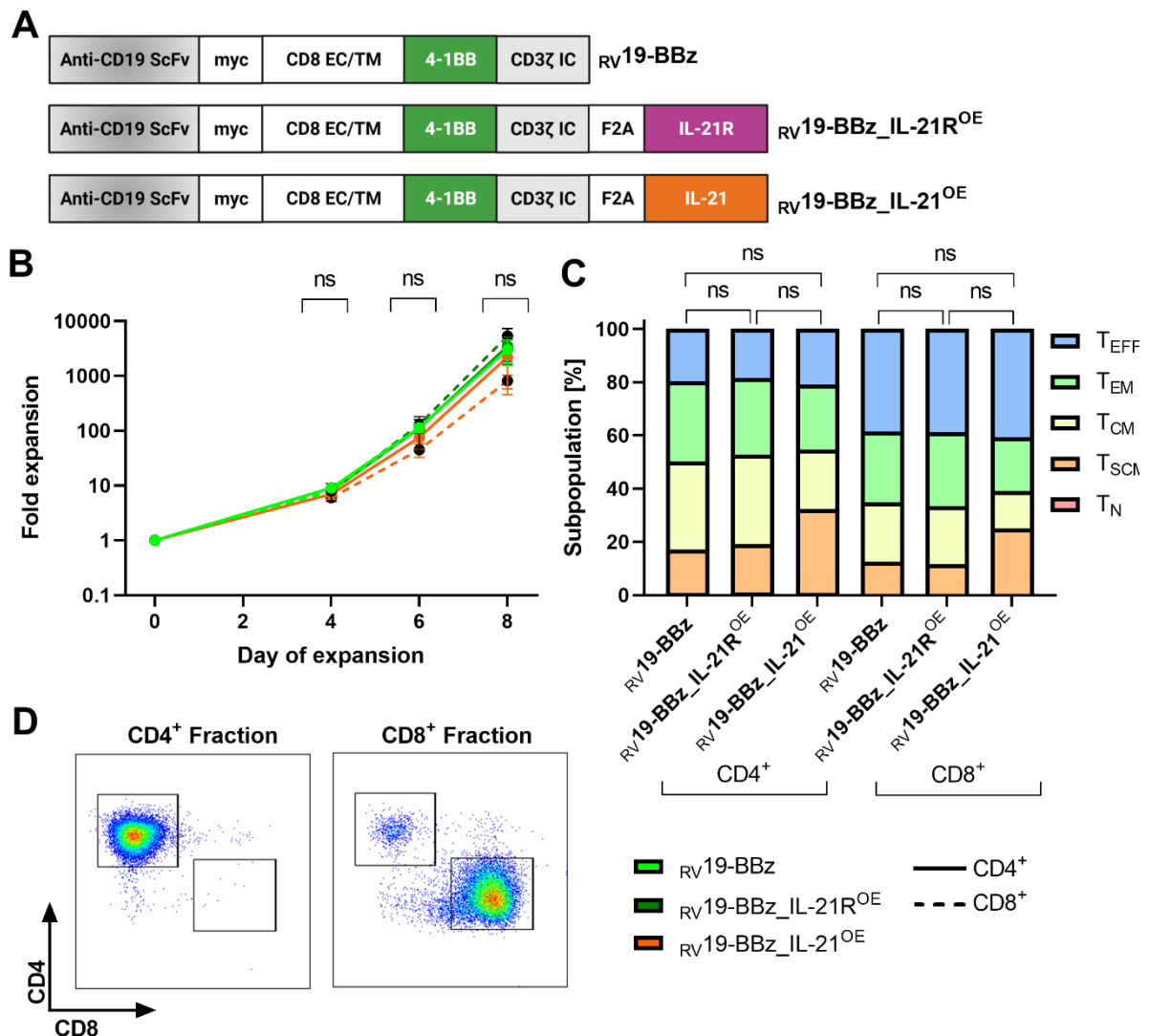


Figure 6.19 Generation of purified CD4⁺ and CD8⁺ second-generation CAR T cells with IL-21R and IL-21 overexpression

A. Schematic drawing of the three generated second-generation CAR constructs with a 4-1BB endodomain: conventional (RV19-BBz), IL-21R overexpressing (RV19-BBz_IL-21R^{OE}), and IL-21 overexpressing (RV19-BBz_IL-21^{OE}) CAR T cells. **B.** CD4⁺ and CD8⁺ T cells were isolated, activated and transduced with one of three CAR constructs and expanded separately. Expansion rate was determined every two to three days via cell counting after staining with trypan blue. Fold expansion is relative to the number of cells used for transduction and no differences were found among tested constructs. **C.** On the last day of expansion, transduced CD4⁺ cell showed a high percentage of less differentiated stem cell-like memory and central memory cells. CD8⁺ T cells had a more mature phenotype consisting of mostly T_{EFF} and T_{EM}. No significant difference in the sum of T_{SCM} and T_{CM} was seen. **D.** Purity of isolated T cells was controlled via FACS prior to transduction and on the last day of expansion. Data is representative of at least two donors and shown as mean ± SD. One-way ANOVA was used to compare groups. ScFv: single chain variable fragment, EC: extracellular, TM: transmembrane, IC: intracellular, RV: retroviral, OE: overexpression, T_N: naïve T cells, T_{SCM}: stem cell-like memory T cells, T_{CM}: central memory T cells, T_{EM}: effector memory T cells, T_{EFF}: effector T cells, NK cells: natural killer cells, NK T cells: natural killer T cells.

As a final investigation of in vitro functionality, the interaction between IL-21 producing CD4⁺ and IL-21R expressing CD8⁺ T cells in physiology was mimicked in a CAR setting. For this purpose, CD4⁺ and CD8⁺ T cells were isolated separately from PBMCs, activated and transduced with one of three second-generation CAR constructs containing a 4-1BB co-stimulatory domain: a conventional (RV19-BBz), an IL-21R overexpressing (RV19-BBz_IL-21R^{OE}), and an IL-21 overexpressing (RV19-BBz_IL-21^{OE}) CAR construct (Figure 6.19.A). CD4⁺ and CD8⁺ CAR T cells were then expanded separately and no significant differences in fold expansion could be measured between conditions (Figure 6.19.B). IL-2 was used for the expansion of CD8⁺ CAR T cells in order to ensure sufficient cell numbers, since CD8⁺ T cell expansion was very low when using IL-7 and IL-15, as documented in the methods' section (5.1.1). IL-21 secretion was determined via ELISA and supernatants from RV19-BBz_IL-21^{OE} CAR T cells had a significantly higher concentration of the ligand compared to UT and other CAR T cells (data not shown).

On last day of expansion of cells from two donors, a mean of 51.7% of all CD4⁺ CAR T cells consisted of T_{SCM} and T_{CM} cells. No significant differences could be measured between CD4⁺ conditions overexpressing either the IL-21R alpha chain or IL-21 (mean sum of T_{SCM} and T_{CM} 51.9% in RV19-BBz_IL-21R^{OE} vs. 53.9% in RV19-BBz_IL-21^{OE}, p=0.996), and these were both comparable to CD4⁺ cells with a conventional second-generation CAR. In contrast, CD8⁺ T cells had a more mature phenotype after expansion in IL-2, made up mostly of T_{EFF} and T_{EM}, with the mean percentage of T_{SCM} and T_{CM} being only 35.4%. Of note is the higher percentage of stem-cell like memory cells in both CD4⁺ and CD8⁺ CAR T cells overexpressing IL-21, even though no significant difference between CAR constructs could be detected (for CD4⁺, mean 31.6% vs. 18.2% in RV19-BBz_IL-21R^{OE}, p=0.602, for CD8⁺, mean 24.5% vs. 11.3% in RV19-BBz_IL-21R^{OE}, p=0.820). The isolated cell product was characterized prior to transduction and on the last day of expansion and demonstrated purity of CD4⁺ and CD8⁺ T cells exceeding 95% and 90%, respectively. Exemplary FACS plots of CD4⁺ and CD8⁺ population of conventional CAR T cells from one donor can be seen in Figure 6.19.D.

6.4.2 Functionality of IL-21R and IL-21 overexpressing CD4⁺ and CD8⁺ anti-CD19 CAR T cells

After successful generation of separate populations of CD4⁺ and CD8⁺ CAR T cells overexpressing IL-21 or IL-21R, CD4⁺ RV19-BBz_IL-21^{OE} and CD8⁺ RV19-BBz_IL-21R^{OE} CAR T cells were combined at a 1:1 ratio in a co-culture with CD19⁺ Nalm6 target cells, with the aim of mimicking the biological interaction between IL-21 and its receptor (a schematic drawing of the experimental setup can be seen in Figure 6.20.A). IFN- γ secretion of the CD8⁺ c-myc⁺ CAR T cells was measured 24 hours after co-culture and compared to that of other combinations of CD4⁺ and CD8⁺ CAR T cells. The intracellular cytokine staining assay was chosen, as it most prominently and sensitively showed differences between experimental conditions in previous experiments. Some data for this experiment were generated by Semjon Willier.

The experimental setting consisting of CD4⁺ RV19-BBz_IL-21^{OE} and CD8⁺ RV19-BBz_IL-21R^{OE} cells was compared to a 1:1 CD4⁺ to CD8⁺ mix of conventional second-generation CAR T cells (RV19-BBz), since therapy with a similar second-generation CAR construct is currently in clinical use. In this case, interaction between IL-21 and IL-21R in the respective overexpressing CAR T cells was superior in terms of CD8⁺ CAR T cell IFN- γ secretion when compared to the current standard of care (mean 17.2%, range 12.9% to 23.7% vs. mean 8.5% in CD4⁺ RV19-BBz and CD8⁺ RV19-BBz, range 5% to 12.9%, p=0.003). Similar results were obtained on comparison of the original condition to a combination of IL-21R overexpressing CD4⁺ and IL-21 overexpressing CD8⁺ CAR T cells (vs. mean 11%, range 6.3% to 19%, p=0.015). This demonstrates that the interaction between the ligand and its receptor is most potent when IL-21 is produced by CD4⁺ and IL-21R expressed by CD8⁺ CAR T cells. The effect is also more pronounced when both molecules are overexpressed, since conventional CAR T cells with physiological interaction between IL-21 and IL-21R secreted less. Overexpression of IL-21 in CD4⁺ CAR T cells generally demonstrated a beneficial effect on IFN- γ secretion, irrespective of the CAR construct in CD8⁺ CAR T cells. Nonetheless, even though no significance was reached, overexpression of the IL-21 receptor alpha chain in CD8⁺ CAR T cells led to a higher mean percentage of CD8⁺ c-myc⁺ IFN- γ ⁺ cells when compared to the condition with basal IL-21R expression (vs. mean 13.9% in CD4⁺ RV19-BBz_IL-21^{OE} and CD8⁺ RV19-BBz,

range 13.4% to 18.1%, $p=0.077$) and with IL-21 overexpression (vs. mean 13.4% in $CD4^+_{RV19-BBz_IL-21^{OE}}$ and $CD8^+_{RV19-BBz_IL-21^{OE}}$, range 6% to 23.9%, $p=0.170$). The other combinations of cells not seen in this figure were inferior in terms of IFN- γ secretion when compared to $CD4^+_{RV19-BBz_IL-21^{OE}}$ and $CD8^+_{RV19-BBz_IL-21R^{OE}}$ cells (data not shown).

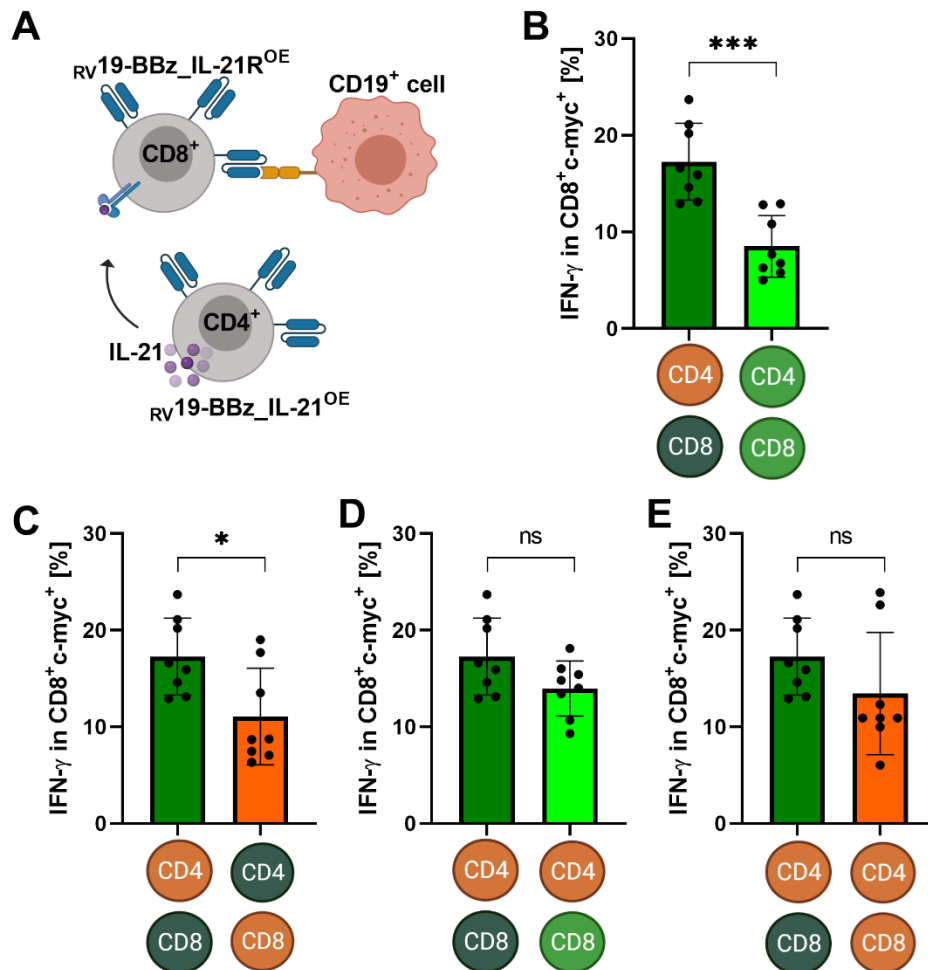


Figure 6.20 Overview of the intracellular cytokine staining assay and IFN- γ secretion of $CD8^+$ CAR T cells with IL-21R and IL-21 overexpression

CAR T cells were co-cultured with the same number of $CD19^+$ target cells for 24h. The T cell product consisted of an even percentage of $CD4^+$ and $CD8^+$ CAR T cells, both of which were transduced with one of the three CAR constructs. After addition of Brefeldin A for 2 hours, cells were fixed, permeabilized and stained, and cytokine secretion was measured via FACS. **A.** An exemplary drawing of one of the assay conditions: $CD19^+$ Nalm6 cells were co-cultured with $CD4^+$ IL-21 producing and $CD8^+$ IL-21R overexpressing CAR T cells. IFN- γ secretion of $CD8^+$ c-myc $^+$ CAR T cells in the condition consisting of $CD4^+_{RV19-BBz_IL-21^{OE}}$ and $CD8^+_{RV19-BBz_IL-21R^{OE}}$ was compared to: **B.** $CD4^+$ and $CD8^+$ CAR T cells with a conventional construct. **C.** $CD4^+$ CAR T cells overexpressing the IL-21R receptor and $CD8^+$ CAR T cells producing the ligand. **D.** $CD4^+_{RV19-BBz_IL-21^{OE}}$ and conventional $CD8^+$ CAR T cells. **E.** $CD4^+$ and $CD8^+$ CAR T cells both overexpressing IL-21. Data is representative of four donors, shown as mean (\pm SD) and experiments were performed in technical duplicates. Generation of CAR T cells from donor #2-4 and ICS assay were performed by Semjon Willier. The two-tailed, unpaired Student's t-test was used to compare each separate group.

These results demonstrate the in vitro benefit of mimicking the IL-21/IL-21R interaction in CD4 and CD8 T cell specific way in an anti-CD19 CAR context, which will be further examined in an in vivo murine model of leukemia.

7 Discussion

Despite successful treatment of relapsed/refractory B-cell precursor ALL via adoptive transfer of anti-CD19 CAR T cells, several mechanisms of therapy failure have been described²⁴. The lack of *in vivo* persistence due to T cell exhaustion is a major limitation of current T cell-based therapies. Exhausted T cells are characterized by reduced expansion, terminal differentiation and increased surface expression of co-inhibitory molecules such as TIM-3⁹⁰. Unpublished research from our group denotes an important role of the interleukin-21 receptor (IL-21R) in CD8⁺ T cells, since its expression is significantly reduced in bone marrow CD8⁺ T cells of pediatric BCP-ALL patients compared to healthy donors.

As a part of the common gamma chain cytokine receptor family¹¹⁸, IL-21R consists of two chains: the IL-21R alpha chain (IL-21R), which binds interleukin-21 (IL-21) secreted by a variety of immune cells, such as CD4⁺ T cells⁷⁹, and the common gamma chain (CD132, γ_c), which is essential for downstream signal transduction¹⁰⁰. Phosphorylation of STAT3¹⁰⁰ and other transcription factors after the ligand-receptor interaction mediates various effects on CD8⁺ T cells, such as improved expansion and a retained memory phenotype *in vivo*⁹⁵, which may be beneficial for the long-time persistence of CAR T cells for immunotherapy¹¹⁹.

Research on the role of IL-21R alpha chain expression in the setting of CAR T cell therapy is lacking, therefore this project aims to characterize the impact of the ligand-receptor interaction on functionality of CD8⁺ T cells *in vitro*. For this purpose, IL-21R expression was manipulated by CRISPR/Cas9 or retroviral transduction in order to evaluate its potential to improve anti-CD19 CAR T cell persistence.

7.1 Altered IL-21R expression and its effect on primary T cells

To characterize the effect of IL-21 receptor expression on primary T cells, a CRISPR/Cas9 genomic knock-out ($_{CR}IL-21R^{KO}$) and a retroviral overexpression of the receptor alpha chain ($_{RV}IL-21R^{OE}$) were performed. Electroporated control ($_{CR}Control$) and untransduced cells (UT) served as controls to the genetically modified cells. The altered expression of IL-21R could be validated in both instances by utilizing different methods, such as a receptor expression induction assay or PCR and Sanger sequencing.

Previous research has shown that the ligand-receptor interaction has a modest effect on CD8⁺ proliferation *in vitro* but can cooperate with IL-7 and IL-15⁹⁸. Contrary to expectations, however, overexpressing IL-21R in T cells led to a reduced expansion rate compared to untransduced controls, despite inclusion of the cytokines IL-7 and IL-15 in the growth medium. All common gamma chain receptors signal via the common γ_c , which has been defined as the limiting factor for effective downstream signaling^{120,121}. Moreover, asymmetric cross-talk between the common gamma chain cytokine receptors has been observed, since the IL-7R was shown to recruit the common γ_c even prior to IL-7 stimulation, thus limiting availability for other cytokine receptors such as IL-21R¹²².

In our experiments, however, bulk CD4⁺CD8⁺ T cells were used. IL-21R in CD4⁺ T cells could hamper their proliferation, as they do not physiologically express that molecule. Moreover, it is possible that endogenous production of IL-21 by T helper subsets, together with the unphysiologically high surface expression of the IL-21R alpha chain could have bound all available common γ_c , thereby limiting the interaction of IL-7 and IL-15 with their respective receptors and thus inhibited proliferation of $_{RV}IL-21R^{OE}$ cells. Alternatively, CRISPR/Cas9 genomic knock-out of IL-21R did not impair T cell expansion, hinting at a functional redundancy of IL-21 signaling in regard to the proliferative stimuli imparted by IL-7 and IL-15.

An efficient way to measure downstream T cell signaling is intracellular phospho-protein staining and FACS¹²³. Interestingly, overexpressing the IL-21R on the surface of T cells led to no increased percentage of pSTAT3, which has been described as one of the main downstream signaling pathways after ligand-receptor interaction¹⁰⁰. This result indicates that either maximal phosphorylation can be achieved by all

cells expressing normal amounts of IL-21R in the presence of excess IL-21 or that the increased availability of the IL-21R alpha chain cannot be advantageously utilized due to only basal expression of the common γ_c . Since IL-21 requires the IL-21R alpha chain for binding^{85,101}, lack of the IL-21 receptor led to hardly any detection of pSTAT3, which also validates the CRISPR/Cas9 genomic knock-out of the receptor.

The functionality of T cells with altered IL-21R expression was examined in a co-culture with CD19⁺ Nalm6 target cells, a B-cell ALL cell line which has been widely used in both in vitro and in vivo experiments^{124,125}. Contact between CD3⁺ T and CD19⁺ tumor cells was facilitated via the bi-specific antibody blinatumomab¹⁹ with addition of IL-21. Dose-dependent cytotoxicity of target cells was observed in both $_{CR}IL-21R^{KO}$ and $_{RV}IL-21R^{OE}$ cells and no difference was noted on comparison with respective control cells, despite a slight increase in killing after addition of IL-21 to the co-culture with IL-21R overexpressing cells.

At the end of expansion, $_{RV}IL-21R^{OE}$ cells demonstrated a trend towards a less differentiated phenotype, consistent with previous research^{91,98}. The generation of long-lived stem cell-like memory (T_{SCM}) and central memory (T_{CM}) cells, which express CD95 and CD62L with additional expression of CD45RO in T_{CM} , is of great interest for adoptive cell therapy, as these demonstrate improved expansion and anti-tumor effects in vivo^{126,127}. However, after co-culture with CD19⁺ target cells, this slight advantage of IL-21R overexpressing cells was abrogated, as the sum of T_{CM} and T_{SCM} cells was comparable among all T cells tested.

A study by Hinrichs et al. demonstrated that IL-21 inhibits the differentiation of less mature into effector CD8⁺ T cells, which are characterized by an increased cytolytic activity and secretion of the Th1 cytokine, interferon- γ (IFN- γ)⁹¹. In line with this finding, our experiments showed that overexpression of the IL-21R led to a reduced IFN- γ and TNF- α secretion by cytotoxic lymphocytes in comparison to UT control cells. Despite a slight rise in secretion of the pro-inflammatory cytokines upon stimulation with IL-21, $_{RV}IL-21R^{OE}$ cells still had lower percentages of CD8⁺ IFN- γ ⁺ and TNF- α ⁺ cells. In T cells with CRISPR/Cas9 genomic knock-out of the receptor, even though basal cytokine secretion in co-culture was not impaired, no interaction with IL-21 could occur and addition of the ligand had no effect on IFN- γ and TNF- α secretion. T cells for adoptive cell transfer are often evaluated in vitro based on their cytotoxicity and secretion of pro-inflammatory cytokines, as in these experiments. However, research has shown that improved in vivo persistence of CD8⁺ T cells correlates with a higher percentage of less differentiated subsets, and not with the superior cytolytic activity in vitro seen in effector (T_{EFF}) cells¹²⁸. From this viewpoint, the reduced secretion of pro-inflammatory cytokines in vitro by IL-21R overexpressing CD8⁺ T cells may prove to be of clinical benefit in vivo.

In summary, the generation of primary T cells with altered expression of the IL-21 receptor was feasible. The CRISPR/Cas9 genomic knock-out had no obvious effect on expansion, phenotype and functionality when compared to the electroporated $_{CR}Control$ cells. As expected, stimulation with IL-21 had hardly any effect on $_{CR}IL-21R^{KO}$ cells, as demonstrated by the lack of signal transduction via STAT3 phosphorylation. In contrast, IL-21R overexpressing cells had a lower expansion rate with a slightly less differentiated phenotype and secreted less pro-inflammatory cytokines than their counterparts in a co-culture setting.

7.2 Overexpression of the common gamma chain does not improve IL-21/IL-21R signaling

The common γ_c has been studied in the setting of X-linked severe combined immunodeficiency (X-SCID)⁸¹, and its preclinical reconstitution in murine models of the disease proved successful in restoring T cell functionality^{129,130}. These results paved the way for retrovirus-mediated human gene therapy for X-SCID¹³¹. Based on the observation that downstream signaling after stimulation with IL-21, as measured by pSTAT3%, did not differ between UT cells with a basal expression of IL-21R and $_{RV}IL-21R^{OE}$ cells, we

decided to test if increasing the availability of the common γ_C (CD132) would improve STAT3 phosphorylation and IL-21/IL-21R signaling in the setting of IL-21R alpha chain overabundance.

For this purpose, CD132 ($_{RV}CD132^{OE}$) and a bicistronic construct ($_{RV}IL-21R_CD132^{OE}$) were retrovirally transduced into primary T cells and compared to $_{RV}IL-21R^{OE}$ cells, with UT cells serving as negative control. Even though gain-of-function mutations of CD132 have been described as drivers of leukemic transformation¹³², no such effect was observed after retroviral overexpression of the common γ_C in vitro. The generated T cells expanded in a similar way, with no obvious proliferative advantage after common γ_C overexpression. Despite marked differences in intra- and interdonor surface expression of IL-21R and CD132 in tested T cells, phosphorylation of STAT3 after stimulation with IL-21 was comparable among all conditions. Therefore, basal surface expression of IL-21R seems to effectively mediate signal transduction via STAT3, and neither CD132 nor IL-21R alpha chain overabundance led to an increase in pSTAT3.

Functionality assays were performed in a co-culture with CD19⁺ Nalm6 target cells and blinatumomab. Addition of IL-21 allowed for further characterization of the ligand-receptor interaction in T cells. Even though $_{RV}CD132^{OE}$ cells demonstrated high cytotoxic potential without IL-21, addition of the ligand led to abrogation of this slight advantage and to similar killing rates among all constructs. Interestingly, T cells overexpressing the common γ_C were not affected by the presence of IL-21 in the co-culture, which can be interpreted as a confirmation of hierarchical signaling of the common gamma chain cytokines¹²². In line with our previous experiments, both IL-21R overexpressing conditions ($_{RV}IL-21R_CD132^{OE}$ and $_{RV}IL-21R^{OE}$) responded to stimulation with IL-21.

CD132 overexpression led to the lowest percentage of CD8⁺ IFN- γ ⁺ and TNF- α ⁺ cells and IL-21 had a minimal impact on cytokine secretion in this condition. In contrast, T cells with overabundance of the IL-21 receptor alpha chain demonstrated comparable levels of pro-inflammatory cytokine secretion and, as in previous experiments, stimulation with the ligand increased the percentage of IFN- γ ⁺ cells. Moreover, almost half of CD8⁺ cells in all tested T cell conditions had surface markers indicative of a stem cell-like memory phenotype at the end of expansion. However, in a co-culture setting both constructs overexpressing IL-21R had similar levels of phenotypic differentiation, whereas $_{RV}CD132^{OE}$ cells managed to retain a less mature phenotype despite contact with CD19⁺ target cells. These results underscore the role of the common γ_C in T cell memory formation without augmenting the cytotoxic potential of CD8⁺ T cells, which has already been described¹³³.

These experiments demonstrated that the functionality of both constructs overexpressing the IL-21 receptor was comparable, and co-expression of the common γ_C led to no improvement in expansion, direct cytotoxicity, phenotype or cytokine secretion in primary T cells. Of note, however, is the effect of sole CD132 overexpression on the formation of a less differentiated memory phenotype in vitro, which may have implications for cancer therapy.

Even though specific gamma chain cytokine responses are thought to be mostly dependent on the interaction between cytokines and their respective specific chains¹³⁴ (e.g., IL-21 and IL-21R alpha chain), with the common γ_C just providing a scaffold for the realization of this interaction, research has already demonstrated a more direct role of CD132 in cytokine signaling¹³⁵. With this in mind, we hypothesized a dose-response relationship between CD132 expression and pSTAT3 phosphorylation upon stimulation with IL-21, which could not be proven in our experiments. Nonetheless, the observed differences in T cell functionality, despite similar levels of phosphorylation of STAT3, underscored the availability of other possible downstream signaling pathways¹³⁶, which may be responsible for the observed effects on T cells after ligand-receptor interaction.

7.3 Successful generation of functional anti-CD19 CAR T cells overexpressing IL-21R

Based on the comparable functionality of $_{RV}IL-21R_CD132^{OE}$ and $_{RV}IL-21R^{OE}$ cells seen in the previous experiment, overexpressing the IL-21R alpha chain was regarded as sufficient to further study the effect of the IL-21R/IL-21 interaction in the setting of CAR T cells. For this reason, first- and second-generation bicistronic CAR constructs overexpressing IL-21R were generated. Three conventional CAR constructs served as controls.

A consistently lower CAR transduction rate was observed in the IL-21R co-expressing CAR T cells compared to their respective control cells, probably due to the greater length of the bicistronic constructs. Nonetheless, stable expression of the chimeric receptor in the range of 46% to 79.5% was achieved among all constructs. Moreover, in contrast to results in primary T cell, no differences in expansion rate could be detected, even if IL-21R was overexpressed. A possible reason for this could be the tonic signaling and activation due to the presence of the CAR, especially in second-generation constructs^{53,137}. The CAR T cell product at the end of expansion showed mostly CD4⁺ cells, closely followed by CD8⁺ cells, with a predominance of less differentiated T_{SCM} and T_{CM} cells in all constructs, which has been shown to benefit CAR T cell functionality¹³⁸.

A functionality screen was initially performed with the first- ($_{RV}19z_IL-21R^{OE}$) and second-generation CAR T cells with a CD28 co-stimulatory domain ($_{RV}19-28z_IL-21R^{OE}$) in a co-culture with CD19⁺ Nalm6 target cells. As in previous experiments, IL-21 was added to the co-culture to enable interaction with the IL-21 receptor. Direct cytotoxic activity was comparable between CAR constructs and functionality was preserved even at the lowest E:T ratio. As further proof of anti-CD19 specificity, all constructs proliferated upon stimulation with CD19⁺ target cells. A specific effect of IL-21R overexpression on cytotoxicity and proliferation in vitro could not be demonstrated, since basal surface expression of IL-21R seemed to be sufficient for interaction with the ligand. In general, IL-21R overexpressing CAR T cells could be successfully generated and showed comparable functionality to conventional CAR cells.

Based on our previous observations in primary T cells, the secretion of pro-inflammatory cytokines as markers of effector functionality¹³⁹ after CD19 antigen contact was of particular interest. Both constructs overexpressing the IL-21R secreted INF- γ and TNF- α on target cell contact. Despite similarities in TNF- α secretion, INF- γ production was markedly lower in $_{RV}19z_IL-21R^{OE}$ and $_{RV}19-28z_IL-21R^{OE}$ cells compared to their respective controls. IL-21 partially reversed this trend, however, mimicking the effect seen in $_{RV}IL-21R^{OE}$ T cells. Nevertheless, IL-21R overexpression was once again associated with less pronounced effector functions, which can be seen as advantageous for in vivo implementation^{47,140}, especially in conjunction with the less mature phenotype at the end of expansion. This effect was most notably observed in the second-generation CAR construct with CD28 co-stimulation. Interestingly, such CAR designs are usually associated with a higher activation potential and accelerated exhaustion in vivo⁵⁵.

7.4 Altered IL-21R expression and its effect on second-generation CAR T cells with 4-1BB co-stimulation

Due to observations on increased in vivo persistence of second-generation CAR T cells with a 4-1BB co-stimulatory domain³², further experiments focused on such a construct overexpressing IL-21R ($_{RV}19-BBz_IL-21R^{OE}$). Moreover, a CRISPR/Cas9 genomic knock-out of the receptor alpha chain ($_{RV}19-BBz_{CR}IL-21R^{KO}$) was performed in conventional CAR T cells to further characterize the ligand-receptor interaction. Electroporated ($_{RV}19-BBz_{CR}Control$) and conventional second-generation CAR T cells ($_{RV}19-BBz$) served as controls.

Despite predominance of effector memory (T_{EM}) T cells on the last day of expansion, $_{RV}19-BBz_IL-21R^{OE}$ CAR T cells demonstrated the highest percentage of T_{SCM} and T_{CM}. High T cell purity of the cell product was achieved in all CAR constructs, with CD4⁺ cells being the most numerous. Consistent with previous

results, the CRISPR/Cas9 knock-out of IL-21R led to no detrimental effects on expansion, phenotype and cellular composition when compared to electroporated control cells.

When CAR T cell functionality was tested in a co-culture with CD19⁺ target cells, direct cytotoxicity was comparable among constructs. Normal or increased expression of IL-21R led to a slight rise in killing potential on addition of IL-21, whereas it had no effect in particular on $_{RV19-BBz_{CR}}IL-21R^{KO}$ CAR T cells, a further proof of high knock-out efficiency. As in previous experiments, the cytometry-based cytotoxicity assay¹⁴¹ was not sensitive enough to show marked differences between the genetically modified cells.

In contrast, a pronounced positive effect of the IL-21/IL-21R interaction on the expansion of CD8⁺ $_{RV19-BBz_IL-21R^{OE}}$ CAR T cells could be observed upon stimulation, as these demonstrated the highest proliferative capacity among all tested constructs on addition of IL-21. Overabundance of the receptor alpha chain was clearly necessary for this proliferative effect, since basal expression of IL-21R in conventional $_{RV19-BBz}$ cells did not lead to such a marked increase in antigen-dependent expansion. This supports prior reports from in vitro studies on the effect of the ligand on the proliferation of cytotoxic T cells^{95,96,142}.

Moreover, in line with previous experiments, secretion of the cytokines INF- γ and TNF- α after contact with CD19⁺ targets was lowest in IL-21R overexpressing CAR T cells, whereas addition of IL-21 led to a pronounced increase in pro-inflammatory cytokine secretion. This rapid increase in effector activity upon stimulation with IL-21, coupled with the already described superior ability to self-renew can be seen as first proof that anti-CD19 CAR T cells overexpressing the IL-21 receptor may be beneficial for in vivo persistence, which has been reported previously in a non-CAR context⁵¹. The electroporated conditions generally retained their baseline proliferative rate and cytokine secretion independent of IL-21 in the co-culture.

In the setting of cancer immunotherapy, antigen-dependent effector functionality of CD8⁺ T cells may deteriorate and finally lead to T cell exhaustion⁵², which is characterized by markedly increased expression of co-inhibitory markers such as TIM-3 and PD-1¹⁴³. Upregulation of the inhibitory receptors also correlates with relapse of BCP-ALL^{144,113}. PD-1 and TIM-3 on the cell surface can lead to T cell dysfunction and abrogate T cell response to chronic infections and cancer¹⁴⁵. This effect can be reversed by blockade of the co-inhibitory markers¹⁴⁶. Since IL-21 led to such a dramatic rise in INF- γ and TNF- α secretion in CD8⁺ $_{RV19-BBz_IL-21R^{OE}}$ CAR T cells, expression of the co-inhibitory receptors was investigated as a marker of early T cell dysfunction. For this purpose, TIM-3 and PD-1 upregulation upon stimulation with IL-21 was compared between conventional and IL-21R overexpressing CAR T cells in co-culture with CD19⁺ target cells. Both constructs showed comparable expression of the inhibitory receptors, thus no short-term T cell dysfunction was detectable.

To further elucidate the effect of IL-21 on the characteristics of IL-21R overexpressing CAR T cells, the concentration of multiple pro-inflammatory cytokines was determined via multiplex immunoassay from supernatants after co-culture with Nalm6 cells. The presence of the ligand augmented the concentration of IFN- γ , granzyme B, granulysin and soluble Fas in all tested constructs with normal or increased expression of the IL-21 receptor alpha chain, but not in $_{RV19-BBz_{CR}}IL-21R^{KO}$ cells. These ligands are known to improve T cell cytotoxic functions¹⁴⁷. T-bet is a transcription factor known to be responsible for the expression of the Th1 hallmark cytokine, IFN- γ ^{148,149}, and can be induced by IL-21¹⁵⁰. The positive effect of IL-21 on production of granzyme B and granulysin by CD8⁺ cytotoxic lymphocytes in a STAT3-dependent manner has also been described^{98,151,152}. Our results confirm the role of IL-21/IL-21R interaction for efficient production and secretion of ligands which mediate anti-tumor activity by CD8⁺ T cells.

Of particular interest in this setting, however, is the unique cytokine profile of $_{RV19-BBz_IL-21R^{OE}}$ CAR T cells, which makes them stand out from the conventional CAR T cells with just basal expression of IL-21R. IL-21 contact led to a rise in concentration of both IL-2 and IL-10 in IL-21R overexpressing CAR T

cells. IL-21 and IL-2 are both members of the common gamma chain cytokine family and have been described to mediate context-dependent and even opposing effects on T cell functionality *ex vivo*⁸⁷. On the other hand, the ability to produce IL-2, especially in conjunction with enhanced IFN- γ secretion, serves as a marker for polyfunctionality and improved *in vivo* persistence of effector T cells^{153,154}. After stimulation with IL-21, CAR T cells with basal or increased expression of the IL-21 receptor alpha chain increased their secretion of IL-2. This effect was most pronounced in IL-21R overexpressing T cells. The ligand/receptor interaction led to no change when a CRISPR/Cas9 knock-out of the receptor was performed. This can be seen as a further benefit of the IL-21/IL-21R axis in producing more functional CAR T cells.

IL-10 is generally associated with anti-inflammatory and immunosuppressive properties¹⁵⁵. Nonetheless, several studies have challenged this perception of IL-10, since the cytokine has been shown to promote the formation of CD8⁺ memory T cells¹⁵⁶ and Th1 cytokine production¹⁵⁷. Furthermore, a synergistic effect of IL-21 and IL-10 on the formation of long-lived antigen-specific memory CD8⁺ T cells via the STAT3 pathway has been described¹⁰⁴. In this context, the marked increase in IL-10 secretion by $_{RV19-BBz_IL-21R^{OE}}$ CAR T cells after addition of IL-21 to the co-culture may signal a similar IL-21/IL-10 synergy leading to the formation of a CD8⁺ memory population that is not terminally exhausted. Similar to the effects of IL-21, interleukin-10 seems to act in a context-dependent manner and its role on CD8⁺ T cell functionality should be further characterized.

For this purpose, the population of CD4⁺ second-generation CAR T cells was analyzed to screen for phenotypic differences that could be due to the overabundance of the IL-21 receptor alpha chain within CD4⁺ T cells and its interaction with IL-21. Of particular interest in this regard are CD4⁺ Th17 cells, since they not only produce interleukin-21, but may also be stimulated in an autocrine manner by the same ligand⁸⁶. Moreover, the Th17 population has been shown to mediate a superior anti-tumor response due to its increased persistence *in vivo*^{50,158}. In our experiments, there was a significant increase in this population after antigen contact of the CAR T cells with their CD19⁺ targets. However, neither IL-21R overexpression nor presence of IL-21 in the co-culture led to a pronounced expansion of this population. This was also the case regarding other investigated T helper populations, such as Th1, Th2 and Th1Th17.

In summary, interaction of IL-21 with its receptor in the setting of $_{RV19-BBz_IL-21R^{OE}}$ CAR T cells led to enhanced proliferation and pro-inflammatory cytokine secretion. Compared to conventional second-generation CAR T cells, IL-21R overabundance was associated with a lower basal rate of IFN- γ secretion, which could be starkly increased on addition of IL-21. The ligand/receptor interaction furthermore improved production of other pro-inflammatory cytokines, and at the same time induced IL-10 secretion. Thus, IL-21 seems to mediate adequate effector functionality, while simultaneously preserving a less differentiated state of CD8⁺ T cells. This effect is, however, dependent on the increased expression of the IL-21 receptor on the surface of CAR T cells and the presence of IL-21.

7.5 Superior functionality after combination of IL-21 producing CD4⁺ and IL-21R overexpressing CD8⁺ CAR T cells

Due to its pleiotropic effects¹¹², *in vivo* administration of IL-21 may lead to unexpected effects on a variety of immune cell populations. As our *in vitro* experiments demonstrate, however, the presence of IL-21 is essential for the functionality of CAR T cells overexpressing the IL-21 receptor alpha chain. To mimic the ligand/receptor interaction in a system closely resembling physiologic conditions¹⁵⁹, IL-21 was overexpressed in CD4⁺ and IL-21R in CD8⁺ CAR T cells, respectively. Tailoring this system in the context of CAR T cells allows for direct interaction between IL-21 and its receptor in direct vicinity of CD19⁺ leukemic blasts. Both T cell populations could be expanded successfully, with no intrapopulation differences in expansion or phenotype.

CD4⁺ $_{RV19-BBz_IL-21^{OE}}$ and CD8⁺ $_{RV19-BBz_IL-21R^{OE}}$ CAR T cells were then co-cultured with CD19⁺ target cells and IFN- γ secretion measured. Interaction of the ligand with its receptor led to a high percentage

of CD8⁺ c-myc⁺ IFN- γ ⁺ CAR T cells. This effect was superior in comparison to either conventional second-generation CAR T cells or a combination of IL-21R overexpressing CD4⁺ and IL-21 overexpressing CD8⁺ CAR T cells. Therefore, production of IL-21 by CD4⁺ CAR T cells mediated a potent anti-tumor effect on IL-21R overexpressing CD8⁺ CAR T cells and improved the functionality of standard-of-care CAR T cells.

Based on previous results, IL-21R overexpression seems to play a vital role for the positive effects seen after ligand/receptor interaction. Even though increased secretion of IL-21 by CD4⁺ CAR T cells (RV19-BBz_IL-21^{OE}) led to similar levels of IFN- γ secretion, independent of the CAR construct in CD8⁺ cells (basal IL-21R expression or IL-21 overexpression), the mean percentage of CD8⁺ c-myc⁺ IFN- γ ⁺ cells was highest when IL-21R was overexpressed in cytotoxic lymphocytes. Therefore, it can be concluded that mimicking the physiologic interplay between CD4⁺ and CD8⁺ T cells by use of IL-21 and IL-21R in a CAR setting demonstrated beneficial effects of IL-21R overexpression on CD8⁺ CAR T cell functionality.

7.6 Outlook

Our in vitro experiments show the clinical promise of CAR T cells overexpressing the IL-21 receptor alpha chain. There are, however, several limitations to the clinical application of these CAR constructs. IL-21 has been implicated in a variety of pathways which may overstimulate or inhibit immune reactions¹¹². Even though exogenous application of the cytokine would not be necessary if IL-21 is overproduced by CD4⁺ CAR T cells, the ligand could still be released off-target in vivo and lead to undesirable immune responses and toxicity. Membrane-bound IL-15 in a CAR setting has been shown to mediate superior anti-tumor activity with no aberrant proliferation of the engineered cells¹⁶⁰. A similar strategy in the generation of CD4⁺ CAR T cells overexpressing IL-21 might be of benefit in the clinic.

Another issue that needs to be addressed is the role of IL-10 in IL-21/IL-21R interaction and its effect on the functionality of CAR T cells overexpressing the IL-21 receptor, since interleukin-10 has pleiotropic immune effects¹⁵⁵ which may even limit the anti-tumor effect of immunotherapy in a context-dependent manner. Further study of the interplay between IL-10, IL-21 and their respective receptor complexes in the setting of CAR T cell therapy is needed.

In general, these experiments show that CAR T cells with IL-21R overexpression can be successfully generated and interaction between IL-21 and its receptor mediates several in vitro effects, which may be beneficial for immunotherapy of CD19⁺ malignancies: improved expansion, tendency towards a less differentiated phenotype, retained cytotoxicity, increased secretion of several pro-inflammatory cytokines, as well as no increased expression of co-inhibitory markers. The novel approach to combine IL-21 producing CD4⁺ and IL-21R overexpressing CD8⁺ CAR T cells is also a promising platform to further examine the effects of IL-21 receptor overexpression on T cell functionality in vivo.

8 Summary/Abstract

Adoptive transfer of anti-CD19 chimeric antigen receptor (CAR) T cells has revolutionized the therapy of relapsed/refractory B-cell precursor ALL. High initial remission rates are nevertheless hampered by a lack of long-term persistence due to T cell exhaustion. Sustained proliferation and persistence of less differentiated T cell populations can counteract the effects of exhausted immune cells and confer a superior anti-tumor response to immunotherapy. Of particular interest in this regard is the interaction between interleukin-21, a common gamma chain receptor cytokine, and its receptor complex, IL-21R, which consists of the specific alpha chain and the common gamma chain (γ_c). The ligand/receptor interplay leads to improved proliferation and the generation of long-lived memory CD8⁺ T cells. This in vitro study characterizes the role of IL-21R expression in the setting of CAR T cells with the aim of improving long-term persistence of T cell-based immunotherapy.

First, primary T cells with altered expression of the IL-21R alpha chain were examined. A CRISPR/Cas9 genomic knock-out of the receptor had no detrimental effects on T cell functionality, whereas retroviral overexpression of the IL-21R led to slower expansion, a less differentiated phenotype and reduced secretion of pro-inflammatory cytokines in CD8⁺ cells, even after stimulation with IL-21. Co-expression of the common γ_c played no additional role in the IL-21/IL-21R interaction in primary T cells.

To examine this effect in a CAR setting, first- and second-generation bicistronic CAR constructs overexpressing the IL-21R alpha chain were compared to conventional CAR T cells. Specific anti-CD19 functionality was observed in all CAR constructs, with direct cytotoxicity and proliferation comparable after stimulation with CD19⁺ target cells. Interestingly, INF- γ secretion was consistently lower in IL-21R overexpressing CAR T cells, while addition of IL-21 partially reversed this trend. Further experiments focused on the effect of IL-21/IL-21R interaction in a second-generation CAR construct with a 4-1BB co-stimulatory domain. Not surprisingly, CAR T cells with a CRISPR/Cas9 genomic knock-out of IL-21R performed similarly to conventional CAR T cells. In contrast, IL-21R overexpressing CAR T cells demonstrated signs of improved persistence, as they retained a high proliferative capacity despite the rapid increase in effector functions after addition of IL-21 to the co-culture. No signs of early T cell dysfunction were detected, since no marked rise in expression of the co-inhibitory markers TIM-3 and PD-1 was observed. Moreover, the interplay between IL-21 and its receptor in the setting of IL-21R overexpressing CAR T cells led to the increased secretion of pro-inflammatory cytokines as well as IL-10. In a final experiment, IL-21 was overexpressed in CD4⁺ and IL-21R in CD8⁺ CAR T cells with the aim of mimicking the physiologic interaction between the two T cell populations. This novel approach led to superior functionality when compared to standard-of-care CAR T cells: the highest INF- γ Secretion was observed when IL-21 was overexpressed in CD4⁺ CAR T cells while IL21R was expressed in CD8⁺ CAR T cells.

These promising results underscore the in vitro benefits to T cell functionality after interaction between IL-21 and its receptor, which may improve the long-term persistence of CAR T cell-based immunotherapy. Combining IL-21 producing CD4⁺ with IL-21R overexpressing CD8⁺ CAR T cells can help further examine the in vivo persistence of IL-21 receptor overexpressing CAR T cells.

9 Zusammenfassung

Der adoptive Transfer von anti-CD19 CAR-T-Zellen hat die Therapie der rezidivierten/ refraktären B-Zell-Vorläufer-ALL revolutioniert. Trotz initial hohen Remissionsraten kommt es zu fehlender Langzeitpersistenz dieser Zellen aufgrund von T-Zell-Erschöpfung. Die anhaltende Proliferation und Persistenz von weniger stark differenzierten T-Zell-Populationen können den negativen Auswirkungen erschöpfter Immunzellen entgegenwirken und führen zu einer verbesserten Immunantwort nach Immuntherapie. Von besonderem Interesse in dieser Hinsicht ist die Wechselwirkung zwischen Interleukin-21, einem Zytokin aus der Gammaketten-Rezeptor-Zytokinfamilie, und seinem Rezeptorkomplex IL-21R, der aus einer spezifischen Alpha-Kette und der gemeinsamen Gammakette (γ_c) besteht. Das Ligand/Rezeptor-Wechselspiel führt zu einer verbesserten Proliferation und zur Erzeugung langlebiger CD8⁺-T-Gedächtniszellen. Diese In-vitro-Studie versucht, die Rolle der IL-21R-Expression bei der Erzeugung von CAR-T-Zellen zu charakterisieren, mit dem Ziel, die langfristige Persistenz der T-Zell-basierten Immuntherapie zu verbessern.

Zunächst wurden primäre T-Zellen mit veränderter Expression der IL-21R-Alpha-Kette untersucht. Der genomische CRISPR/Cas9-Knockout des Rezeptors hatte keine nachteiligen Auswirkungen auf die T-Zell-Funktionalität, wohingegen die retrovirale Überexpression des IL-21R zu einer langsameren Expansion, einem wenig stark differenzierten Phänotyp und einer verringerten Sekretion von proinflammatorischen Zytokinen in CD8⁺-T-Zellen führte, sogar nach Stimulation mit IL-21. Eine Überexpression der gemeinsamen Gammakette zusammen mit IL-21R spielte keine zusätzliche Rolle bei der IL-21/IL-21R-Interaktion in primären T-Zellen, außer einer über die gemeinsame Gammakette pSTAT3-vermittelten Signalübertragung. Bi-cistronische CAR-Konstrukte der ersten und zweiten Generation mit Überexpression der IL-21R-Alpha-Kette wurden mit konventionellen CAR-T-Zellen verglichen. In allen CAR-Konstrukten wurde eine spezifische Anti-CD19-Funktionalität beobachtet, wobei die direkte Zytotoxizität und die Proliferation nach Stimulation mit CD19⁺-Tumorzellen vergleichbar waren. Interessanterweise wurde eine erniedrigte INF- γ -Sekretion in IL-21R-überexprimierenden CAR-T-Zellen beobachtet, welche durch die Zugabe von IL-21 erhöht werden konnte. Weitere Experimente konzentrierten sich auf die Auswirkung der IL-21R-Überexpression in einem CAR-Konstrukt der zweiten Generation mit 4-1BB-Kostimulation. CAR-T-Zellen mit einem genomischen CRISPR/Cas9-Knock-out von IL-21R funktionierten ähnlich wie konventionelle CAR-T-Zellen. Im Gegensatz dazu, zeigten IL-21R-überexprimierende CAR-T-Zellen Anzeichen einer verbesserten Persistenz, da sie trotz Effektorfunktionen nach Zugabe von IL-21 eine hohe Proliferation aufwiesen. Es konnten keine Anzeichen einer frühen T-Zell-Dysfunktion festgestellt werden, da die Expression der co-inhibitorischen Marker TIM-3 und PD-1 auf basalem Niveau blieb. Darüber hinaus führte das Zusammenspiel zwischen IL-21 und seinem Rezeptor in IL-21R überexprimierenden CAR-T-Zellen zu einer erhöhten Sekretion sowohl von proinflammatorischen Zytokinen als auch von IL-10. In einem letzten Experiment wurden IL-21 in CD4⁺- und IL-21R in CD8⁺-CAR-T-Zellen überexprimiert, um die physiologische Interaktion zwischen den beiden T-Zellpopulationen nachzuahmen. Dieser neuartige Ansatz führte zu einer verbesserten Funktionalität im Vergleich zu konventionellen CAR-T-Zellen: die höchste INF- γ -Sekretion konnte bei der Interaktion zwischen IL-21 produzierenden CD4⁺- und IL-21R überexprimierenden CD8⁺-CAR-T-Zellen erreicht werden.

Diese vielversprechenden Ergebnisse zeigen die vorteilhaften In-vitro-Effekte nach Interaktion zwischen IL-21 und seinem Rezeptor, die eine langfristige Persistenz der CAR-T-Zell-basierten Immuntherapie bewirken könnten. Die Kombination von IL-21 produzierenden CD4⁺- und IL-21R überexprimierenden CD8⁺-CAR-T-Zellen ist ein geeigneter Ansatz, um die In-vivo-Persistenz von IL-21-Rezeptor überexprimierenden CAR-T-Zellen weiter untersuchen zu können.

10 References

1. Cunningham, R. M., Walton, M. A. & Carter, P. M. The Major Causes of Death in Children and Adolescents in the United States. *New Engl J Med* **379**, 2468–2475 (2018).
2. Longo, D. L., Hunger, S. P. & Mullighan, C. G. Acute Lymphoblastic Leukemia in Children. *New Engl J Medicine* **373**, 1541–1552 (2015).
3. Michaelis, J. & Kaatsch, P. Deutsches Kinderkrebsregister. *Der Onkologe* **19**, 1058–1064 (2013).
4. Inaba, H. & Mullighan, C. G. Pediatric acute lymphoblastic leukemia. *Haematologica* **105**, 0–0 (2020).
5. Duffield, A. S., Mullighan, C. G. & Borowitz, M. J. International Consensus Classification of acute lymphoblastic leukemia/lymphoma. *Virchows Arch* **482**, 11–26 (2023).
6. Clarke, R. T. *et al.* Clinical presentation of childhood leukaemia: a systematic review and meta-analysis. *Arch Dis Child* **101**, 894 (2016).
7. Roberts, K. G. & Mullighan, C. G. The Biology of B-Progenitor Acute Lymphoblastic Leukemia. *Csh Perspect Med* **10**, a034835 (2020).
8. Sidney, F., K., D., Louis, D., M., Robert, F., S., Robert & A., W., James. Temporary Remissions in Acute Leukemia in Children Produced by Folic Acid Antagonist, 4-Aminopteroyl-Glutamic Acid (Aminopterin). *New Engl J Medicine* **238**, 787–793 (1948).
9. Anja, M. *et al.* Dexamethasone vs prednisone in induction treatment of pediatric ALL: results of the randomized trial AIEOP-BFM ALL 2000. *Blood* **127**, 2101–2112 (2016).
10. M., M., Regina *et al.* Humanized CD19-Targeted Chimeric Antigen Receptor (CAR) T Cells in CAR-Naive and CAR-Exposed Children and Young Adults With Relapsed or Refractory Acute Lymphoblastic Leukemia. *J Clin Oncol* **39**, 3044–3055 (2021).
11. Cooper, S. L. & Brown, P. A. Treatment of Pediatric Acute Lymphoblastic Leukemia. *Pediatr Clin N Am* **62**, 61–73 (2015).
12. Kato, M. & Manabe, A. Treatment and biology of pediatric acute lymphoblastic leukemia. *Pediatr Int* **60**, 4–12 (2018).
13. Borowitz, M. J. *et al.* Clinical significance of minimal residual disease in childhood acute lymphoblastic leukemia and its relationship to other prognostic factors: a Children’s Oncology Group study. *Blood* **111**, 5477–5485 (2008).
14. Schrappe, M. *et al.* Outcomes after Induction Failure in Childhood Acute Lymphoblastic Leukemia. *New Engl J Medicine* **366**, 1371–1381 (2012).
15. Ko, R. H. *et al.* Outcome of Patients Treated for Relapsed or Refractory Acute Lymphoblastic Leukemia: A Therapeutic Advances in Childhood Leukemia Consortium Study. *J Clin Oncol* **28**, 648–654 (2009).

16. Freyer, D. R. *et al.* Postrelapse survival in childhood acute lymphoblastic leukemia is independent of initial treatment intensity: a report from the Children's Oncology Group. *Blood* **117**, 3010–3015 (2011).
17. Sun, W. *et al.* Outcome of children with multiply relapsed B-cell acute lymphoblastic leukemia: a therapeutic advances in childhood leukemia & lymphoma study. *Leukemia* **32**, 2316–2325 (2018).
18. Gökbüget, N. *et al.* Outcome of relapsed adult lymphoblastic leukemia depends on response to salvage chemotherapy, prognostic factors, and performance of stem cell transplantation. *Blood* **120**, 2032–2041 (2012).
19. Löffler, A. *et al.* A recombinant bispecific single-chain antibody, CD19 × CD3, induces rapid and high lymphoma-directed cytotoxicity by unstimulated T lymphocytes. *Blood* **95**, 2098–2103 (2000).
20. Mark, S. Blinatumomab: First Global Approval. *Drugs* **75**, 321–327 (2015).
21. Kantarjian, H. *et al.* Blinatumomab versus Chemotherapy for Advanced Acute Lymphoblastic Leukemia. *New Engl J Medicine* **376**, 836–847 (2017).
22. Locatelli, F. *et al.* Effect of Blinatumomab vs Chemotherapy on Event-Free Survival Among Children With High-risk First-Relapse B-Cell Acute Lymphoblastic Leukemia. *Jama* **325**, 843–854 (2021).
23. A., B., Patrick *et al.* A Randomized Phase 3 Trial of Blinatumomab Vs. Chemotherapy As Post-Reinduction Therapy in High and Intermediate Risk (HR/IR) First Relapse of B-Acute Lymphoblastic Leukemia (B-ALL) in Children and Adolescents/Young Adults (AYAs) Demonstrates Superior Efficacy and Tolerability of Blinatumomab: A Report from Children's Oncology Group Study AALL1331. *Blood* **134**, LBA-1-LBA-1 (2019).
24. June, C. H., O'Connor, R. S., Kawalekar, O. U., Ghassemi, S. & Milone, M. C. CAR T cell immunotherapy for human cancer. *Science* **359**, 1361–1365 (2018).
25. Eshhar, Z., Waks, T., Gross, G. & Schindler, D. G. Specific activation and targeting of cytotoxic lymphocytes through chimeric single chains consisting of antibody-binding domains and the gamma or zeta subunits of the immunoglobulin and T-cell receptors. *Proc National Acad Sci* **90**, 720–724 (1993).
26. Hombach, A. *et al.* Tumor-Specific T Cell Activation by Recombinant Immunoreceptors: CD3 ζ Signaling and CD28 Costimulation Are Simultaneously Required for Efficient IL-2 Secretion and Can Be Integrated Into One Combined CD28/CD3 ζ Signaling Receptor Molecule. *J Immunol* **167**, 6123–6131 (2001).
27. Maher, J., Brentjens, R. J., Gunset, G., Rivière, I. & Sadelain, M. Human T-lymphocyte cytotoxicity and proliferation directed by a single chimeric TCR ζ /CD28 receptor. *Nat Biotechnol* **20**, 70–75 (2002).
28. Imai, C. *et al.* Chimeric receptors with 4-1BB signaling capacity provoke potent cytotoxicity against acute lymphoblastic leukemia. *Leukemia* **18**, 676–684 (2004).
29. Kochenderfer, J. N. *et al.* Eradication of B-lineage cells and regression of lymphoma in a patient treated with autologous T cells genetically engineered to recognize CD19. *Blood* **116**, 4099–4102 (2010).
30. Jensen, M. C. *et al.* Antitransgene Rejection Responses Contribute to Attenuated Persistence of Adoptively Transferred CD20/CD19-Specific Chimeric Antigen Receptor Redirected T Cells in Humans. *Biol Blood Marrow Tr* **16**, 1245–1256 (2010).

31. Savoldo, B. *et al.* CD28 costimulation improves expansion and persistence of chimeric antigen receptor–modified T cells in lymphoma patients. *J Clin Invest* **121**, 1822–1826 (2011).
32. H, L., Adrienne *et al.* 4-1BB costimulation ameliorates T cell exhaustion induced by tonic signaling of chimeric antigen receptors. *Nat Med* **21**, 581–590 (2015).
33. Grupp, S. A. *et al.* Chimeric Antigen Receptor–Modified T Cells for Acute Lymphoid Leukemia. *New Engl J Medicine* **368**, 1509–1518 (2013).
34. Maude, S. L. *et al.* Chimeric Antigen Receptor T Cells for Sustained Remissions in Leukemia. *New Engl J Medicine* **371**, 1507–1517 (2014).
35. Maude, S. L. *et al.* Tisagenlecleucel in Children and Young Adults with B-Cell Lymphoblastic Leukemia. *New Engl J Medicine* **378**, 439–448 (2018).
36. Laetsch, T. W. *et al.* Three-Year Update of Tisagenlecleucel in Pediatric and Young Adult Patients With Relapsed/Refractory Acute Lymphoblastic Leukemia in the ELIANA Trial. *J Clin Oncol* **41**, 1664–1669 (2023).
37. Vairy, S., Garcia, J. L., Teira, P. & Bittencourt, H. CTL019 (tisagenlecleucel): CAR-T therapy for relapsed and refractory B-cell acute lymphoblastic leukemia. *Drug Des Dev Ther* **12**, 3885–3898 (2018).
38. Klebanoff, C. A., Yamamoto, T. N. & Restifo, N. P. Treatment of aggressive lymphomas with anti-CD19 CAR T cells. *Nat Rev Clin Oncol* **11**, 685–686 (2014).
39. Turtle, C. J. *et al.* CD19 CAR–T cells of defined CD4+:CD8+ composition in adult B cell ALL patients. *J Clin Invest* **126**, 2123–2138 (2016).
40. Pillai, V. *et al.* CAR T-cell therapy is effective for CD19-dim B-lymphoblastic leukemia but is impacted by prior blinatumomab therapy. *Blood Adv* **3**, 3539–3549 (2019).
41. June, C. H. & Sadelain, M. Chimeric Antigen Receptor Therapy. *New Engl J Med* **379**, 64–73 (2018).
42. Suntharalingam, G. *et al.* Cytokine Storm in a Phase 1 Trial of the Anti-CD28 Monoclonal Antibody TGN1412. *New Engl J Medicine* **355**, 1018–1028 (2006).
43. Margherita, N. *et al.* Monocyte-derived IL-1 and IL-6 are differentially required for cytokine-release syndrome and neurotoxicity due to CAR T cells. *Nat Med* **24**, 739–748 (2018).
44. Giavridis, T. *et al.* CAR T cell–induced cytokine release syndrome is mediated by macrophages and abated by IL-1 blockade. *Nat Med* **24**, 731–738 (2018).
45. Bhoj, V. G. *et al.* Persistence of long-lived plasma cells and humoral immunity in individuals responding to CD19-directed CAR T-cell therapy. *Blood* **128**, 360–370 (2016).
46. Kansagra, A. J. *et al.* Clinical utilization of Chimeric Antigen Receptor T-cells (CAR-T) in B-cell acute lymphoblastic leukemia (ALL)—an expert opinion from the European Society for Blood and Marrow Transplantation (EBMT) and the American Society for Blood and Marrow Transplantation (ASBMT). *Bone Marrow Transpl* **54**, 1868–1880 (2019).

47. Fraietta, J. A. *et al.* Determinants of response and resistance to CD19 chimeric antigen receptor (CAR) T cell therapy of chronic lymphocytic leukemia. *Nat Med* **24**, 563–571 (2018).
48. Gattinoni, L. *et al.* Removal of homeostatic cytokine sinks by lymphodepletion enhances the efficacy of adoptively transferred tumor-specific CD8+ T cells. *J Exp Medicine* **202**, 907–912 (2005).
49. Klebanoff, C. A., Khong, H. T., Antony, P. A., Palmer, D. C. & Restifo, N. P. Sinks, suppressors and antigen presenters: how lymphodepletion enhances T cell-mediated tumor immunotherapy. *Trends Immunol* **26**, 111–117 (2005).
50. Muranski, P. *et al.* Th17 Cells Are Long Lived and Retain a Stem Cell-like Molecular Signature. *Immunity* **35**, 972–985 (2011).
51. Crespo, J., Sun, H., Welling, T. H., Tian, Z. & Zou, W. T cell anergy, exhaustion, senescence, and stemness in the tumor microenvironment. *Curr Opin Immunol* **25**, 214–221 (2013).
52. Wherry, E. J. & Kurachi, M. Molecular and cellular insights into T cell exhaustion. *Nat Rev Immunol* **15**, 486–499 (2015).
53. Gomes-Silva, D. *et al.* Tonic 4-1BB Costimulation in Chimeric Antigen Receptors Impedes T Cell Survival and Is Vector-Dependent. *Cell Reports* **21**, 17–26 (2017).
54. Love, P. E. & Hayes, S. M. ITAM-mediated Signaling by the T-Cell Antigen Receptor. *Csh Perspect Biol* **2**, a002485 (2010).
55. Feucht, J. *et al.* Calibration of CAR activation potential directs alternative T cell fates and therapeutic potency. *Nat Med* **25**, 82–88 (2019).
56. Sara, G. *et al.* Enhanced CAR T cell expansion and prolonged persistence in pediatric patients with ALL treated with a low-affinity CD19 CAR. *Nat Med* **25**, 1408–1414 (2019).
57. J., O., Elena *et al.* Genetic mechanisms of target antigen loss in CAR19 therapy of acute lymphoblastic leukemia. *Nat Med* **24**, 1504–1506 (2018).
58. Sotillo, E. *et al.* Convergence of Acquired Mutations and Alternative Splicing of CD19 Enables Resistance to CART-19 Immunotherapy. *Cancer Discov* **5**, 1282–1295 (2015).
59. Fischer, J. *et al.* CD19 Isoforms Enabling Resistance to CART-19 Immunotherapy Are Expressed in B-ALL Patients at Initial Diagnosis. *J Immunother* **40**, 187–195 (2017).
60. Jacoby, E. *et al.* CD19 CAR immune pressure induces B-precursor acute lymphoblastic leukaemia lineage switch exposing inherent leukaemic plasticity. *Nat Commun* **7**, 12320 (2016).
61. Ahmad, R., L., M., Richard & M., O., Maureen. Lineage Switch in MLL-Rearranged Infant Leukemia Following CD19-Directed Therapy. *Pediatr Blood Cancer* **63**, 1113–1115 (2016).
62. Hamieh, M. *et al.* CAR T cell trogocytosis and cooperative killing regulate tumour antigen escape. *Nature* **568**, 112–116 (2019).
63. Braig, F. *et al.* Resistance to anti-CD19/CD3 BiTE in acute lymphoblastic leukemia may be mediated by disrupted CD19 membrane trafficking. *Blood* **129**, 100–104 (2017).

64. Fry, T. J. *et al.* CD22-targeted CAR T cells induce remission in B-ALL that is naive or resistant to CD19-targeted CAR immunotherapy. *Nat Med* **24**, 20–28 (2018).
65. Cordoba, S. *et al.* CAR T cells with dual targeting of CD19 and CD22 in pediatric and young adult patients with relapsed or refractory B cell acute lymphoblastic leukemia: a phase 1 trial. *Nat Med* **27**, 1797–1805 (2021).
66. R., T., Kirk, R., F., Kim & R., C., Mario. High frequency targeting of genes to specific sites in the mammalian genome. *Cell* **44**, 419–428 (1986).
67. D., U., Fyodor *et al.* Highly efficient endogenous human gene correction using designed zinc-finger nucleases. *Nature* **435**, 646–651 (2005).
68. Ishino, Y., Shinagawa, H., Makino, K., Amemura, M. & Nakata, A. Nucleotide sequence of the *iap* gene, responsible for alkaline phosphatase isozyme conversion in *Escherichia coli*, and identification of the gene product. *J Bacteriol* **169**, 5429–5433 (1987).
69. Bolotin, A., Quinquis, B., Sorokin, A. & Ehrlich, S. D. Clustered regularly interspaced short palindrome repeats (CRISPRs) have spacers of extrachromosomal origin. *Microbiology+* **151**, 2551–2561 (2005).
70. E., G., Josiane *et al.* The CRISPR/Cas bacterial immune system cleaves bacteriophage and plasmid DNA. *Nature* **468**, 67–71 (2010).
71. Gasiunas, G., Barrangou, R., Horvath, P. & Siksnys, V. Cas9–crRNA ribonucleoprotein complex mediates specific DNA cleavage for adaptive immunity in bacteria. *Proc National Acad Sci* **109**, E2579–E2586 (2012).
72. Jinek, M. *et al.* A Programmable Dual-RNA–Guided DNA Endonuclease in Adaptive Bacterial Immunity. *Science* **337**, 816–821 (2012).
73. Anders, C., Niewoehner, O., Duerst, A. & Jinek, M. Structural basis of PAM-dependent target DNA recognition by the Cas9 endonuclease. *Nature* **513**, 569–573 (2014).
74. Simeonov, D. R. & Marson, A. CRISPR-Based Tools in Immunity. *Annu Rev Immunol* **37**, 1–27 (2019).
75. Jasin, M. & Haber, J. E. The democratization of gene editing: Insights from site-specific cleavage and double-strand break repair. *Dna Repair* **44**, 6–16 (2016).
76. Jinek, M. *et al.* RNA-programmed genome editing in human cells. *Elife* **2**, e00471 (2013).
77. Ran, F. A. *et al.* Genome engineering using the CRISPR-Cas9 system. *Nat Protoc* **8**, 2281–2308 (2013).
78. Beltra, J.-C. & Decaluwe, H. Cytokines and persistent viral infections. *Cytokine* **82**, 4–15 (2016).
79. Parrish-Novak, J. *et al.* Interleukin 21 and its receptor are involved in NK cell expansion and regulation of lymphocyte function. *Nature* **408**, 57–63 (2000).
80. Shourian, M., Beltra, J.-C., Bourdin, B. & Decaluwe, H. Common gamma chain cytokines and CD8 T cells in cancer. *Semin Immunol* **42**, 101307 (2019).

81. Noguchi, M. *et al.* Interleukin-2 receptor γ chain mutation results in X-linked severe combined immunodeficiency in humans. *Cell* **73**, 147–157 (1993).
82. Croce, M., Rigo, V. & Ferrini, S. IL-21: A Pleiotropic Cytokine with Potential Applications in Oncology. *J Immunol Res* **2015**, 1–15 (2015).
83. Katsutoshi, O., Kristine, K., David, M., R., Y., Peter & J., L., Warren. Cloning of a type I cytokine receptor most related to the IL-2 receptor β chain. *Proc National Acad Sci* **97**, 11439 (2000).
84. Jin, H., Carrio, R., Yu, A. & Malek, T. R. Distinct Activation Signals Determine whether IL-21 Induces B Cell Costimulation, Growth Arrest, or Bim-Dependent Apoptosis. *J Immunol* **173**, 657–665 (2004).
85. Kotlarz, D. *et al.* Loss-of-function mutations in the IL-21 receptor gene cause a primary immunodeficiency syndrome. *J Exp Med* **210**, 433–443 (2013).
86. Wei, L., Laurence, A., Elias, K. M. & O’Shea, J. J. IL-21 Is Produced by Th17 Cells and Drives IL-17 Production in a STAT3-dependent Manner. *J Biol Chem* **282**, 34605–34610 (2007).
87. Attridge, K. *et al.* IL-21 inhibits T cell IL-2 production and impairs Treg homeostasis. *Blood* **119**, 4656–4664 (2012).
88. Recher, M. *et al.* IL-21 is the primary common γ chain-binding cytokine required for human B-cell differentiation in vivo. *Blood* **118**, 6824–6835 (2011).
89. Katsutoshi, O. *et al.* A Critical Role for IL-21 in Regulating Immunoglobulin Production. *Science* **298**, 1630 (2002).
90. McLane, L. M., Abdel-Hakeem, M. S. & Wherry, E. J. CD8 T Cell Exhaustion During Chronic Viral Infection and Cancer. *Annu Rev Immunol* **37**, 1–39 (2015).
91. Hinrichs, C. S. *et al.* IL-2 and IL-21 confer opposing differentiation programs to CD8⁺ T cells for adoptive immunotherapy. *Blood* **111**, 5326–5333 (2008).
92. Markley, J. C. & Sadelain, M. IL-7 and IL-21 are superior to IL-2 and IL-15 in promoting human T cell-mediated rejection of systemic lymphoma in immunodeficient mice. *Blood* **115**, 3508–3519 (2010).
93. Yi, J. S., Du, M. & Zajac, A. J. A Vital Role for Interleukin-21 in the Control of a Chronic Viral Infection. *Science* **324**, 1572–1576 (2009).
94. Allard, E. *et al.* Overexpression of IL-21 promotes massive CD8⁺ memory T cell accumulation. *Eur J Immunol* **37**, 3069–3077 (2007).
95. Fröhlich, A. *et al.* IL-21R on T Cells Is Critical for Sustained Functionality and Control of Chronic Viral Infection. *Science* **324**, 1576–1580 (2009).
96. Li, Y., Bleakley, M. & Yee, C. IL-21 Influences the Frequency, Phenotype, and Affinity of the Antigen-Specific CD8 T Cell Response. *J Immunol* **175**, 2261–2269 (2005).
97. Moroz, A. *et al.* IL-21 Enhances and Sustains CD8⁺ T Cell Responses to Achieve Durable Tumor Immunity: Comparative Evaluation of IL-2, IL-15, and IL-21. *J Immunol* **173**, 900–909 (2004).

98. Zeng, R. *et al.* Synergy of IL-21 and IL-15 in regulating CD8⁺ T cell expansion and function. *J Exp Medicine* **201**, 139–148 (2005).
99. Chapuis, A. G. *et al.* Transferred WT1-Reactive CD8⁺ T Cells Can Mediate Antileukemic Activity and Persist in Post-Transplant Patients. *Sci Transl Med* **5**, 174ra27-174ra27 (2013).
100. Habib, T., Senadheera, S., Weinberg, K. & Kaushansky, K. The Common γ Chain (γ c) Is a Required Signaling Component of the IL-21 Receptor and Supports IL-21-Induced Cell Proliferation via JAK3 \dagger . *Biochemistry-us* **41**, 8725–8731 (2002).
101. Asao, H. *et al.* Cutting Edge: The Common γ -Chain Is an Indispensable Subunit of the IL-21 Receptor Complex. *J Immunol* **167**, 1–5 (2001).
102. Siegel, A. M. *et al.* A Critical Role for STAT3 Transcription Factor Signaling in the Development and Maintenance of Human T Cell Memory. *Immunity* **35**, 806–818 (2011).
103. Zeng, R. *et al.* The molecular basis of IL-21–mediated proliferation. *Blood* **109**, 4135–4142 (2007).
104. Cui, W., Liu, Y., Weinstein, J. S., Craft, J. & Kaech, S. M. An Interleukin-21- Interleukin-10-STAT3 Pathway Is Critical for Functional Maturation of Memory CD8⁺ T Cells. *Immunity* **35**, 792–805 (2011).
105. Mesas-Fernández, A. *et al.* Interleukin-21 in autoimmune and inflammatory skin diseases. *Eur. J. Immunol.* 2250075 (2023) doi:10.1002/eji.202250075.
106. Bubier, J. A. *et al.* A critical role for IL-21 receptor signaling in the pathogenesis of systemic lupus erythematosus in BXSB-Yaa mice. *Proc National Acad Sci* **106**, 1518–1523 (2009).
107. McPhee, C. G. *et al.* IL-21 Is a Double-Edged Sword in the Systemic Lupus Erythematosus–like Disease of BXSB.Yaa Mice. *J Immunol* **191**, 4581–4588 (2013).
108. Niu, X. *et al.* IL-21 regulates Th17 cells in rheumatoid arthritis. *Hum Immunol* **71**, 334–341 (2010).
109. Carbone, G. *et al.* Interleukin-6 Receptor Blockade Selectively Reduces IL-21 Production by CD4 T Cells and IgG4 Autoantibodies in Rheumatoid Arthritis. *Int J Biol Sci* **9**, 279–288 (2013).
110. Ménoret, E. *et al.* IL-21 Stimulates Human Myeloma Cell Growth through an Autocrine IGF-1 Loop. *J Immunol* **181**, 6837–6842 (2008).
111. Scheeren, F. A. *et al.* IL-21 is expressed in Hodgkin lymphoma and activates STAT5: evidence that activated STAT5 is required for Hodgkin lymphomagenesis. *Blood* **111**, 4706–4715 (2008).
112. Spolski, R. & Leonard, W. J. Interleukin-21: a double-edged sword with therapeutic potential. *Nat Rev Drug Discov* **13**, 379–395 (2014).
113. Blaeschke, F. *et al.* Leukemia-induced dysfunctional TIM-3⁺CD4⁺ bone marrow T cells increase risk of relapse in pediatric B-precursor ALL patients. *Leukemia* **34**, 2607–2620 (2020).
114. Ghani, K. *et al.* Efficient Human Hematopoietic Cell Transduction Using RD114- and GALV-Pseudotyped Retroviral Vectors Produced in Suspension and Serum-Free Media. *Hum Gene Ther* **20**, 966–974 (2009).

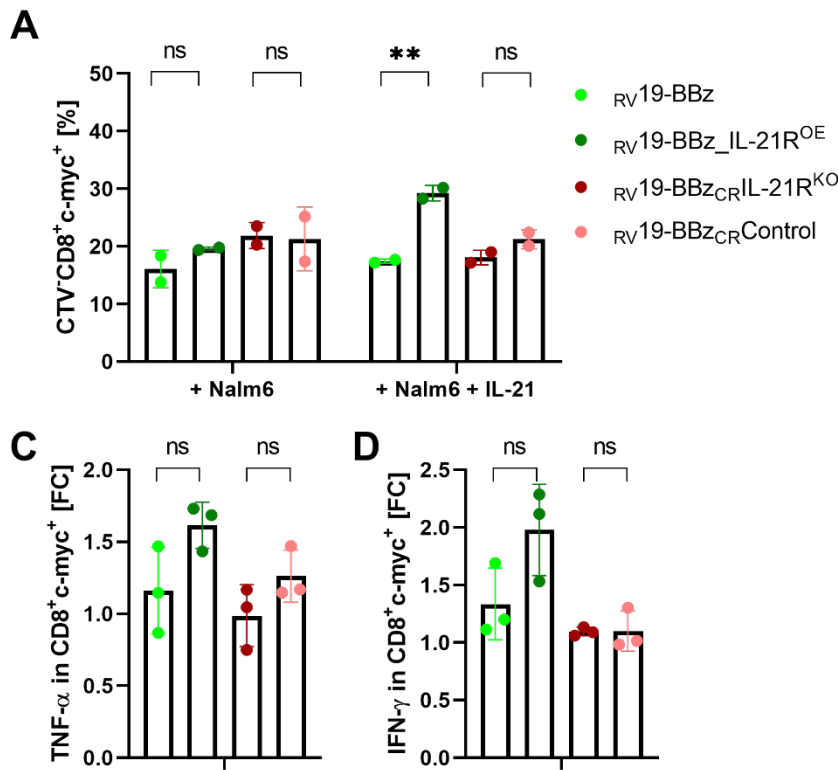
115. Chicaybam, L. *et al.* An Efficient Electroporation Protocol for the Genetic Modification of Mammalian Cells. *Frontiers Bioeng Biotechnology* **4**, 99 (2017).
116. Huyer, G. *et al.* Mechanism of Inhibition of Protein-tyrosine Phosphatases by Vanadate and Pervanadate*. *J Biol Chem* **272**, 843–851 (1997).
117. Brinkman, E. K., Chen, T., Amendola, M. & van Steensel, B. Easy quantitative assessment of genome editing by sequence trace decomposition. *Nucleic Acids Res* **42**, e168–e168 (2014).
118. Dwyer, C. J. *et al.* Fueling Cancer Immunotherapy With Common Gamma Chain Cytokines. *Front Immunol* **10**, 263 (2019).
119. Maus, M. V. *et al.* Adoptive Immunotherapy for Cancer or Viruses. *Annu Rev Immunol* **32**, 189–225 (2014).
120. Smyth, C. M., Ginn, S. L., Deakin, C. T., Logan, G. J. & Alexander, I. E. Limiting γ c expression differentially affects signaling via the interleukin (IL)-7 and IL-15 receptors. *Blood* **110**, 91–98 (2007).
121. Kuijpers, T. W. *et al.* A reversion of an IL2RG mutation in combined immunodeficiency providing competitive advantage to the majority of CD8+ T cells. *Haematologica* **98**, 1030–1038 (2013).
122. Gonnord, P. *et al.* A hierarchy of affinities between cytokine receptors and the common gamma chain leads to pathway cross-talk. *Sci Signal* **11**, eaal1253 (2018).
123. Krutzik, P. O. & Nolan, G. P. Intracellular phospho-protein staining techniques for flow cytometry: Monitoring single cell signaling events. *Cytom Part A* **55A**, 61–70 (2003).
124. MacLeod, R. A. F. *et al.* Human Leukemia and Lymphoma Cell Lines as Models and Resources. *Curr Med Chem* **15**, 339–359 (2008).
125. Brentjens, R. J. *et al.* Genetically Targeted T Cells Eradicate Systemic Acute Lymphoblastic Leukemia Xenografts. *Clin Cancer Res* **13**, 5426–5435 (2007).
126. Gattinoni, L. *et al.* A human memory T cell subset with stem cell–like properties. *Nat Med* **17**, 1290–1297 (2011).
127. Wang, X. *et al.* Phase 1 studies of central memory–derived CD19 CAR T–cell therapy following autologous HSCT in patients with B-cell NHL. *Blood* **127**, 2980–2990 (2016).
128. Gattinoni, L. *et al.* Acquisition of full effector function in vitro paradoxically impairs the in vivo antitumor efficacy of adoptively transferred CD8+ T cells. *J Clin Invest* **115**, 1616–1626 (2005).
129. Lo, M. *et al.* Restoration of lymphoid populations in a murine model of X-linked severe combined immunodeficiency by a gene-therapy approach. *Blood* **94**, 3027–36 (1999).
130. Soudais, C. *et al.* Stable and functional lymphoid reconstitution of common cytokine receptor gamma chain deficient mice by retroviral-mediated gene transfer. *Blood* **95**, 3071–7 (2000).
131. Fischer, A. & Hacein-Bey-Abina, S. Gene therapy for severe combined immunodeficiencies and beyond. *J Exp Med* **217**, e20190607 (2019).

132. Kiel, M. J. *et al.* Integrated genomic sequencing reveals mutational landscape of T-cell prolymphocytic leukemia. *Blood* **124**, 1460–1472 (2014).
133. Decaluwe, H. *et al.* γ c deficiency precludes CD8+ T cell memory despite formation of potent T cell effectors. *Proc National Acad Sci* **107**, 9311–9316 (2010).
134. Rochman, Y., Spolski, R. & Leonard, W. J. New insights into the regulation of T cells by γ c family cytokines. *Nat Rev Immunol* **9**, 480–490 (2009).
135. Hong, C. *et al.* Activated T Cells Secrete an Alternatively Spliced Form of Common γ -Chain that Inhibits Cytokine Signaling and Exacerbates Inflammation. *Immunity* **40**, 910–923 (2014).
136. Tian, Y. & Zajac, A. J. IL-21 and T Cell Differentiation: Consider the Context. *Trends Immunol* **37**, 557–568 (2016).
137. Frigault, M. J. *et al.* Identification of Chimeric Antigen Receptors That Mediate Constitutive or Inducible Proliferation of T Cells. *Cancer Immunol Res* **3**, 356–367 (2015).
138. Blaeschke, F. *et al.* Induction of a central memory and stem cell memory phenotype in functionally active CD4+ and CD8+ CAR T cells produced in an automated good manufacturing practice system for the treatment of CD19+ acute lymphoblastic leukemia. *Cancer Immunol Immunother* **67**, 1053–1066 (2018).
139. Wherry, E. J. T cell exhaustion. *Nat Immunol* **12**, 492–499 (2011).
140. Fraietta, J. A. *et al.* Disruption of TET2 promotes the therapeutic efficacy of CD19-targeted T cells. *Nature* **558**, 307–312 (2018).
141. Stefan, K., C., M., John, K., C., Navin, Zachary, T. & S., A., Prasad. Comparative analysis of assays to measure CAR T-cell-mediated cytotoxicity. *Nat Protoc* **16**, 1331–1342 (2021).
142. Santegoets, S. J. *et al.* IL-21 promotes the expansion of CD27+CD28+ tumor infiltrating lymphocytes with high cytotoxic potential and low collateral expansion of regulatory T cells. *J Transl Med* **11**, 37 (2013).
143. Fourcade, J. *et al.* Upregulation of Tim-3 and PD-1 expression is associated with tumor antigen-specific CD8+ T cell dysfunction in melanoma patients. *J Exp Med* **207**, 2175–2186 (2010).
144. Feucht, J. *et al.* T-cell responses against CD19 + pediatric acute lymphoblastic leukemia mediated by bispecific T-cell engager (BiTE) are regulated contrarily by PD-L1 and CD80/CD86 on leukemic blasts. *Oncotarget* **5**, 76902–76919 (2014).
145. Zhu, C. *et al.* The Tim-3 ligand galectin-9 negatively regulates T helper type 1 immunity. *Nat Immunol* **6**, 1245–1252 (2005).
146. Wolf, Y., Anderson, A. C. & Kuchroo, V. K. TIM3 comes of age as an inhibitory receptor. *Nat Rev Immunol* **20**, 173–185 (2020).
147. Andersen, M. H., Schrama, D., Straten, P. thor & Becker, J. C. Cytotoxic T Cells. *J Invest Dermatol* **126**, 32–41 (2006).

148. Szabo, S. J. *et al.* A Novel Transcription Factor, T-bet, Directs Th1 Lineage Commitment. *Cell* **100**, 655–669 (2000).
149. Sullivan, B. M., Juedes, A., Szabo, S. J., Herrath, M. von & Glimcher, L. H. Antigen-driven effector CD8 T cell function regulated by T-bet. *Proc National Acad Sci* **100**, 15818–15823 (2003).
150. Strengell, M., Sareneva, T., Foster, D., Julkunen, I. & Matikainen, S. IL-21 Up-Regulates the Expression of Genes Associated with Innate Immunity and Th1 Response. *J Immunol* **169**, 3600–3605 (2002).
151. Hogg, A. E., Bowick, G. C., Herzog, N. K., Cloyd, M. W. & Endsley, J. J. Induction of granulysin in CD8+ T cells by IL-21 and IL-15 is suppressed by human immunodeficiency virus-1. *J Leukocyte Biol* **86**, 1191–1203 (2009).
152. Wu, Y. *et al.* The Biological Effects of IL-21 Signaling on B-Cell-Mediated Responses in Organ Transplantation. *Front Immunol* **7**, 319 (2016).
153. Almeida, J. R. *et al.* Superior control of HIV-1 replication by CD8+ T cells is reflected by their avidity, polyfunctionality, and clonal turnover. *J Exp Medicine* **204**, 2473–2485 (2007).
154. Zimmerli, S. C. *et al.* HIV-1-specific IFN- γ /IL-2-secreting CD8 T cells support CD4-independent proliferation of HIV-1-specific CD8 T cells. *P Natl Acad Sci Usa* **102**, 7239–7244 (2005).
155. Saraiva, M. & O’Garra, A. The regulation of IL-10 production by immune cells. *Nat Rev Immunol* **10**, 170–181 (2010).
156. Foulds, K. E., Rotte, M. J. & Seder, R. A. IL-10 Is Required for Optimal CD8 T Cell Memory following *Listeria monocytogenes* Infection. *J Immunol* **177**, 2565–2574 (2006).
157. Santin, A. D. *et al.* Interleukin-10 Increases Th1 Cytokine Production and Cytotoxic Potential in Human Papillomavirus-Specific CD8+ Cytotoxic T Lymphocytes. *J Virol* **74**, 4729–4737 (2000).
158. Bowers, J. S. *et al.* Th17 cells are refractory to senescence and retain robust antitumor activity after long-term ex vivo expansion. *Jci Insight* **2**, e90772 (2017).
159. Spolski, R. & Leonard, W. J. Interleukin-21: Basic Biology and Implications for Cancer and Autoimmunity*. *Immunology* **26**, 57–79 (2008).
160. Hurton, L. V. *et al.* Tethered IL-15 augments antitumor activity and promotes a stem-cell memory subset in tumor-specific T cells. *Proc National Acad Sci* **113**, E7788–E7797 (2016).

11 Supplements

11.1 Supplementary figures



Supplementary figure 11.1 Proliferation and intracellular cytokine staining of IL-21R knock-out and overexpressing CAR T cells

A. Proliferation of CAR T cells after 48h of co-culture with Nalm6 target cells, shown for CD8⁺ c-myc⁺ cells. There was a significant increase in the proliferation of IL-21R overexpressing CAR T cells after addition of IL-21. Data is shown for one donor and experiments were performed in technical duplicates. Data is shown as mean ± SD. The two-tailed, unpaired Student's t-test was used to compare each separate group. **B.** and **C.** CAR T cells were co-cultured with CD19⁺ targets ± IL-21 for 24h. For ICS, Brefeldin A was added for 2 hours, cells were fixed, permeabilized and stained, and intracellular cytokine secretion was determined via flow cytometry. Cytokine secretion was evaluated as fold change in cytokine secretion after addition of IL-21 with the respective CAR construct in co-culture without the ligand serving as baseline. **B.** IL-21 increased TNF-α secretion considerably in *RV19-BBz_IL-21^{OE}* CAR T cells, which was as pronounced in the other tested conditions. **C.** A similar effect of IL-21 was observed in regard to the IFN-γ secretion. Data is shown for three donors as mean ± SD. The two-tailed, unpaired Student's t-test was used to compare every separate group. TNF-α: tumor necrosis factor alpha, IFN-γ: interferon gamma, FC: fold change, CTV: cell-trace violet.

11.2 Primer sequences

| | |
|---|----------------------|
| Forward primer IL-21R CRISPR/Cas9 knock-out | TTCACCTGCCCTGTACATGT |
| Reverse primer IL-21R CRISPR/Cas9 knock-out | ATGGACTTCTTGACGCTCCT |

11.3 T cell sequences

The Kozak sequence GCCGCCACC was attached to the 5' end to increase expression of the construct. Restriction sites Not1 and EcoR1 were added for cloning into pMP71.

11.3.1 Sequence of _{RV19z} CAR

```
ATGCTTCTCCTGGTGACAAGCCTTCTGCTCTGTGAGTTACCACACCCAGCATTCCCTCCTGATCCCAGACATCCAGA
TGACACAGACTACATCCTCCCTGTCTGCCTCTCTGGGAGACAGAGTCACCATCAGTTGCAGGGCAAGTCAGGAC
ATTAGTAAATATTTAAATTGGTATCAGCAGAAACCAGATGGAAGTGTAAACTCCTGATCTACCATACATCAAGA
TTACTCAGGAGTCCCATCAAGGTTCAAGTGGCAGTGGGTCTGGAACAGATTATTCTCTCACCATTAGCAACCTG
GAGCAAGAAGATATTGCCACTTACTTTTGCCAACAGGGTAATACGCTTCCGTACACGTTCCGGAGGGGGACTAA
GTTGGAAATAACAGGCTCCACCTCTGGATCCGGCAAGCCCGGATCTGGCGAGGGATCCACCAAGGGCGAGGTG
AAACTGCAGGAGTCAGGACCTGGCCTGGTGGCGCCCTCACAGAGCCTGTCCGTACATGCACTGTCTCAGGGGT
CTCATTACCCGACTATGGTGTAAAGCTGGATTCCGACGCTCCACGAAAGGGTCTGGAGTGGCTGGGAGTAATAT
GGGGTAGTGAACACATACTATAATTCAGCTCTCAAATCCAGACTGACCATCATCAAGGACAACCTCAAGAGCC
AAGTTTTCTTAAAAATGAACAGTCTGCAAACTGATGACACAGCCATTTACTACTGTGCCAAACATTATTACTACGG
TGGTAGCTATGCTATGGACTACTGGGGTCAAGGAACCTCAGTCACCGTCTCCTCAGAGCAAAGCTCATTTCTGA
AGAGGACTTGTTCTGCGCGTCTTCTGCCAGCGAAGCCACCACGACGCCAGCGCCGCGACCACCAACACCGG
CGCCACCATCGCGTCGCAGCCCCTGTCCTGCGCCCAGAGGCGTCCGGCCAGCGGCGGGGGGCGCAGTGCA
CACGAGGGGGCTGGACTTCGCTGTGATATCTACATCTGGGCGCCCTTGGCCGGGACTTGTGGGGTCTTCTCCT
GTCACTGGTTATCACCCCTTACTGCAACCACAGGAACAGAGTGAAGTTCAGCAGGAGCGCAGACGCCCCCGCGT
ACCAGCAGGGCCAGAACCAGCTCTATAACGAGCTCAATCTAGGACGAAGAGAGGAGTACGATGTTTTGGACAA
GAGACGTGGCCGGGACCCTGAGATGGGGGGAAAGCCGAGAAGGAAGAACCCTCAGGAAGGCCTGTACAATGA
ACTGCAGAAAGATAAGATGGCGGAGGCCTACAGTGAGATTGGGATGAAAGGCGAGCGCCGGAGGGGGCAAGG
GGCACGATGGCCTTACCAGGGTCTCAGTACAGCCACCAAGGACACCTACGACGCCCTTACATGCAGGCCCTG
CCCCCTCGCTAA
```

11.3.2 Sequence of _{RV19z_IL-21R^{OE}} CAR

```
ATGCTTCTCCTGGTGACAAGCCTTCTGCTCTGTGAGTTACCACACCCAGCATTCCCTCCTGATCCCAGACATCCAGA
TGACACAGACTACATCCTCCCTGTCTGCCTCTCTGGGAGACAGAGTCACCATCAGTTGCAGGGCAAGTCAGGAC
ATTAGTAAATATTTAAATTGGTATCAGCAGAAACCAGATGGAAGTGTAAACTCCTGATCTACCATACATCAAGA
TTACTCAGGAGTCCCATCAAGGTTCAAGTGGCAGTGGGTCTGGAACAGATTATTCTCTCACCATTAGCAACCTG
GAGCAAGAAGATATTGCCACTTACTTTTGCCAACAGGGTAATACGCTTCCGTACACGTTCCGGAGGGGGACTAA
GTTGGAAATAACAGGCTCCACCTCTGGATCCGGCAAGCCCGGATCTGGCGAGGGATCCACCAAGGGCGAGGTG
AAACTGCAGGAGTCAGGACCTGGCCTGGTGGCGCCCTCACAGAGCCTGTCCGTACATGCACTGTCTCAGGGGT
CTCATTACCCGACTATGGTGTAAAGCTGGATTCCGACGCTCCACGAAAGGGTCTGGAGTGGCTGGGAGTAATAT
GGGGTAGTGAACACATACTATAATTCAGCTCTCAAATCCAGACTGACCATCATCAAGGACAACCTCAAGAGCC
AAGTTTTCTTAAAAATGAACAGTCTGCAAACTGATGACACAGCCATTTACTACTGTGCCAAACATTATTACTACGG
TGGTAGCTATGCTATGGACTACTGGGGTCAAGGAACCTCAGTCACCGTCTCCTCAGAGCAAAGCTCATTTCTGA
AGAGGACTTGTTCTGCGCGTCTTCTGCCAGCGAAGCCACCACGACGCCAGCGCCGCGACCACCAACACCGG
CGCCACCATCGCGTCGCAGCCCCTGTCCTGCGCCCAGAGGCGTCCGGCCAGCGGCGGGGGGCGCAGTGCA
CACGAGGGGGCTGGACTTCGCTGTGATATCTACATCTGGGCGCCCTTGGCCGGGACTTGTGGGGTCTTCTCCT
GTCACTGGTTATCACCCCTTACTGCAACCACAGGAACAGAGTGAAGTTCAGCAGGAGCGCAGACGCCCCCGCGT
ACCAGCAGGGCCAGAACCAGCTCTATAACGAGCTCAATCTAGGACGAAGAGAGGAGTACGATGTTTTGGACAA
GAGACGTGGCCGGGACCCTGAGATGGGGGGAAAGCCGAGAAGGAAGAACCCTCAGGAAGGCCTGTACAATGA
ACTGCAGAAAGATAAGATGGCGGAGGCCTACAGTGAGATTGGGATGAAAGGCGAGCGCCGGAGGGGGCAAGG
GGCACGATGGCCTTACCAGGGTCTCAGTACAGCCACCAAGGACACCTACGACGCCCTTACATGCAGGCCCTG
CCCCCTCGCGTGAACAGACTTTGAATTTTACCTTCTCAAGTTGGCGGGAGACGTGGAGTCCAACCCAGGCCC
GCCGCGTGGCTGGGCCGCCCTTGTCTCTGCTGCTCCAGGGAGGCTGGGGTCCCCGACCTCGTCTGCT
ACACCGATTACCTCCAGACGGTCTATCTGCATCCTGGAAATGTGGAACCTCCACCCAGCACGCTCACCCCTACCT
GGCAAGACCAGTATGAAGAGCTGAAGGACGAGGCCACCTCCTGCAGCCTCCACAGGTCGGCCACAATGCCAC
```

GCATGCCACCTACACCTGCCACATGGATGTATTCCACTTCATGGCCGACGACATTTTCAGTGTCAACATCACAGAC
CAGTCTGGCAACTACTCCCAGGAGTGTGGCAGCTTTCTCCTGGCTGAGAGCATCAAGCCGGCTCCCCCTTTCAAC
GTGACTGTGACCTTCTCAGGACAGTATAATATCTCCTGGCGCTCAGATTACGAAGACCCCTGCCTTCTACATGCTG
AAGGGCAAGCTTCAAGTATGAGCTGCAGTACAGGAACCGGGGAGACCCCTGGGCTGTGAGTCCGAGGAGAAAG
CTGATCTCAGTGGACTCAAGAAGTGTCTCCCTCCTCCCCCTGGAGTTCGCAAAGACTCGAGCTATGAGCTGCAG
GTGCGGGCAGGGCCCATGCCTGGCTCCTCCTACCAGGGGACCTGGAGTGAATGGAGTGACCCGGTCATCTTTCA
GACCCAGTCAGAGGAGTTAAAGGAAGGCTGGAACCCCTCACCTGCTGCTTCTCCTCCTGCTTGTATAGTCTTCAT
TCCTGCCTTCTGGAGCCTGAAGACCCATCCATTGTGGAGGCTATGGAAGAAGATATGGGCCGTCCCCAGCCCTG
AGCGGTTCTTTCATGCCCTGTACAAGGGCTGCAGCGGAGACTTCAAGAAATGGGTGGGTGCACCCTTCACTGGC
TCCAGCCTGGAGCTGGGACCCTGGAGCCCAGAGGTGCCCTCCACCCTGGAGGTGTACAGCTGCCACCCACCACG
GAGCCCGGCCAAGAGGCTGCAGCTCACGGAGCTACAAGAACCAGCAGAGCTGGTGGAGTCTGACGGTGTGCC
AAGCCCAGCTTCTGGCCGACAGCCCAGAAGCTCGGGGGGCTCAGCTTACAGTGAGGAGAGGGATCGGCCATACG
GCCTGGTGTCCATTGACACAGTGAAGTGTGCTAGATGCAGAGGGGCCATGCACCTGGCCCTGCAGCTGTGAGGAT
GACGGTACCCAGCCCTGGACCTGGATGCTGGCCTGGAGCCCAGCCAGCCCTAGAGGACCCACTCTTGGATGC
AGGGACCACAGTCTGTCTGTGGCTGTGTCTCAGCTGGCAGCCCTGGGCTAGGAGGGCCCTGGGAAGCCTCC
TGGACAGACTAAAGCCACCCCTTGCAGATGGGGAGGACTGGGCTGGGGGACTGCCCTGGGGTGGCCGGTACC
TGGAGGGGTCTCAGAGAGTGAGGCGGGCTCACCCCTGGCCGGCCTGGATATGGACACGTTTTCAGTGGCTTT
GTGGGCTCTGACTGCAGCAGCCCTGTGGAGTGTGACTTACCAGCCCCGGGACGAAGGACCCCCCGGAGCT
ACCTCCGCCAGTGGGTGGTCACTTCTCCGCCACTTTCGAGCCCTGGACCCAGGCCAGCTAA

11.3.3 Sequence of *rv19-28z* CAR

ATGCTTCTCCTGGTGACAAGCCTTCTGCTCTGTGAGTTACCACACCCAGCATTCTCCTGATCCCAGACATCCAGA
TGACACAGACTACATCCTCCCTGTCTGCCTCTCTGGGAGACAGAGTACCATCAGTTGCAGGGCAAGTCAGGAC
ATTAGTAAATATTTAAATTGGTATCAGCAGAAACCAGATGGAAGTGTAAACTCCTGATCTACCATACATCAAGA
TTACTACTCAGGAGTCCCATCAAGGTTCAAGTGGCAGTGGGTCTGGAACAGATTATTCTCTCACCATTAGCAACCTG
GAGCAAGAAGATATTGCCACTTACTTTTGCCAACAGGGTAATACGCTTCCGTACACGTTCCGAGGGGGGACTAA
GTTGGAAATAACAGGCTCCACCTCTGGATCCGGCAAGCCCGGATCTGGCGAGGGATCCACCAAGGGCGAGGTG
AAACTGCAGGAGTCAGGACCTGGCCTGGTGGCGCCCTCACAGAGCCTGTCCGTACATGCACTGTCTCAGGGT
CTCATTACCCGACTATGGTGTAAAGCTGGATTGCGCCAGCCTCCACGAAAGGGTCTGGAGTGGCTGGGAGTAATAT
GGGGTAGTGAACACATACTATAATTCAGCTCTCAAATCCAGACTGACCATCATCAAGGACAACCTCAAGAGCC
AAGTTTTCTTAAAAATGAACAGTCTGCAAAGTATGACACAGCCATTTACTACTGTGCCAAACATTATTACTACGG
TGGTAGCTATGCTATGGACTACTGGGGTCAAGGAACCTCAGTACCCTCTCCTCAGAGCAAAGCTCATTTCTGA
AGAGGACTTGTTCGTGCCGGTCTTCTGCCAGCGAAGCCACCACGACGCCAGCGCCGCGACCACCAACACCGG
CGCCACCATCGCGTCGAGCCCTGTCCCTGCGCCAGAGGCGTCCGGCCAGCGCGGGGGGCGCAGTGCA
CACGAGGGGGCTGGACTTCGCTGTGATATCTACATCTGGGCGCCCTTGGCCGGGACTTGTGGGGTCTTCTCCT
GTCCTGGTTATCACCTTTACTGCAACCACAGGAACAGAGTGAAGTTCAGCAGGAGCGCAGACGCCCCGCGT
ACCAGCAGGGCCAGAACCAGCTCTATAACGAGCTCAATCTAGGACGAAGAGAGGAGTACGATGTTTTGGACAA
GAGACGTGGCCGGGACCCTGAGATGGGGGAAAGCCGAGAAGGAAGAACCCTCAGGAAGGCCTGTACAATGA
ACTGCAGAAAGATAAGATGGCGGAGGCCTACAGTGAAGTGGGATGAAAGGCGAGCGCCGGAGGGGCAAGG
GGCAGATGGCCTTACCAGGGTCTCAGTACAGCCACCAAGGACACCTACGACGCCCTTACATGCAGGCCCTG
CCCCCTCGC

11.3.4 Sequence of *rv19-28z_IL-21R^{OE}* CAR

ATGCTTCTCCTGGTGACAAGCCTTCTGCTCTGTGAGTTACCACACCCAGCATTCTCCTGATCCCAGACATCCAGA
TGACACAGACTACATCCTCCCTGTCTGCCTCTCTGGGAGACAGAGTACCATCAGTTGCAGGGCAAGTCAGGAC
ATTAGTAAATATTTAAATTGGTATCAGCAGAAACCAGATGGAAGTGTAAACTCCTGATCTACCATACATCAAGA
TTACTACTCAGGAGTCCCATCAAGGTTCAAGTGGCAGTGGGTCTGGAACAGATTATTCTCTCACCATTAGCAACCTG
GAGCAAGAAGATATTGCCACTTACTTTTGCCAACAGGGTAATACGCTTCCGTACACGTTCCGAGGGGGGACTAA
GTTGGAAATAACAGGCTCCACCTCTGGATCCGGCAAGCCCGGATCTGGCGAGGGATCCACCAAGGGCGAGGTG
AAACTGCAGGAGTCAGGACCTGGCCTGGTGGCGCCCTCACAGAGCCTGTCCGTACATGCACTGTCTCAGGGT
CTCATTACCCGACTATGGTGTAAAGCTGGATTGCGCCAGCCTCCACGAAAGGGTCTGGAGTGGCTGGGAGTAATAT

GGGGTAGTGAAACCACATACTATAATTGAGCTCTCAAATCCAGACTGACCATCATCAAGGACAACCTCCAAGAGCC
AAGTTTTCTTAAAAATGAACAGTCTGCAAACCTGATGACACAGCCATTTACTACTGTGCCAAACATTATTACTACGG
TGGTAGCTATGCTATGGACTACTGGGGTCAAGGAACCTCAGTCACCGTCTCCTCAGAGCAAAGCTCATTTCTGA
AGAGGACTTGTTCTGTGCCGGTCTTCCTGCCAGCGAAGCCACCACGACGCCAGCGCCGCGACCACCAACACCGG
CGCCACCATCGCGTCGCAGCCCCTGTCCCTGCGCCCAGAGGCGTGCCGGCCAGCGGCGGGGGGCGCAGTGCA
CACGAGGGGGCTGGACTTCGCCTGTGATATCTACATCTGGGCGCCCTTGGCCGGGACTTGTGGGGTCTTCTCCT
GTCACTGGTTATCACCTTTACTGCAACCACAGGAACAGGAGTAAGAGGAGCAGGCTCCTGCACAGTGACTACA
TGAACATGACTCCCCGCCGCCCGGGCCACCCGCAAGCATTACCAGCCCTATGCCCCACCACGCGACTTCGCAG
CCTATCGCTCCAGAGTGAAGTTCAGCAGGAGCGCAGACGCCCCCGCGTACCAGCAGGGCCAGAACCAGCTCTAT
AACGAGCTCAATCTAGGACGAAGAGAGGAGTACGATGTTTTGGACAAGAGACGTGGCCGGGACCCTGAGATG
GGGGGAAAGCCGAGAAGGAAGAACCCTCAGGAAGGCTGTACAATGAACTGCAGAAAGATAAGATGGCGGAG
GCCTACAGTGAGATTGGGATGAAAGGCGAGCGCCGGAGGGGCAAGGGGCACGATGGCCTTTACCAGGGTCTC
AGTACAGCCACCAAGGACACCTACGACGCCCTTACATGCAGGCCCTGCCCCCTCGCGTGAACAGACTTTGAAT
TTTGACCTTCTCAAGTTGGCGGGAGACGTGGAGTCCAACCCAGGCCCGCCGCGTGGCTGGGCCGCCCTTGCT
CCTGCTGCTGCTCCAGGGAGGCTGGGGCTGCCCCGACCTCGTCTGCTACACCGATTACCTCCAGACGGTCATCTG
CATCCTGGAATGTGGAACCTCCACCCAGCAGCTCACCTTACCTGGCAAGACCAGTATGAAGAGCTGAAGG
ACGAGGCCACCTCCTGCAGCCTCCACAGGTGGGCCACAATGCCACGCATGCCACCTACACCTGCCACATGGATG
TATCCACTTCATGGCCGACGACATTTTCAGTGTCAACATCACAGACCAGTCTGGCAACTACTCCAGGAGTGTG
GCAGCTTCTCCTGGCTGAGAGCATCAAGCCGGCTCCCCCTTCAACGTGACTGTGACCTTCTCAGGACAGTATA
ATATCTCCTGGCGCTCAGATTACGAAGACCCTGCCTTCTACATGCTGAAGGGCAAGCTTCAGTATGAGCTGCAGT
ACAGGAACCGGGGAGACCCTGGGCTGTGAGTCCGAGGAGAAAGCTGATCTCAGTGGACTCAAGAAGTGTCTC
CCTCCTCCCCCTGGAGTTCGCAAAAGACTCGAGCTATGAGCTGCAGGTGCGGGCAGGGCCCATGCCTGGCTCCT
CCTACCAGGGGACCTGGAGTGAATGGAGTGACCCGGTCACTTTTCAGACCCAGTCAGAGGAGTTAAAGGAAGG
CTGGAACCTCACCTGCTGCTTCTCCTCCTGCTTGTATAGTCTTATTCTGCTTCTGGAGCCTGAAGACCCATC
CATTGTGGAGGCTATGGAAGAAGATATGGGCCGTCCCCAGCCCTGAGCGGTTCTTCATGCCCTGTACAAGGGC
TGCAGCGGAGACTTCAAGAAATGGGTGGGTGCACCCTTCACTGGCTCCAGCCTGGAGCTGGGACCCTGGAGCC
CAGAGGTGCCCTCCACCTGGAGGTGTACAGCTGCCACCCACCACGGAGCCCAGGCAAGAGGCTGCAGCTCAC
GGAGCTACAAGAACCAGCAGAGCTGGTGGAGTCTGACGGTGTGCCAAGCCAGCTTCTGGCCGACAGCCAG
AACTCGGGGGGCTCAGCTTACAGTGAGGAGAGGGATCGGCCATACGGCCTGGTGTCCATTGACACAGTGACTG
TGCTAGATGCAGAGGGGCCATGCACCTGGCCCTGCAGCTGTGAGGATGACGGCTACCCAGCCCTGGACCTGGA
TGCTGGCCTGGAGCCCAGCCAGGCCTAGAGGACCCACTTTGGATGCAGGGACCACAGTCTGCTGCTGTGGCT
GTGTCTCAGCTGGCAGCCCTGGGCTAGGAGGGCCCTGGGAAGCCTCCTGGACAGACTAAAGCCACCCCTTGCA
GATGGGGAGGACTGGGCTGGGGGACTGCCCTGGGGTGGCCGGTCACTGGAGGGGTCTCAGAGAGTGAGGC
GGGCTCACCCCTGGCCGGCCTGGATATGGACACGTTTGACAGTGGCTTTGTGGGCTCTGACTGCAGCAGCCCTG
TGGAGTGTGACTTACCAGCCCCGGGACGAAGGACCCCCCGGAGCTACCTCCGCCAGTGGGTGGTCATTCTC
CCGCCACTTTCGAGCCCTGGACCCAGGCCAGCTAA

11.3.5 Sequence of ^{RV}19-BBz CAR

ATGCTTCTCCTGGTGACAAGCCTTCTGCTCTGTGAGTTACCACACCCAGCATTCTCCTGATCCCAGACATCCAGA
TGACACAGACTACATCCTCCCTGTCTGCCTCTCTGGGAGACAGAGTCACCATCAGTTGCAGGGCAAGTCAGGAC
ATTAGTAAATATTTAAATTGGTATCAGCAGAAACCAGATGGAACCTGTTAAACTCCTGATCTACCATACATCAAGA
TTACTACTCAGGAGTCCCATCAAGGTTCAAGTGGCAGTGGGTCTGGAACAGATTATTCTCTCACCATAGCAACCTG
GAGCAAGAAGATATTGCCACTTACTTTTGCCAACAGGGTAATACGCTTCCGTACACGTTCCGAGGGGGGACTAA
GTTGGAAATAACAGGCTCCACCTCTGGATCCGGCAAGCCCGGATCTGGCGAGGGATCCACCAAGGGCGAGGTG
AAACTGCAGGAGTCAGGACCTGGCCTGGTGGCGCCCTCACAGAGCCTGTCCGTACATGCACTGTCTCAGGGT
CTCATTACCCGACTATGGTGTAAAGCTGGATTGCGCCAGCCTCCACGAAAGGGTCTGGAGTGGCTGGGAGTAATAT
GGGGTAGTGAAACCACATACTATAATTGAGCTCTCAAATCCAGACTGACCATCATCAAGGACAACCTCCAAGAGCC
AAGTTTTCTTAAAAATGAACAGTCTGCAAACCTGATGACACAGCCATTTACTACTGTGCCAAACATTATTACTACGG
TGGTAGCTATGCTATGGACTACTGGGGTCAAGGAACCTCAGTCACCGTCTCCTCAGAGCAAAGCTCATTTCTGA
AGAGGACTTGTTCTGTGCCGGTCTTCCTGCCAGCGAAGCCACCACGACGCCAGCGCCGCGACCACCAACACCGG
CGCCACCATCGCGTCGCAGCCCCTGTCCCTGCGCCCAGAGGCGTGCCGGCCAGCGGCGGGGGGCGCAGTGCA

CACGAGGGGGCTGGACTTCGCCTGTGATATCTACATCTGGGCGCCCTTGGCCGGGACTTGTGGGGTCCTTCTCCT
GTCACTGGTTATCACCTTTACTGCAACCACAGGAACAAACGGGGCAGAAAGAACTCCTGTATATATTCAAACA
ACCATTTATGAGACCAGTACAACTACTCAAGAGGAAGATGGCTGTAGCTGCCGATTTCCAGAAGAAGAAGAAG
GAGGATGTGAACTGAGAGTGAAGTTCAGCAGGAGCGCAGACGCCCCCGGTACCAGCAGGGCCAGAACCAGC
TCTATAACGAGCTCAATCTAGGACGAAGAGAGGAGTACGATGTTTTGGACAAGAGACGTGGCCGGGACCCTGA
GATGGGGGGAAAGCCGAGAAGGAAGAACCCTCAGGAAGGCCTGTACAATGAACTGCAGAAAGATAAGATGGC
GGAGGCCTACAGTGAGATTGGGATGAAAGGCGAGCGCCGGAGGGGGCAAGGGGCACGATGGCCTTACCAGGG
TCTCAGTACAGCCACCAAGGACACCTACGACGCCCTTACATGCAGGGCCTGCCCCCTCGCTAA

11.3.6 Sequence of *rv19-BBz_IL-21R^{OE} CAR*

ATGCTTCTCCTGGTGACAAGCCTTCTGCTCTGTGAGTTACCACACCCAGCATTCTCCTGATCCCAGACATCCAGA
TGACACAGACTACATCCTCCCTGTCTGCCTCTCTGGGAGACAGAGTACCATCAGTTGCAGGGCAAGTCAGGAC
ATTAGTAAATATTTAAATTGGTATCAGCAGAAACCAGATGGAAGTGTAAACTCCTGATCTACCATACATCAAGA
TTACTCAGGAGTCCCATCAAGGTTCAAGTGGCAGTGGGTCTGGAACAGATTATTCTCTACCATTAGCAACCTG
GAGCAAGAAGATATTGCCACTTACTTTGCCAACAGGGTAATACGCTTCCGTACACGTTCCGAGGGGGGACTAA
GTTGAAATAACAGGCTCCACCTCTGGATCCGGCAAGCCGGATCTGGCGAGGGATCCACCAAGGGCGAGGTG
AAACTGCAGGAGTCAGGACCTGGCCTGGTGGCGCCCTCACAGAGCCTGTCCGTACATGCACTGTCTCAGGGGT
CTCATTACCCGACTATGGTGTAAAGCTGGATTGCCAGCCTCCACGAAAGGGTCTGGAGTGGCTGGGAGTAATAT
GGGGTAGTGAACACATACTATAATTCAGCTCTCAAATCCAGACTGACCATCATCAAGGACAACCTCAAGAGCC
AAGTTTTCTTAAAAATGAACAGTCTGCAAATGATGACACAGCCATTTACTACTGTGCCAAACATTATTACTACGG
TGGTAGCTATGCTATGGACTACTGGGGTCAAGGAACCTCAGTCACCGTCTCCTCAGAGCAAAGCTCATTTCTGA
AGAGGACTTGTTCGTGCCGGTCTTCTGCCAGCGAAGCCACCACGACGCCAGCGCCGCGACCACCAACACCGG
CGCCACCATCGCGTCGAGCCCTGTCCCTGCGCCAGAGGCGTCCGCGCCAGCGGCGGGGGGCGCAGTGCA
CACGAGGGGGCTGGACTTCGCCTGTGATATCTACATCTGGGCGCCCTTGGCCGGGACTTGTGGGGTCCTTCTCCT
GTCACTGGTTATCACCTTTACTGCAACCACAGGAACAAACGGGGCAGAAAGAACTCCTGTATATATTCAAACA
ACCATTTATGAGACCAGTACAACTACTCAAGAGGAAGATGGCTGTAGCTGCCGATTTCCAGAAGAAGAAGAAG
GAGGATGTGAACTGAGAGTGAAGTTCAGCAGGAGCGCAGACGCCCCCGGTACCAGCAGGGCCAGAACCAGC
TCTATAACGAGCTCAATCTAGGACGAAGAGAGGAGTACGATGTTTTGGACAAGAGACGTGGCCGGGACCCTGA
GATGGGGGGAAAGCCGAGAAGGAAGAACCCTCAGGAAGGCCTGTACAATGAACTGCAGAAAGATAAGATGGC
GGAGGCCTACAGTGAGATTGGGATGAAAGGCGAGCGCCGGAGGGGGCAAGGGGCACGATGGCCTTACCAGGG
TCTCAGTACAGCCACCAAGGACACCTACGACGCCCTTACATGCAGGGCCTGCCCCCTCGCGTGAACAGACTTT
GAATTTGACCTTCTCAAGTTGGCGGAGACGTGGAGTCCAACCCAGGCCCCGCGCGTGGCTGGGCCGCCCTT
TGCTCCTGCTGCTCCAGGGAGGCTGGGGCTGCCCCGACCTCGTCTGCTACACCGATTACCTCCAGACGGTCA
TCTGCATCCTGGAATGTGGAACCTCCACCCAGCAGCTACCCCTTACCTGGCAAGACCAGTATGAAGAGCTGA
AGGACGAGGGCACCTCCTGCAGCCTCCACAGGTCGGCCACAATGCCACGCATGCCACCTACACCTGCCACATG
GATGTATTCACTTCATGGCCGACGACATTTTCAGTGTCAACATCACAGACCAGTCTGGCAACTACTCCCAGGAG
TGTGGCAGCTTTCTCCTGGCTGAGAGCATCAAGCCGGTCCCCCTTCAACGTGACTGTGACCTTCTCAGGACAG
TATAATATCTCCTGGCGCTCAGATTACGAAGACCCTGCCTTACATGCTGAAGGGCAAGCTTCAGTATGAGCTG
CAGTACAGGAACCGGGGAGACCCCTGGGCTGTGAGTCCGAGGAGAAAGCTGATCTCAGTGGACTCAAGAAGTG
TCTCCCTCCTCCCCCTGGAGTCCGCAAAGACTCGAGCTATGAGCTGCAGGTGCGGGCAGGGCCATGCCTGGC
TCCTCCTACCAGGGGACCTGGAGTGAATGGAGTGACCCGGTCACTTTTCAGACCCAGTCAGAGGAGTTAAAGGA
AGGCTGGAACCTCACCTGCTGCTTCTCCTCCTGCTGTACATAGTCTTATTCTGCCTTCTGGAGCCTGAAGACC
CATCCATTGTGGAGGCTATGGAAGAAGATATGGGCCGTCCCAGCCCTGAGCGGTTCTTCATGCCCTGTACAA
GGGCTGCAGCGGAGACTTCAAGAAATGGGTGGTGCACCCTTCACTGGCTCCAGCCTGGAGCTGGGACCCTGG
AGCCCAGAGGTGCCCTCCACCTGGAGGTGTACAGCTGCCACCACCACGGAGCCCCGCCAAGAGGCTGCAGC
TCACGGAGCTACAAGAACCAGCAGAGCTGGTGGAGTCTGACGGTGTGCCAAGCCAGCTTCTGGCCGACAGC
CCAGAACTCGGGGGGCTCAGCTTACAGTGAGGAGAGGGATCGGCCATACGGCCTGGTGTCCATTGACACAGTG
ACTGTGCTAGATGCAGAGGGGCCATGCACCTGGCCCTGCAGCTGTGAGGATGACGGTACCCAGCCCTGGACCT
GGATGCTGGCCTGGAGCCCAGCCAGGCCTAGAGGACCCACTTTGGATGCAGGGACCACAGTCTGTCTGTG
GCTGTGTCTCAGCTGGCAGCCCTGGGCTAGGAGGGCCCTGGGAAGCCTCCTGGACAGACTAAAGCCACCCTT
GCAGATGGGGAGGACTGGGCTGGGGGACTGCCCTGGGGTGGCCGGTACCTGGAGGGGTCTCAGAGAGTGA

GGCGGGCTCACCCCTGGCCGGCCTGGATATGGACACGTTTGACAGTGGCTTTGTGGGCTCTGACTGCAGCAGCC
CTGTGGAGTGTGACTTCACCAGCCCCGGGGACGAAGGACCCCCCGGAGCTACCTCCGCCAGTGGGTGGTCATT
CCTCCGCCACTTTGAGCCCTGGACCCCAGGCCAGCTAA

11.3.7 Sequence of *rvCD132*^{OE}

ATGTTGAAGCCATCATTACCATTACATCCCTCTTATTCTGCAGCTGCCCCTGCTGGGAGTGGGGCTGAACACG
ACAATTCTGACGCCAATGGGAATGAAGACACCACAGCTGATTTCTTCTGACCACTATGCCCACTGACTCCCTCA
GTGTTTCCACTCTGCCCTCCCAGAGTTTCACTGTTTTGTGTTCAATGTCGAGTACATGAATTGCACTTGGAAACAG
CAGCTCTGAGCCCCAGCCTACCAACCTCACTCTGCATTATTGGTACAAGAAGTCCGATAATGATAAAGTCCAGAA
GTGCAGCCACTATCTATTCTCTGAAGAAATCACTTCTGGCTGTCAGTTGCAAAAAAAGGAGATCCACCTTACCA
AACATTTGTTGTTTCACTCCAGGACCCACGGGAACCCAGGAGACAGGCCACACAGATGCTAAAAGTGCAGAATC
TGGTGATCCCCTGGGCTCCAGAGAACCTAACACTTCACAACTGAGTGAATCCCAGCTAGAACTGAACTGGAAC
AACAGATTCTTGAACCACTGTTTGGAGCACTTGGTGCAGTACCCGACTGACTGGGACCACAGCTGGACTGAACA
ATCAGTGGATTATAGACATAAGTTCTCCTTGCCTAGTGTGGATGGGCAGAAACGCTACACGTTTTCTGTTCCGGAG
CCGCTTTAACCCTCTGTGGAAGTGTCTCAGCATTGGAGTGAATGGAGCCACCAATCCACTGGGGGAGCAATA
CTTCAAAGAGAATCCTTTCTGTTTGCATTGGAAGCCGTGGTTATCTCTGTTGGCTCCATGGGATTGATTATCAG
CCTTCTCTGTGTATTCTGGCTGGAACGGACGATGCCCCGAATTCCCACCCTGAAGAACCTAGAGGATCTTGT
TACTGAATACCACGGGAACTTTTCGGCCTGGAGTGGTGTGTCTAAGGGACTGGCTGAGAGTCTGCAGCCAGACT
ACAGTGAACGACTCTGCCTCGTCAGTGAGATCCCCAAAAGGAGGGGCCCTTGGGGAGGGGCTGGGGCCTC
CCCATGCAACCAGCATAGCCCCTACTGGGCCCCCCATGTTACACCCTAAAGCCTGAAACCTGA

11.3.8 Sequence of *rvIL-21R*^{OE}

ATGCCGCGTGGCTGGGCCGCCCTTGCTCCTGCTGCTGCTCCAGGGAGGCTGGGGCTGCCCGACCTCGTCTG
CTACACCGATTACCTCCAGACGGTCACTGCATCCTGGAAATGTGGAACCTCCACCCAGCAGCTCACCCCTTACC
TGGCAAGACCAGTATGAAGAGCTGAAGGACGAGGCCACCTCCTGCAGCCTCCACAGGTGGGCCACAATGCCA
CGCATGCCACCTACACCTGCCACATGGATGTATTCCACTTCATGGCCGACGACATTTTCACTGTCAACATCACAGA
CCAGTCTGGCAACTACTCCCAGGAGTGTGGCAGCTTTCTCCTGGCTGAGAGCATCAAGCCGGCTCCCCCTTCAA
CGTGACTGTGACCTTCTCAGGACAGTATAATATCTCCTGGCCTCAGATTACGAAGACCCTGCCTTCTACATGCT
GAAGGGCAAGCTTCACTATGAGCTGCAGTACAGGAACCCGGGAGACCCCTGGGCTGTGAGTCCGAGGAGAAA
GCTGATCTCAGTGGACTCAAGAAGTGTCTCCCTCCTCCCCCTGGAGTTCCGCAAAGACTCGAGCTATGAGCTGCA
GGTGCGGGCAGGGCCATGCCTGGCTCCTCTACCAGGGGACCTGGAGTGAATGGAGTGACCCGGTCACTTTT
AGACCCAGTCAAGAGGAGTTAAAGGAAGGCTGGAACCCCTCACCTGCTGCTTCTCCTCCTGCTTGTATAGTCTTCA
TTCCTGCCTTCTGGAGCCTGAAGACCCATCATTGTGGAGGCTATGGAAGAAGATATGGGCCGTCCCCAGCCCT
GAGCGGTTCTTATGCCCTGTACAAGGGCTGCAGCGGAGACTTCAAGAAATGGGTGGGTGCACCCCTTACTGG
CTCCAGCCTGGAGCTGGGACCCTGGAGCCCAGAGGTGCCCTCCACCCTGGAGGTGTACAGCTGCCACCCACCAC
GGAGCCCGCCAAGAGGCTGCAGCTCACGGAGCTACAAGAACCAGCAGAGCTGGTGGAGTCTGACGGTGTGC
CCAAGCCCAGCTTCTGGCCGACAGCCCAGAAGTCCGGGGGCTCAGCTTACAGTGAAGGAGGGATCGGCCATA
CGGCCTGGTGTCCATTGACACAGTACTGTGCTAGATGCAGAGGGGCCATGCACCTGGCCCTGCAGCTGTGAG
GATGACGGCTACCCAGCCCTGGACCTGGATGCTGGCCTGGAGCCCAGCCAGGCCCTAGAGGACCCACTCTTGA
TGCAGGGACCACAGTCTGTCTGTGGCTGTGTCTCAGCTGGCAGCCCTGGGCTAGGAGGGCCCTGGGAAGC
CTCCTGGACAGACTAAAGCCACCCCTTGCAGATGGGGAGGACTGGGCTGGGGGACTGCCCTGGGGTGGCCGGT
CACCTGGAGGGGTCTCAGAGAGTGAAGCGGGCTCACCCCTGGCCGGCCTGGATATGGACACGTTTGCAGTGG
CTTTGTGGGCTCTGACTGCAGCAGCCCTGTGGAGTGTGACTTACCAGCCCCGGGGACGAAGGACCCCCCGGA
GCTACCTCCGCCAGTGGGTGGTCACTTCTCCGCCACTTTCGAGCCCTGGACCCCAGGCCAGCTAA

11.3.9 Sequence of *rvIL-21R_CD132*^{OE}

ATGTTGAAGCCATCATTACCATTACATCCCTCTTATTCTGCAGCTGCCCCTGCTGGGAGTGGGGCTGAACACG
ACAATTCTGACGCCAATGGGAATGAAGACACCACAGCTGATTTCTTCTGACCACTATGCCCACTGACTCCCTCA
GTGTTTCCACTCTGCCCTCCCAGAGTTTCACTGTTTTGTGTTCAATGTCGAGTACATGAATTGCACTTGGAAACAG
CAGCTCTGAGCCCCAGCCTACCAACCTCACTCTGCATTATTGGTACAAGAAGTCCGATAATGATAAAGTCCAGAA
GTGCAGCCACTATCTATTCTCTGAAGAAATCACTTCTGGCTGTCAGTTGCAAAAAAAGGAGATCCACCTTACCA

AACATTTGTTGTTTCAGCTCCAGGACCCACGGGAACCCAGGAGACAGGCCACACAGATGCTAAAACCTGCAGAATC
TGGTGATCCCCTGGGCTCCAGAGAACCTAACACTTCACAAACTGAGTGAATCCCAGCTAGAACTGAACTGGAAC
AACAGATTCTTGAACCACTGTTTGGAGCACTTGGTGCAGTACCGGACTGACTGGGACCACAGCTGGACTGAACA
ATCAGTGGATTATAGACATAAGTTCTCCTTGCCTAGTGTGGATGGGCAGAAACGCTACACGTTTTCTGTTCCGGAG
CCGCTTTAACCCACTCTGTGGAAGTGCTCAGCATTGGAGTGAATGGAGCCACCCAATCCACTGGGGGAGCAATA
CTTCAAAGAGAATCCTTTCTGTTTGCATTGGAAGCCGTGGTTATCTCTGTTGGCTCCATGGGATTGATTATCAG
CCTTCTCTGTGTATTCTGGCTGGAACGGACGATGCCCCGAATCCCACCCTGAAGAACCTAGAGGATCTTGT
TACTGAATACCACGGGAACTTTTCGGCCTGGAGTGGTGTGTCTAAGGGACTGGCTGAGAGTCTGCAGCCAGACT
ACAGTGAACGACTCTGCCTCGTCAGTGAGATTCCCCAAAAGGAGGGGCCCTTGGGGAGGGGCCTGGGGCCTC
CCCATGCAACCAGCATAGCCCCTACTGGGCCCCCCATGTTACACCCTAAAGCCTGAAACCGTGAAACAGACTTT
GAATTTTGACCTTCTCAAGTTGGCGGGAGACGTGGAGTCCAACCCAggcccgCCGCGTGGCTGGGCCCCCCCTT
GCTCCTGCTGCTGCTCCAGGGAGGCTGGGGCTGCCCGACCTCGTCTGCTACACCGATTACCTCCAGACGGTCAT
CTGCATCCTGGAATGTGGAACCTCCACCCCAGCACGCTCACCTTACCTGGCAAGACCAGTATGAAGAGCTGA
AGGACGAGGCCACCTCCTGCAGCCTCCACAGGTCGGCCACAATGCCACGCATGCCACCTACACCTGCCACATG
GATGTATTCCACTTCATGGCCGACGACATTTTCAGTGTCAACATCACAGACCAGTCTGGCAACTACTCCCAGGAG
TGTGGCAGCTTTCTCCTGGCTGAGAGCATCAAGCCGGCTCCCCCTTCAACGTGACTGTGACCTTCTCAGGACAG
TATAATATCTCCTGGCGCTCAGATTACGAAGACCCTGCCTTCTACATGCTGAAGGGCAAGCTTCAGTATGAGCTG
CAGTACAGGAACCGGGGAGACCCCTGGGCTGTGAGTCCGAGGAGAAAGCTGATCTCAGTGGACTCAAGAAGTG
TCTCCCTCCTCCCCCTGGAGTTCGCAAAAGACTCGAGCTATGAGCTGCAGGTGCGGGCAGGGCCCATGCCTGGC
TCCTCCTACCAGGGGACCTGGAGTGAATGGAGTGACCCGGTCATCTTTCAGACCCAGTCAGAGGAGTTAAAGGA
AGGCTGGAACCCTCACCTGCTGCTTCTCCTCCTGCTTGTGCATAGTCTTCATTCTGCCTTCTGGAGCCTGAAGACC
CATCCATTGTGGAGGCTATGGAAGAAGATATGGGCCGTCCCCAGCCCTGAGCGGTTCTTCATGCCCTGTACAA
GGGCTGCAGCGGAGACTTCAAGAAATGGGTGGGTGCACCCTTCACTGGCTCCAGCCTGGAGCTGGGACCCTGG
AGCCCAGAGGTGCCCTCCACCCTGGAGGTGTACAGCTGCCACCACCGGAGCCCCGCAAGAGGCTGCAGC
TCACGGAGCTACAAGAACCAGCAGAGCTGGTGGAGTCTGACGGTGTGCCAAGCCCAGCTTCTGGCCGACAGC
CCAGAACTCGGGGGGCTCAGCTTACAGTGAGGAGAGGGATCGGCCATACGGCCTGGTGTCCATTGACACAGTG
ACTGTGCTAGATGCAGAGGGGCCATGCACCTGGCCCTGCAGCTGTGAGGATGACGGCTACCCAGCCCTGGACCT
GGATGCTGGCCTGGAGCCCAGCCCAGGCCTAGAGGACCCACTCTTGATGCAGGGACCACAGTCCTGTCCTGTG
GCTGTGCTCAGCTGGCAGCCCTGGGCTAGGAGGGCCCCTGGGAAGCCTCCTGGACAGACTAAAGCCACCCCTT
GCAGATGGGGAGGACTGGGCTGGGGGACTGCCCTGGGGTGGCCGTCACCTGGAGGGGTCTCAGAGAGTGA
GGCGGGCTCACCCCTGGCCGGCCTGGATATGGACACGTTTGACAGTGGCTTTGTGGGCTCTGACTGCAGCAGCC
CTGTGGAGTGTGACTTCACCAGCCCCGGGGACGAAGGACCCCCCGGAGCTACCTCCGCCAGTGGGTGGTCATT
CCTCCGCCACTTTCGAGCCCTGGACCCCAGGCCAGCTAA